SYNTHESIS, MOLECULAR DOCKING, PHARMACOKINETICS, DFT STUDIES AND EVALUATION OF ANTIBACTERIAL AND ANTIOXIDANT ACTIVITIES OF SOME NEW PYRAZOLE DERIVATIVES

ABICHO TESHALE BEDASO

A THESIS SUBMITTED TO THE DEPARTMENT OF APPLIED CHEMISTRY
SCHOOL OF APPLIED NATURAL SCIENCE

PRESENTED IN PARTIAL FULFILLMENT OF THE REQUIREMENT FOR THE DEGREE OF MASTER OF SCIENCE IN APPLIED CHEMISTRY

OFFICE OF GRADUATE STUDIES
ADAMA SCIENCE AND TECHNOLOGY UNIVERSITY

ADAMA, ETHIOPIA

JULY, 2021

SYNTHESIS, MOLECULAR DOCKING, PHARMACOKINETICS, DFT STUDIES AND EVALUATION OF ANTIBACTERIAL AND ANTIOXIDANT ACTIVITIES OF SOME NEW PYRAZOLE DERIVATIVES

ABICHO TESHALE BEDASO

MAJOR ADVISOR: AMAN DEKEBO (PhD) PROFESSOR

CO-ADVISOR: ANKITA GARG (PhD)

A THESIS SUBMITTED TO THE DEPARTMENT OF APPLIED CHEMISTRY
SCHOOL OF APPLIED NATURAL SCIENCE

PRESENTED IN PARTIAL FULFILLMENT OF THE REQUIREMENT FOR THE DEGREE OF MASTER OF SCIENCE IN APPLIED CHEMISTRY

OFFICE OF GRADUATE STUDIES
ADAMA SCIENCE AND TECHNOLOGY UNIVERSITY

ADAMA, ETHIOPIA
JULY, 2021

Approval Sheet

We, the advisors of the thesis entitled "Synthesis, Molecular Docking, Pharmacokinetics, DFT Studies and Evaluation of Antibacterial and Antioxidant Activities of Some New Pyrazole Derivatives" and prepared by Abicho Teshale, hereby certify that the recommendation and suggestions made by the board of examiners are appropriately incorporated into the final version of the thesis.

Aman Dekebo (Prof.)		Sept. 9, 2021
Major Advisor	Signature	Date
_____	_____	_____
Co-advisor	Signature	Date

We, the undersigned, members of the Board of Examiners of the thesis by Abicho Teshale have read and evaluated the thesis entitled "Synthesis, Molecular Docking, Pharmacokinetics, DFT Studies and Evaluation of Antibacterial and Antioxidant Activities of Some New Pyrazole Derivatives" and examined the candidate during open defense. This is, therefore, to certify that the thesis is accepted for partial fulfillment of the requirement of the degree of Master of Science in Synthetic Organic Chemistry.

_____	_____	_____
Chairperson	Signature	Date
_____	_____	_____
Internal Examiner	Signature	Date
Negera Abdissa, PhD		09. Sept. 2021
External Examiner	Signature	Date

Final approval and acceptance of the thesis is contingent upon submission of its final copy to the Office of Postgraduate Studies (OPGS) through the Department Graduate Council (DGC) and School Graduate Committee (SGC).

_____	_____	_____
Department Head	Signature	Date
_____	_____	_____
School Dean	Signature	Date
_____	_____	_____
Office of Postgraduate Studies, Dean	Signature	Date

DECLARATION

I hereby declare that this master thesis entitled "Synthesis, Molecular Docking, Pharmacokinetics, DFT Studies and Evaluation of Antibacterial and Antioxidant Activities of Some New Pyrazole Derivatives" is my original work. That is, it has not been submitted for the award of any academic degree, diploma or certificate in any other university. All sources of materials that are used for this thesis have been duly acknowledged through citation.

_____	_____	_____
Name of student	Signature	Date

RECOMMENDATION

We, the advisor(s) of this thesis, hereby certify that we have read the revised version of the thesis "Synthesis, Molecular Docking, Pharmacokinetics, DFT Studies and Evaluation of Antibacterial and Antioxidant Activities of Some New Pyrazole Derivatives" prepared under our guidance by Abicho Teshale submitted in partial fulfillment of the requirements for the degree of Masters of Science in Applied Chemistry with specialization in Synthetic Organic Chemistry. Therefore, we recommend the submission of revised version of the thesis to the department following the applicable procedures.

Aman Dekebo (Prof.)		Sept. 9, 2021
Maior Advisor	Signature	Date
_____	_____	_____
Co-advisor	Signature	Date

ACKNOWLEDGMENTS

I am grateful to the almighty of ALLAH for the good health and wellbeing that were necessary to complete this studies. Surely goodness and mercy shall follow me all the day of my life. Throughout the writing of this thesis, I have received a great deal of support and assistance. My genuine apologies, if I miss to mention some who deserve to be acknowledge!

I would first like to express my deepest thanks and sincerely appreciation to my major advisor Aman Dekabo (Professor) for his valuable advice, instructions, expert guidance, comments and suggestions, without which I would not have succeeded in carrying out this thesis. I'm really indebted!

As well as I wish to express my deepest and sincere gratitude to my co-advisor Ankita Garg (PhD) for her innovative ideas, advice, encouragement, guidance, coaching, unreserved assistance, giving materials, fruitful discussion and scientific knowledge with which she has inspired me profoundly during this research and write up of the thesis.

I would like to thank Department of Applied Chemistry, Adama Science and Technology University for giving me the chance to pursue graduate study. My sincere acknowledgement also goes to Addis Ababa University for providing the NMR Spectroscopic facility.

I would like to thank my friends and supportive colleagues; Yoseph Samuel, Bayan Abdi, Lencho Alemaheyow, Tekalign Worku and all others who gave me valuable suggestion, materials and chemical for my thesis work. Especial thanks goes to Mr. Arabu Husen for financial support and positive attitude on this thesis.

Finally, I would like to express my deepest gratitude and appreciation to my family for providing me the unconditional love, advice and continuous support throughout my life. Without their inspiration, advice and continuous support, it's difficult to finish this research work.

TABLE OF CONTENTS

LIST OF SCHEMES

LIST OF TABLES

LIST OF FIGURES

LIST OF APPENDICES

LIST OF ACRONMYS AND ABBERVIATIONS

ADME	Absorption, Distribution, Metabolism, and Excretion
d	Doublet
DCM	Dichloromethane
DEPT	Distortion less Enhancement by Polarization Transfer
DFT	Density functional theory
DMF	Dimethylformamide
DMSO	Dimethyl sulfoxide
DPPH	Diphenyl-2-picryl-hydrazyl
Hz	Hertz
IC_{50}	Half Maximal Inhibitory Concentration
m	Multiplicity
MIC	Minimum Inhibition Concentration
MHz	Megahertz
NMR	Nuclear Magnetic Resonance
Rf	Retention factor
s	Singlet
SD	Standard Deviation
TEA	Triethylamine
TLC	Thin Layer Chromatography
UV-Vis	Ultra Violet Visible

ABSTRACT

*Pyrazole derivatives become a good candidate and potential classes of organic compound to play an important role towards medicinal chemistry. This study was aimed to synthesize some pyrazole derivatives via condensation reaction between substituted acetophenone and phenyl hydrazine. Further phenyl hydrazone derivatives treated with Vilsmeier-reagent (DMF and $POCl_3$), after a complete addition of $POCl_3$ to afford the target compound pyrazole derivatives. In present study, compound **97**, **102a** and **102b** were synthesized with 75%, 84% and 86% yield respectively. The synthesized compounds were purified by recrystallization and characterized by spectroscopic techniques (^{1}H-NMR and ^{13}C-NMR). Furthermore, the synthesized compounds were evaluated for their in vitro antibacterial activity against two Gram-negative bacterial strains (E. coli, and P. aeruginosa**)** and two Gram-positive bacteria **(**S. pyogenes and S. aureus) by disk diffusion method. Among synthesized compounds, compound **102a** showed modern inhibitory activity against tested bacterial strains with 12.5±0.707- 25±0.707 mm zone of inhibition compared to standard drug Ceftazidime (13.5±0.707- 26.0±1.414 mm) at 100 mg/mL. All the synthesized compounds showed high inhibitory activity against Gram-positive, S. aureus at 100 mg/mL with 15.5±0.707 – 7.50±0.040 mm zone of inhibition. The radical scavenging property of these compound was evaluated using DPPH radical assay and among the synthesized compounds, compound **97** and **102b** were showed the strongest activity with IC_{50} values of 1.90 and 1.805 μg/mL, respectively. While, the IC_{50} value of ascorbic acid was 1.636 μg/mL. The synthesized compounds were evaluated for their in silico molecular docking analysis using tyrosyl-tRNA synthetase and were found to have minimum binding energy ranging from – 8.0 to –8.4 kcal/mol. Compound **97** and **102a** scored better docking efficiency with binding affinity of – 8.3 kcal/mol and – 8.4 kcal/mol respectively. The result of in silico molecular docking study of the synthetic compounds against Human myeloperoxidase was in good agreement with in vitro antibacterial and antioxidant analysis. Compound **102a** has shown the best binding score (– 9.3 kcal/mol). The drug likeness of the synthesized compound was performed and satisfies the Lipinski's rule of five with zero violations. The method used here to synthesize the compounds was efficient for the preparation of various pyrazole derivatives of enhanced biological activities in drug discovery program.*

Key words: *Pyrazole, Vilsmeier-reagent, Antibacterial, Antioxidant, Molecular docking*

1. INTRODUTION

Heterocycles are an extraordinarily important and unique class of compounds; they make up more than half of all known organic compounds and have a wide range of physical, chemical and biological properties spanning a broad spectrum of reactivity and stability (Karrouchi *et al*., 2018). Heterocyclic compounds are extensively distributed in nature and have versatile synthetic applicability and biological activity which helped the medicinal chemist to plan, organize and implement new approaches towards the discovery of novel drugs (De *et al*., 2021).

Pyrazole **1** is an aromatic heterocyclic compound that constitute a class of compounds particularly useful in organic synthesis and one of the most studied groups of compounds among the azole family. It is a five-membered ring with two nitrogen atoms bound to each other and three carbon atoms. Nitrogen atom 1 (N1) is ‘‘pyrrole-like and Nitrogen atom 2 (N2) is ‘‘pyridine-like”. The N1 nitrogen is not reactive but is deprotonated in the presence of a base-forming anion. Due to the differences between the nitrogen atoms, pyrazoles react with both acids and basis (Figure 1). Another important structural characteristic of pyrazole is prototropic isomerism. Three isomers are possible in unsubstituted pyrazoles (Figure 2) (Venância *et al*., 2017).

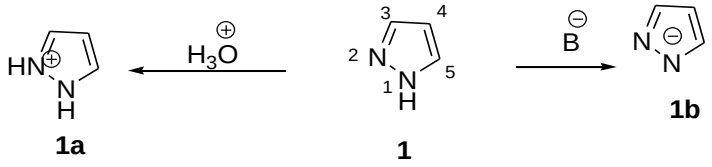

Figure 1: Amphoteric properties of pyrazole

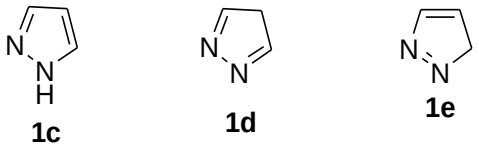

Figure 2: Isomers of unsubstituted pyrazole

Pyrazole framework plays an essential role in biologically active compounds and therefore represents an interesting template for combinatorial as well as medicinal chemistry. Pyrazole derivatives have been reported to wide range of biological activity. Pyrazole derivatives have received a considerable interest in the field of drug discovery and therefore pyrazole ring

constitutes a relevant synthetic target in pharmaceutical industry. In fact, such a heterocyclic moiety represents the core structure of a number of drugs. The wide range of biological activity of pyrazoles has made them popular synthetic targets. There are a number of book chapters and literature reviews dedicated to the synthesis of pyrazole and condensed pyrazoles. The compounds containing pyrazole nucleus has wide applications in medicinal chemistry as well as considerable interest in the chemotherapeutic activity (Anam Ansari *et al.*, 2017).

Pyrazole, it self, is a volatile, colorless, crystalline solid with a pyridine like odour. It is soluble in water, ethanol, and ether to lesser extent, benzene and cyclohexane. It is insoluble in petroleum ether. Much of the basic information obtained about the chemistry of the pyrazole moiety was its aromatic properties compared to those of benzene derivatives. Pyrazole constitute an important heterocyclic family covering a broad range of synthetic as well as natural products that display innumerable chemical, biological, agrochemical and pharmacological properties (Mantzanidou *et al*., 2021).

Pyrazole derivatives represent one of the most active classes of compounds and possess a wide spectrum of biological activities. Pyrazole derivatives play an important role in antitumor agents because of their good inhibitory activity against BRAF(V600E), EGFR, telomerase, ROS Receptor Tyrosine Kinase and Aurora-A kinase. In addition, pyrazole derivatives also show good anti-inflammatory and antibacterial activities. Several drugs have been developed from pyrazole derivatives. For example, celecoxib **2** demonstrates anti-inflammatory effects and inhibits COX-2; rimonabant **3** functions as a cannabinoid receptor and is utilized to treat obesity; fomepizole **4** inhibits alcohol dehydrogenase; and sildenafil **5** inhibits phosphodiesterase (Figure 3) (Altun *et al.*, 2014).

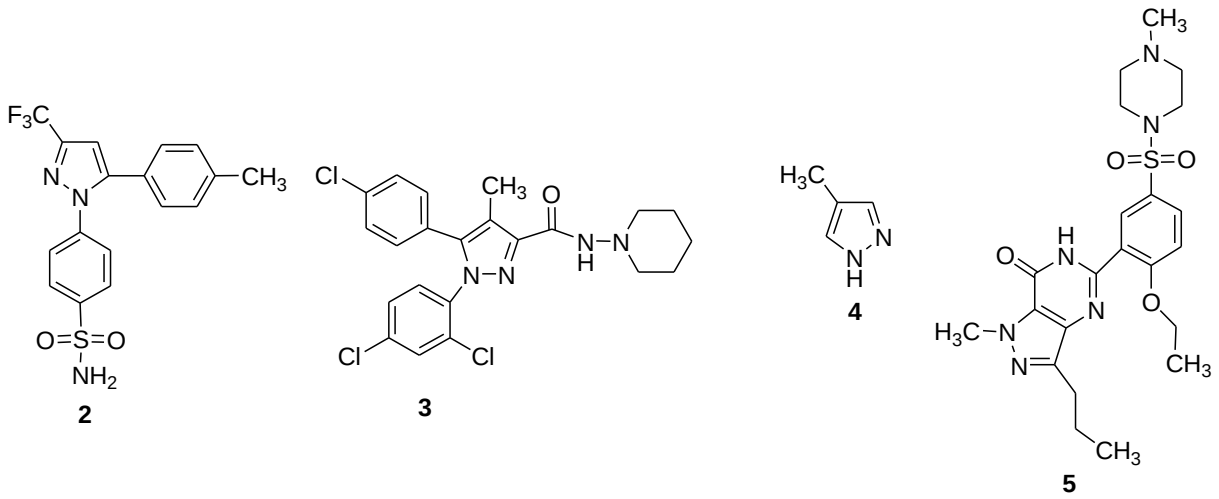

Figure 3: Chemical structure of some drugs containing pyrazole scaffolds.

1.1. Statement of Problem

Infectious diseases are a significant issue in developing countries. Current reports from the World Health Organization (WHO) expressed that public health has become a significant issues due to the population explosion and an increase in endemic and epidemic diseases (Holst, 2020). The increase in resistance to many commercially produced synthetic antimicrobial agents by microorganisms has been increasing with time. The majority of the bacterial and parasitic microorganisms have shown the ability of developing resistance from some of commercially accessible antimicrobial agents. This has led to the search for new, cheap and effective antimicrobial agents that can combat the increasing resistance by the pathogenic microbes. To address this dilemma, it is critical to develop new compounds with more effective antimicrobial activity with least side effects. Across the world, many researcher synthesize pyrazole derivative containing heteroatom scaffold for their biological activity. Synthesis of novel pyrazole derivatives are one of technique used for controlling the growth of pathogenic microorganism. Therefore, this study was aimed to find new and potent antibacterial compounds, and were led to consider the synthesis of some new pyrazole derivatives with the main objective to improve their activity as antimicrobial against some Gram-negative and Gram-positive bacterial strains.

1.2. Objectives of the Study

1.2.1. General Objective

- The overall objective of this study was to synthesize pyrazole derivatives and evaluate their *in silico* molecular docking, pharmacokinetics, antibacterial and antioxidant activities.

1.2.2. Specific Objectives

- To synthesize pyrazole derivatives *via* Vilsmeier-Haack reaction and condensation reaction methods.
- To characterize the structure of the synthesized compounds by spectroscopic techniques such as 1D NMR (^{1}H-NMR, ^{13}C-NMR and DEPT 135).
- To evaluate antibacterial activity of the synthesized compound using disk diffusion method against selected Gram-negative bacterial strains *(E. coli and P. aeruginosa)* and Gram-positive bacteria *(S. pyogenes* and *S. aureus).*
- To evaluate antioxidant activity of synthesized compounds using DPPH assay method.
- To examine *in silico* molecular docking study of synthesized compounds against *S. aureus tyrosyl-tRNA synthetase* (PDB ID 1JIJ) and Human *myeloperoxidase* (PDB ID 1DNU) using Autodoc version 4.2.6.
- To know Pharmacokinetics activities of synthesized compounds.
- To perform DFT study of synthesized Compounds.

1.3. Significance of the Study

The results of this study might provide:-

- Information about the synthesis of pyrazole derivatives that might have application in the pharmaceutical industries to assist their efforts in further research in the development of new drug entities.
- Information about antibacterial activities of synthesized pyrazole derivatives against selected bacterial strains.
- Information about molecular docking, Pharmacokinetics, and DFT study of pyrazole derivatives.

- Documentary information that can be referred by other researchers interested to work on the identification of lead compound and synthesis of related compounds.

2. LITERATURE RIVIEW

2.1. Synthetic Approaches towards Pyrazole Derivatives

The pyrazole ring is prominent structural motif found in numerous pharmaceutically active compounds. This mainly due to its ease of preparation and pharmacological activity. It has also been found that the selective functionalization of the pyrazole with diverse substituents improves their range of action in various fields. Pyrazole is a π-excess aromatic heterocyclic compound. Electrophilic substitution reactions occur preferentially at position 4 and nucleophilic attacks at positions 3 and 5. In this section, we review the evolution and present the methods generally used to access substituted pyrazoles, such as, Vilsmeier-Haack reaction and condensation reaction. As a part of the continuing interest in pyrazole derivatives, numerous compounds with pyrazole ring have been reported.

Abdel-wahab *et al*., reported the synthesized compound of 3,6-di(pyrazol-4-yl)carbazoles **8**. The reaction of compound **6** used as starting material of the target compound with phenyl hydrazine yields diacetylcarbazoles **7**. The reaction of the Vilsmeier reagent with hydrazones of diacetylcarbazoles **7** afford the corresponding pyrazole dicarbaldehydes **8** in good yields (Scheme 1) (Abdel-wahab *et al*., 2011).

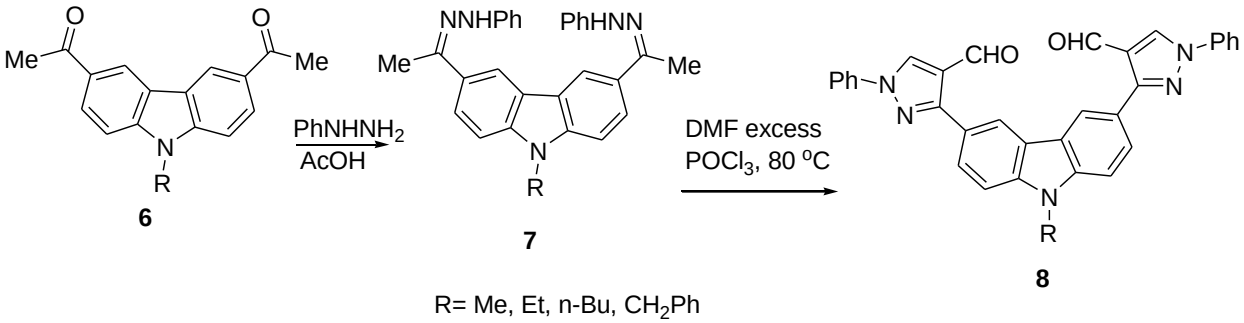

Scheme 1: Synthesis of 3, 6-di (pyrazol-4-yl)carbazole **8**

Hu research group (Hu *et al.,* 2010) have been reported 2,6-dichloro-4-trifluoromethylphenylhydrazine **10** was synthesized from amine **9** through diazotization, followed by reduction using $SnCl_2$/HCl. Phenylhydrazones **11** were next synthesized in almost

quantitative yields by the reaction between the phenyl hydrazine **10** and aryl methyl ketones. When hydrazones **11** reacted with three equivalents of Vilsmeier reagent at 80-90 °C for 4h gave 1-[(2,6-dichloro-4 trifluoromethyl)phenyl]-3-aryl-1*H*-pyrazole-4carbaldehydes **12** in good yields (Scheme 2).

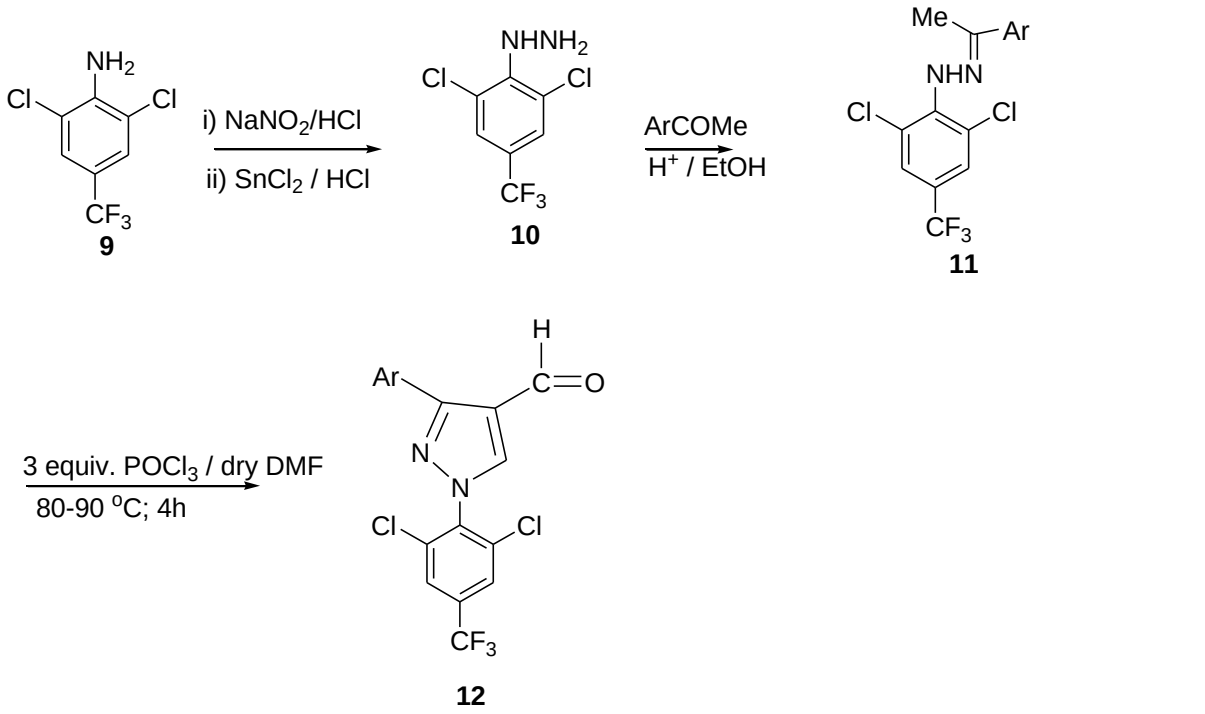

Ar = Ph, 4-ClC_6H_4, 3-ClC_6H_4, 4-BrC_6H_4, 3-BrC_6H_4, 4-$MeOC_6H_4$, 4-$CF_3C_6H_4$, 4-$NO_2C_6H_4$

Scheme 2: Synthesis of pyrazole derivatives **12**

Assali *et al.*, synthesized and reported synthesis of pyrazole derivatives **(16a–16g)**. Pyrazole derivatives **(16a–16g)** were synthesized in two steps (Assali *et al.*, 2020). First, hydrazone compounds **(15a–15g)** were generated by reacting compounds of acetophenone derivatives **13** with phenyl hydrazine derivatives **14** in ethanol using acetic acid glacial as an acid catalyst. After that, hydrazones were reacted with Vilsmeier–Haack reagent which was produced by reacting DMF with $POCl_3$. Various pyrazoles derivatives were synthesized. As illustrated in (Scheme 3).

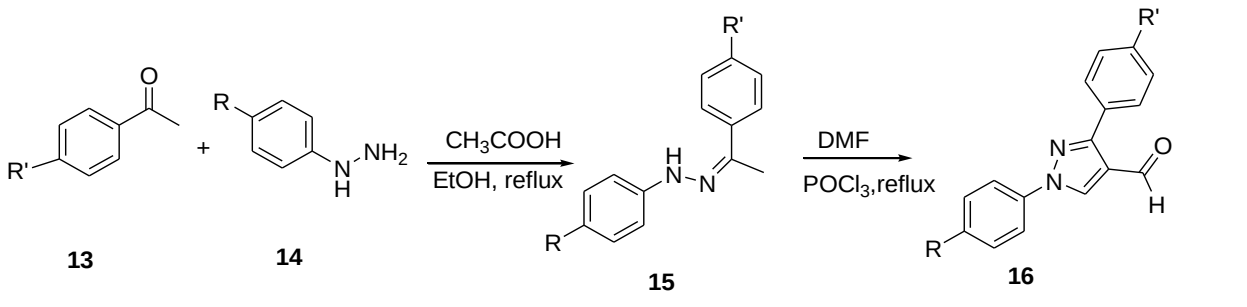

13 **14** **15** **16**

13a R' = SO_2CH_3
13b R' = H
13c R' = Br
13d R' = SO_2NH_2

14a R = SO_2NH_2
14b R = H
14c R = BR
14d R = NO_2

15a R=H, R'= SO_2CH_3
15b R=SO_2NH_2, R'=H
15c R=SO_2NH_2, R'=Br
15d R=SO_2NH_2 ,R'=SO_2CH_3
15e R=H, R'=SO_2NH_2
15f R=Br, R'=SO_2CH_3
15g R=NO_2, R'=SO_2CH_3

16a R=H, R'=SO_2CH_3
16b R=SO_2NH_2, R'=H
16c R=SO_2NH_2, R'=BR
16d R=SO_2NH_2, R'=SO_2CH_3
16e R=H, R'=SO_2NH_2
16f R=Br, R'=SO_2CH_3
16g R=NO_2, R'=SO_2CH_3

Scheme 3: Synthesis of pyrazole derivatives (**16a–16g**)

The synthetic routes to pyrazoles **19-21** have been identified and synthesized by Nagy *et al*. (Nagy *et al*., 2019). The starting ylidenemalononitrile **17** treated in basic conditions with sulfur to provide 2-aminothiophene-3carbonitrile derivative **19**. On the other hand, the starting **17** reacted with 2-hydrazinylquinoline to afford 5-amino-4-cyano-3-aryl-pyrazole derivative **20**. Furthermore, the precursor **17** condensed with various aryl ketones according to Michael addition to provide the desired 2-alkyloxy pyridine-3-carbonitriles **21a-h** (Scheme 4).

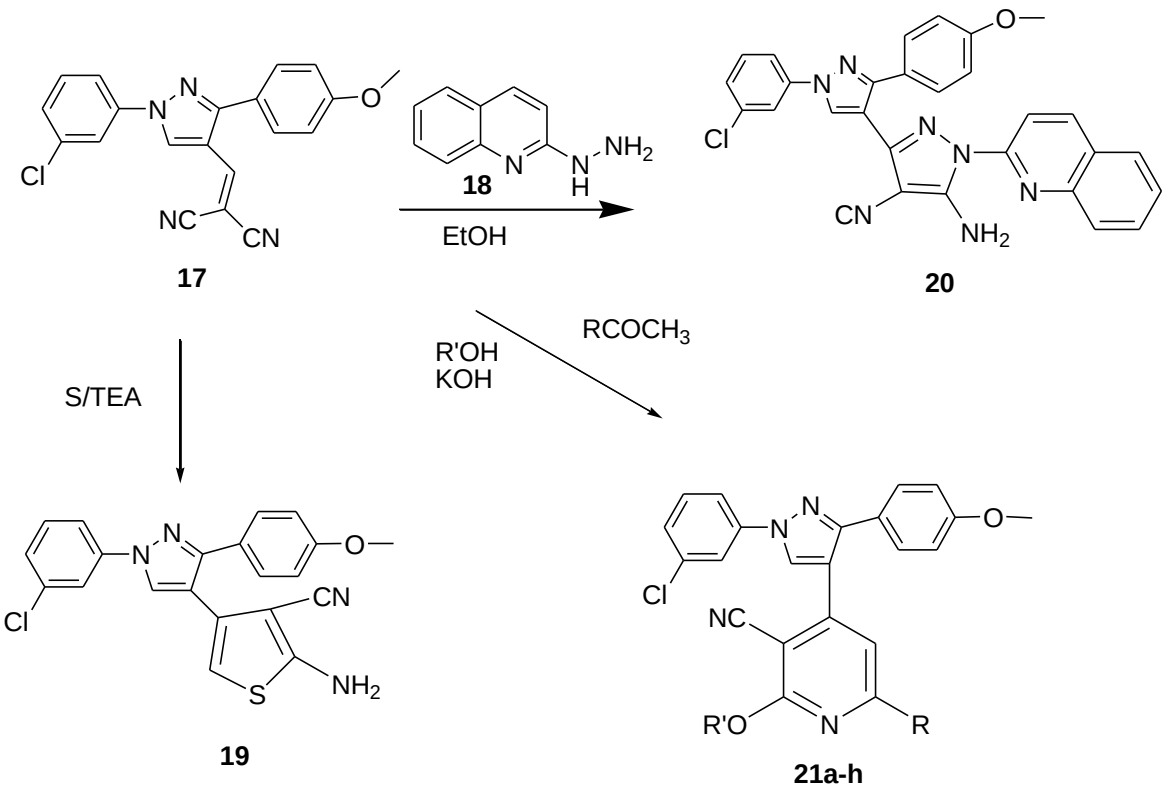

a, R = 3-pyrdinyl, R'= Me
c, R = 2-thienyl, R' =Me
e, R = 4-OH-C_6H_4 R'=Me
g,R = 4-NO_2-C_6H_4, R'=Me

b, R = 3-pyrdinyl, R'= Et
d, R = 2-thienyl, R' =Et
f, R = 4-OH-C_6H_4 R'=Et
h,R = 4-NO_2-C_6H_4, R'=Et

Scheme 4: Synthesis of pyrazole derivatives **19, 20** and **21a-h**

Corresponding to the Hantzsch thiazole synthesis, protocol of thiazolyl hydrazino methylidenepyrazoles **26** synthesized via condensation of *α*-bromoketones **25** with thiosemicarbazones **24** in refluxing EtOH; THF in the presence of sodium acetate (Scheme 5). In this protocol, the starting material 4-formylpyrazoles **22** were treated with thiosemicarbazide **23** in the presence of catalytic amount of acetic acid to afford the corresponding thiosemicarbazones **24** which on subsequent reaction with various *α*-bromoketones **25** afforded the target thiazolyl hydrazino methylidenepyrazoles **26** (Kumar *et al.,* 2012).

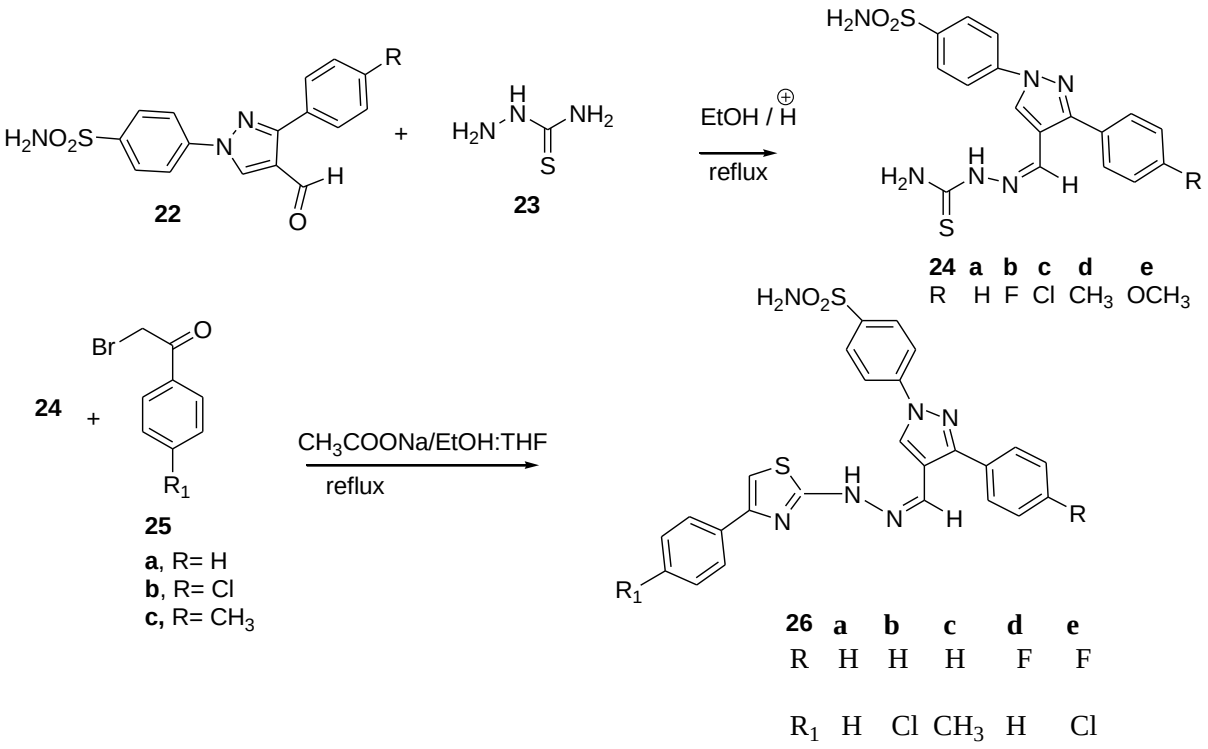

Scheme 5: Synthesis of target compound **24** and **26**

Thuy *et al*., one-pot approach has been applied to prepare a variety of ethyl 1,4,5-triaryl-*1H* pyrazole-3-carboxylates **31** in moderate to high yields from ethyl oxalyl chloride, **28** 1,2-diarylethanones **27** and arylhydrazine hydrochlorides **30** (Scheme 6) (Thuy *et al*., 2019). In this protocol, the *tert*-BuOLi mediated Claisen condensation of 1,2-diarylethanones **27** and ethyl oxalyl chloride **28** efficiently provided the enolized lithium salts of ethyl 2,4-dioxo-3,4-diarylbutanoates, which in situ reacted with arylhydrazine hydrochlorides **30** *via* a hydrochloric acid-promoted Knorr reaction to produce the exquisite triarylpyrazole-3-carboxylates **31**. A process for the preparation of celecoxib was also applied (Scheme 7). 3,4,5-trimethoxyphenyl -1,1,1-trifluoro-2,4 butanedione **33** obtained from a Claisen condensation between acetophenone derivatives **31** and ethyl trifluoroacetate thereby react with 4-sulfamidophenyl hydrazine halide salt to form the 3,4,5-trimethoxyphenyl analog of celecoxib **34.**

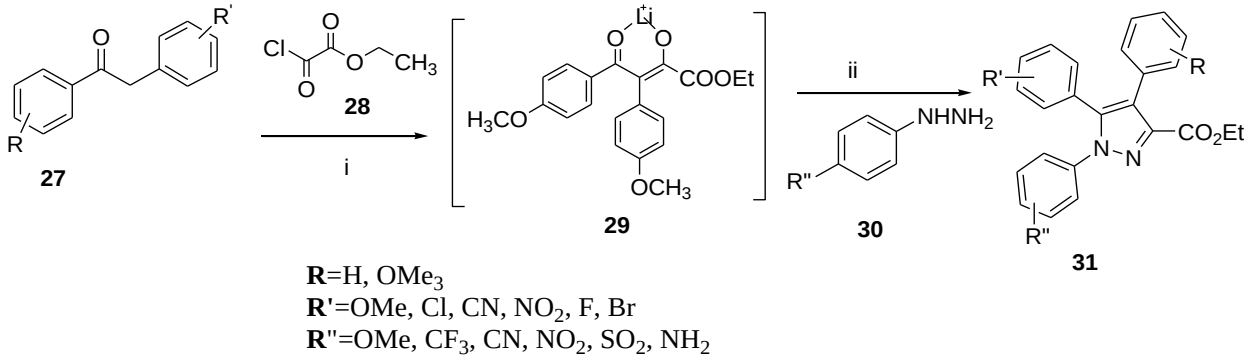

R=H, OMe_3
R'=OMe, Cl, CN, NO_2, F, Br
R"=OMe, CF_3, CN, NO_2, SO_2, NH_2

Scheme 6: Synthesis of ethyl 1,4,5-triaryl-*1H*-pyrazole-3-carboxylates **31**. Reagent and condition (i) Ethyl oxalyl chloride, tert-BuOLi, anhydrous THF,for 6 h under reflux. (ii) EtOH, concentrated HCl, for 6 h under reflux.

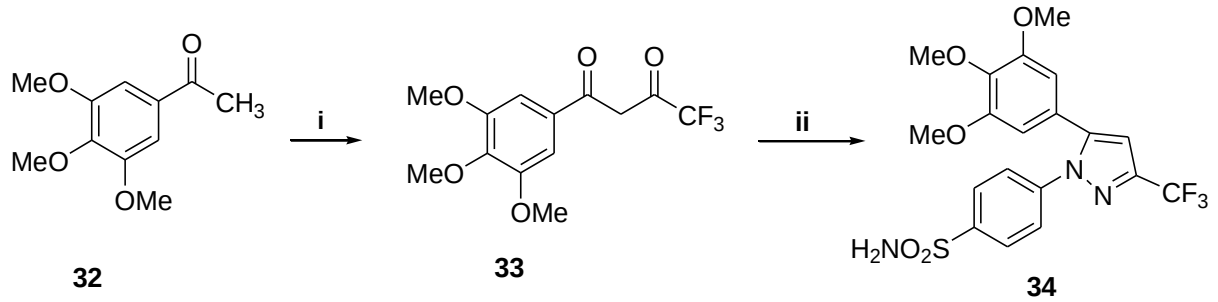

Scheme 7: Synthesis of 3,4,5-trimethoxyphenyl analog of celecoxib **34.** Reagent and conditions: (i) Ethyl trifluoroacetate, NaH, THF, 50°C for 2 hours. (ii) Trifluoroaceticacid, 4-Sulfonamidophenylhydrazine hydrochloride (4SAPH.HCl) (23.0 g, 1.0 mmol) 55°C for one hour.

Balbi *et al*., reported the intermediate 1,3-dicarbonilyc compounds **36** and **38** were obtained by Claisen condensation between 4-methoxyacetophenone **35** and methyl benzoate or ethyl acetate, respectively, under nitrogen atmosphere using sodium hydride as a deprotonating agent whereas **39** was obtained using sodium amide instead of sodium hydride (Balbi *et al.,* 2011). Starting from 1,3-diketones **36, 38 and 39** performed the cyclisation with 2-hydrazinopyridine to pyrazoles **37, 40 and 41** respectively, with the same procedure described above (Scheme 8).

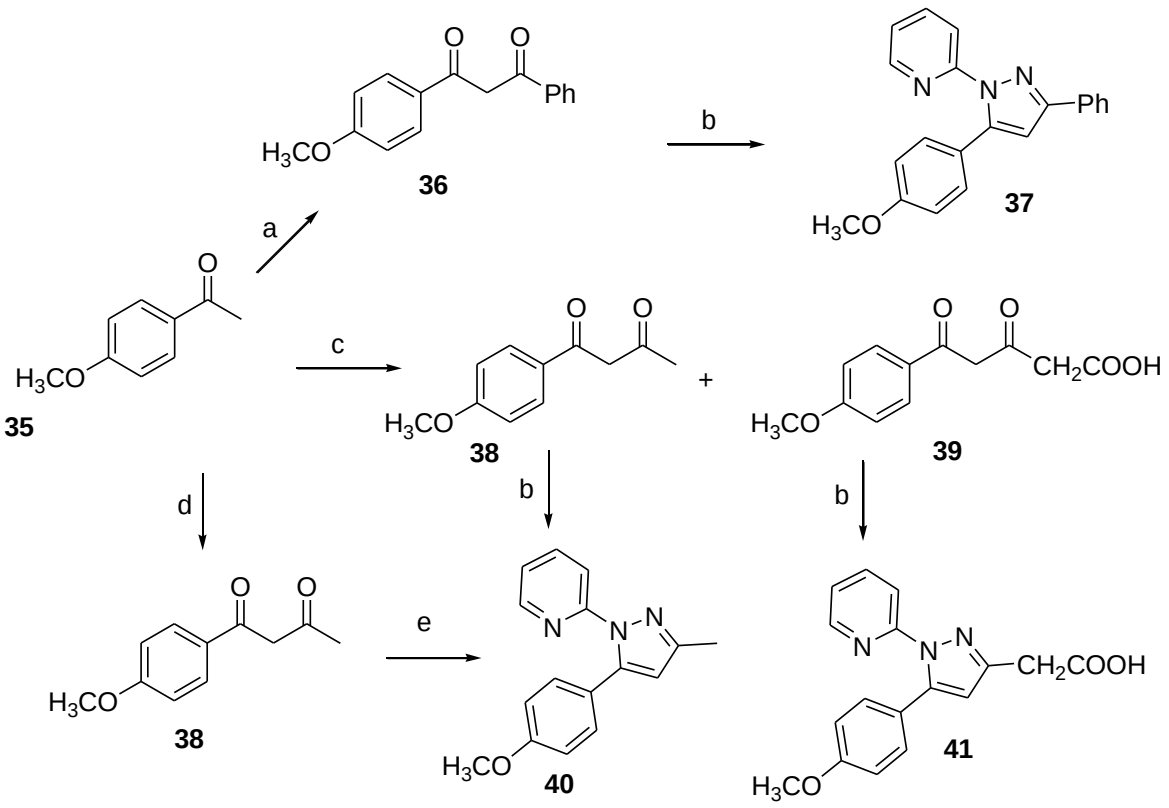

Scheme 8: Synthesis of compound **40** and **41**. Reagent and conditions: (a) $PhCOOCH_3$, NaH, toluene, reflux, N_2; (b) 2-hydrazinopyridine dihydrochloride, EtOH, reflux, (c) AcOEt, $NaNH_2$, toluene, reflux; (d) AcOEt, NaH, toluene, reflux, N_2; (e) 2-hydrazinopyridine dihydrochloride, EtOH, reflux.

Sankappa *et al.,* synthesized and reported the synthetic strategy for the preparation of the chalcones is depicted in scheme 9 (Sankappa *et al.,* 2014). The pyrazole aldehyde **44** was prepared from corresponding acetophenones **42** and semicarbazides and cyclizing the semicarbazone **43** intermediate using $POCl_3$ and DMF. A series of chalcone derivatives **45**(a–e) were synthesized in reasonable yields by the condensation of appropriate acetophenones.

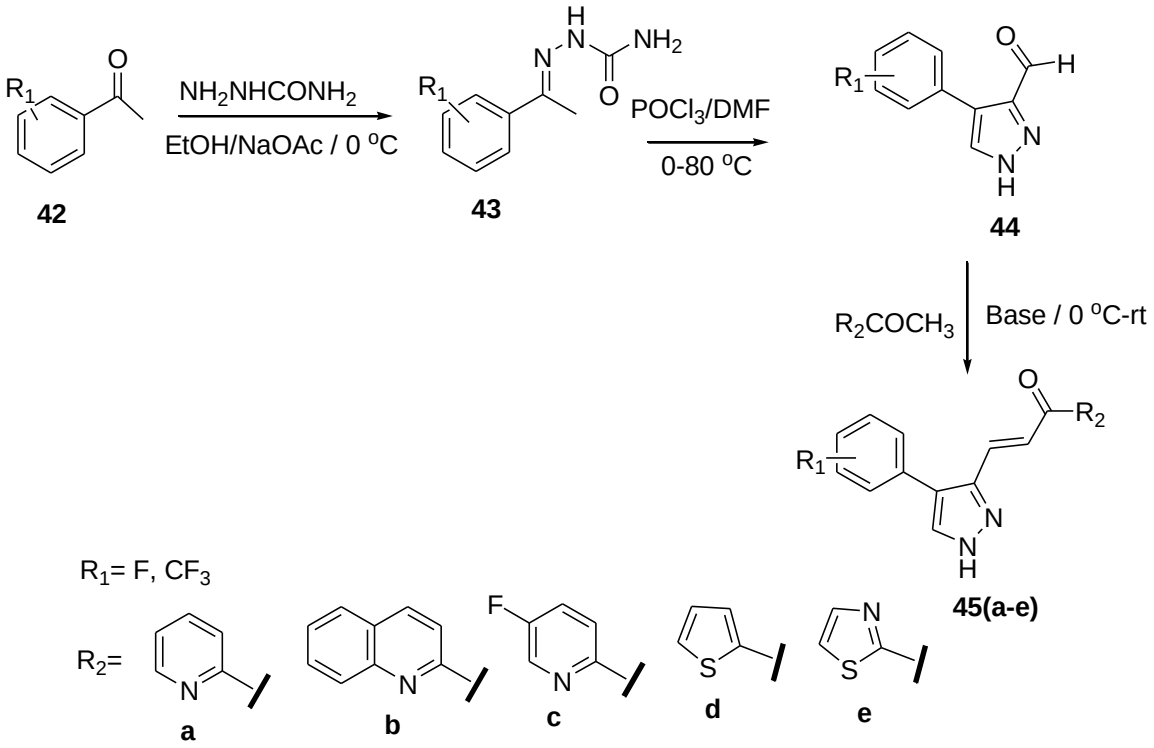

Scheme 9: Synthetic route towards new pyrazole chalcone derivatives 45(a–e)

Rodionor *et al*., reported Claisen condensation of acetyl ferrocene **46** and diethyl oxalate in the presence of NaOEt was reported to furnish ethyl 2,4-dioxo-4-ferrocenylbutanoate **47** in 52% yield (Rodionov *et al.,* 2011). Esters of 1-aryl-5- ferrocenyl-1H-pyrazole-3-carboxylic acids **48** were synthesized in high yields by the condensation between ethyl 2,4-dioxo-4-ferrocenylbutanoate **47** (enol form) and arylhydrazines in boiling ethanol in the presence of a catalytic amount of acetic acid. The corresponding aldehyde **50** were obtained by reduction of esters **49** with $LiAlH_4$ in a mixture of THF and 1,4dioxane. Oxidation with MnO_2 in CH_2Cl_2 at room temperature led to the formation of aldehyde **50** (Scheme 10).

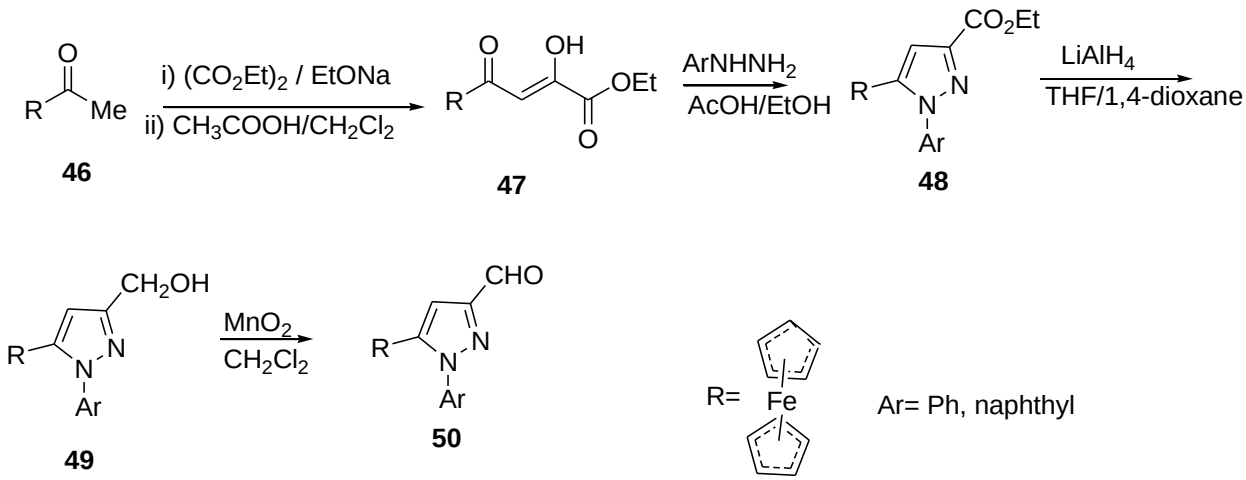

46 **47** **48** **49** **50**

Scheme 10: Synthesis of pyrazole derivatives **50**

1*H*-pyrazole derivatives containing aryl sulfonate moieties acting as COX-2 inhibitors were synthesized by Kendre *et al.*(Kendre *et al.*, 2015) (Scheme 11). In this synthetic route, the intermediate **53(a–e**) was prepared by the reaction of 2-hydroxy acetophenone **51(a–e**) with *N*,*N*-dimethyl formamide dimethyl acetal (DMF-DMA) **52** under microwave irradiation, which furnished **54(a–e)** when reacted with *p*-toluene sulfonyl chloride in the presence of anhydrous K_2CO_3 as catalyst. The desired product **55(a–e**) was obtained by the action of hydrazine hydrate.

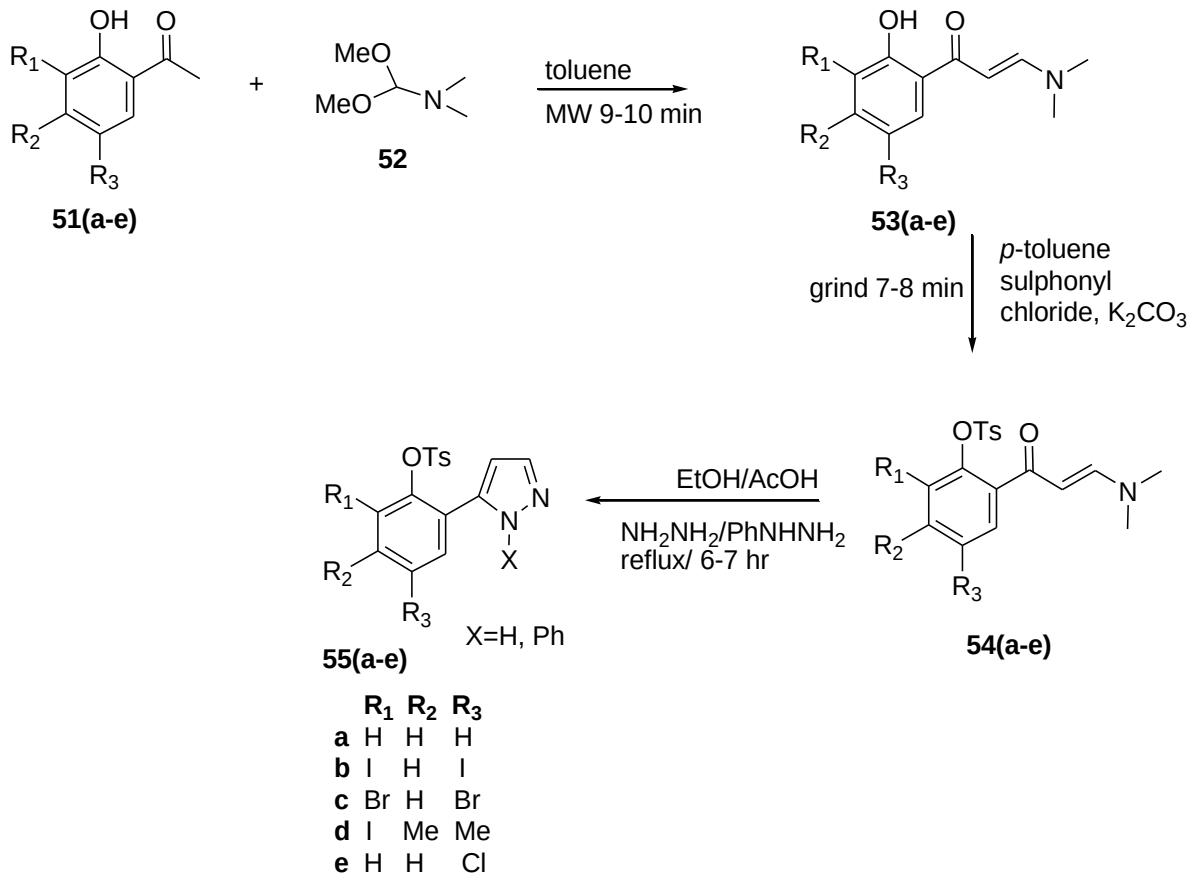

	R_1	R_2	R_3
a	H	H	H
b	I	H	I
c	Br	H	Br
d	I	Me	Me
e	H	H	Cl

Scheme 11: Synthesis of *1H*-pyrazole derivatives **55**(**a–e**)

Another microwave-assisted synthetic route to synthesize pyrazole-4-carbaldehyde with analgesic and anti-inflammatory activity was reported by Selvam *et al.* (Selvam *et al.*, 2012) (Scheme 12). In this approach, acetophenone **56** and substituted aryl hydrazine **57** were exposed to microwave to give 1-substituted phenyl-2-(1-phenylethylidene) hydrazine **58a–e**, which undergo Vilsmeier–Haack reactions to furnish the target compounds **59a–e**.

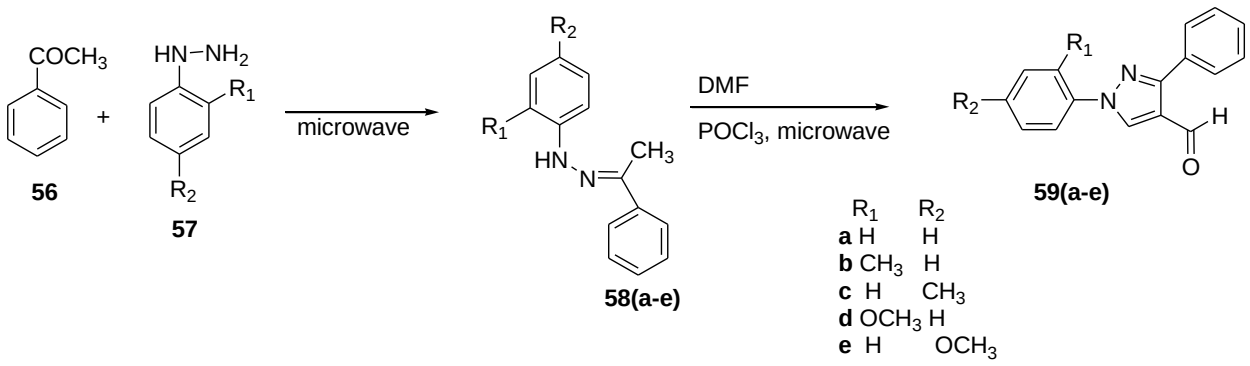

Scheme 12: Microwave-assisted synthetic route for the preparation of pyrazole-4-carbaldehyde derivatives **59**(**a-e**)

2.2. Overview of Biological Potency of Pyrazole Containing Compounds

Pyrazoles are known to be one of the most prominent types of N-containing heterocycles exhibiting large spectrum of biological potencies such as anti-bacterial (Faisal *et al.*, 2019), antifungal (Nagamallu *et al.*, 2015), antitumor (Mohareb, *et al*., 2016), anti-inflammatory (Kohli *et al.*, 2014) and anticancer (Anam *et al*., 2017). The following section describes in brief, the biological activities elucidated by the presence of pyrazole moiety in various compounds.

2.2.1. Anti-Bacterial Potency of Pyrazole Derivatives

Abunada *et al*., prepared 1,3,4,5- tetraaryl-2-pyrazoline, pyrrolo[3,4-c]pyrazole-4,6 dione and 1,3-diaryl-5-(cyanoaminocarbonyl and ethoxycarbonyl)-2-pyrazoline analogues of pyrazole (Abunada *et al.*, 2008). The synthesized derivatives were evaluated for anti-bacterial potency. 1-((4*R*,5*S*)-1,3-bis(4-fluorophenyl)-4-phenyl-4,5dihydro-1H-pyrazol-5-yl)-7-chlorohepta-2,4,6-triyn-1one **60** was reported to be active against *S. aureus* and *E. coli*. Antimicrobial screening results of the compound **60** shows that inhibition zones were 12 mm, 12 mm, 0.0 mm and 10 mm for *E. coli*, *S. aureus*, *A. flavus* and *C. albicans*, respectively (Figure 4).

Chawla *et al*., prepared 3,5-diphenyl-4,5-dihydro-1Hpyrazole-1-carbothioamide derivatives **61a–61f** by making the use of microwave irradiation (MWI) technology (Figure 4) (Chawla *et al.*, 2010). All the prepared pyrazole derivatives were investigated for anti-microbial potency against two Gram positive strains (*B. subtilis* and *S. aureus*) and two Gram-negative strains (*P.*

aeruginosa and *E. coli*). The investigation revealed that derivatives **61a–61f** of synthesized compounds show reasonable anti-bacterial efficacy and noteworthy anti-fungal activity.

Jadhav *et al*., synthesized a new library of 5-(6-metho-xynaphthalen-1-yl)-3-phenyl-4,5-dihydro-1H-pyrazole analogues **62a–62e** (Figure 4) (Jadhav *et al*., 2009). All the constructed pyrazole derivatives were inspected for their anti-microbial power. All the derivatives demonstrated significant to modest anti-microbial capacity.

Kumar *et al*., synthesized a variety of pyrazole derivatives. All the newly developed derivatives were evaluated for their anti-bacterial potency against *B. sublitis*, *E. coli*, *S. aureus* and *K. pneumonia*. The most potent anti-bacterial derivative of the series was **63** (Figure 4) (Kaur *et al.*, 2010). With the, zone of inhibition were 28, 24, 27 and 22mm against *K. pneumoniae*, *S. aureus*, *E. coli*, and *B. sublitis*, respectively.

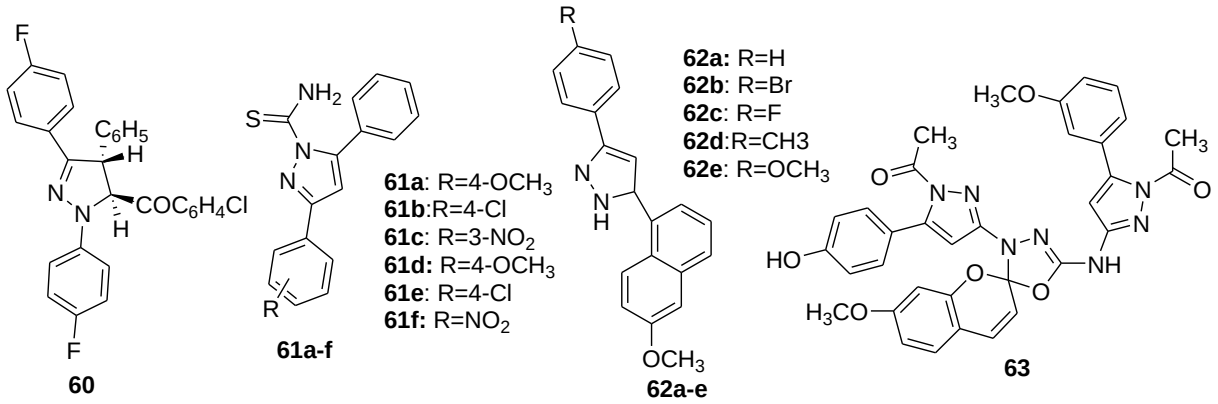

Figure 4: Chemical structures of pyrazole-based potent anti-bacterial compounds.

2.2.2. Antifungal Activity of Pyrazole Derivatives

Synthesis of novel pyrazole-3-carboxylic acid and pyrazole-3,4-dicarboxylic acid derivatives and their antifungal activity are shown in Figure 5 (Venância *et al.*, 2017). The values found were within the range of 25–50 mg/mL against *C. albicans*. Compounds **64**a–b and **65**a–c exhibited MICs of 25 mg/mL compared to nystatin (19 mg/mL). Compounds **64**a–b and **65**a–b were highlighted as the most potent against strains of *C. albicans.*

Nagamallu *et al*., synthesized several coumarin derivatives (Figure 5) (Nagamallu *et al.*, 2015). The compounds showed good activity against three fungal species: *A. niger, A. flavus, and C. albicans.* Compound **66** was identified as the most potent against the three species.

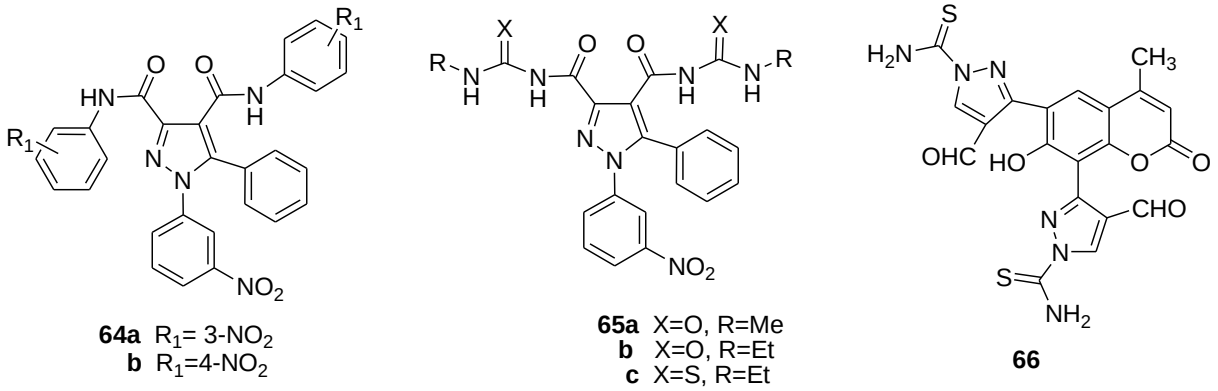

Figure 5: Chemical structures of pyrazole-based potent antifungal compounds.

2.2.3. Antitumor Activity of Pyrazole Derivatives

Cancer is caused by uncontrolled growth of abnormal cells. According to the World Health Organization (WHO), 8.2 million people die from cancer each year, which corresponds to approximately 13% of all deaths around the world. There are three main types of treatment for cancer: surgery, radiation therapy and chemotherapy. With regard to chemotherapy, many research groups have synthesized and evaluated a diverse array of compounds, including substances containing pyrazole rings (Sankappa *et al*., 2014).

Abdelaziz *et al*., synthesized a series of thiophenepyrazole derivatives that were evaluated against three types of tumor cells: breast adenocarcinoma (MCF-7), non-small cell lung cancer (NCI-H460), and CNS cancer (SF-268), also known as glioblastoma (Figure 6) (Mohareb *et al*., 2016). For example, compounds **67a** and **67b** showed good cell growth inhibition when compared to reference drug doxorubicin.

A series of 1-aryl-3,4-substituted-1H-pyrazol-5-ol derivatives were obtained and assayed against cancer antigen-1 (PCA-1 ALKBH3). The best results were obtained for compound **68** (Figure 6), which exhibited high inhibition against the proliferation of DU145 (human hormone independent prostate cancer cells), with no apparent side effects, when administered in a xenografted mouse model (Nakao *et al.*, 2014).

Xing *et al*., synthesized a series of twenty pyrazoles containing an acylhydrazone group. The compounds were evaluated for inhibition of MCF-7 and B16-F10 cancer cell lines. Compound **69** showed the most potent activity against both cell lines (Figure 6) (Xing *et al.,* 2014).

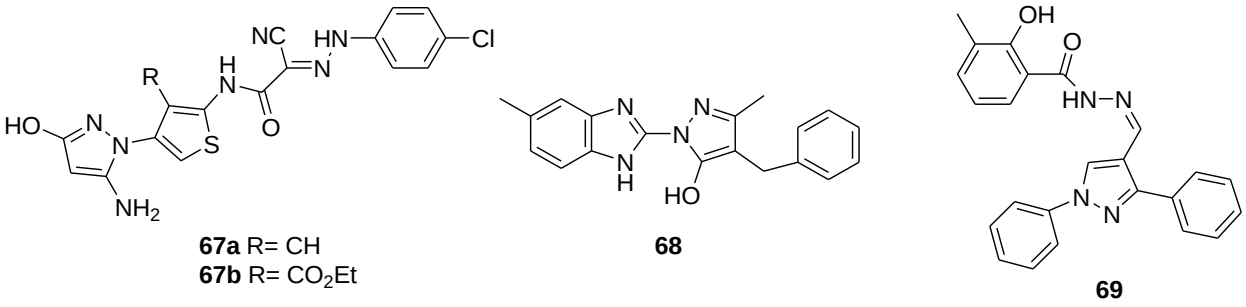

Figure 6: Chemical structure of pyrazoles with antitumor activities.

2.2.4. Anti-Inflammatory Activity of Pyrazole Derivatives

Non-steroidal anti-inflammatory drugs (NSAIDs) provide analgesic and antipyretic effects and are commonly used to treat inflammatory diseases, including rheumatoid arthritis. This anti-inflammatory class inhibits cyclooxygenases enzymes COX-1, COX-2, and COX-3, which are responsible for the production of prostaglandins. NSAIDs have presented a series of side effects, such as gastrointestinal bleeding and stroke. Additionally, an increased cardiovascular risk during treatment with NSAIDs has been reported in patients with a history of myocardial infarction. Dipyrone, celecoxib and lonazolac are pyrazole derivatives used as anti-inflammatory agents (Kohli *et al.,* 2014).

Several new pyrazole derivatives (Figure 7) containing a quinolone moiety were synthesized and tested for their anti-inflammatory and ulcerogenic effect. The most active compound **70** was found to be superior to celecoxib, and demonstrated the highest anti-inflammatory activity as well as the best binding profiles into the COX-2 binding site (El-Feky *et al.,* 2015).

El-Sehemi and his colleagues (El-sehemi *et al.,* 2013) replaced the carboxylic acid group of naproxene, a NSAID, with additional heterocycles. Several compounds were obtained and evaluated with regard to anti-inflammatory, analgesic, and ulcerogenic activities. The derivative **71** showed significant analgesic activity and exhibited no ulcerogenic effect (Figure 7).

Sahu *et al*., prepared various derivatives of 5-phenyl-4-(5-phenyl-4,5-dihydro-1H-pyrazol-3-yl)-4H-1,2,3-triazoles **72** through the reaction of hydrazine monohydrate with chalcones in presence of AcOH (Sahu *et al.,* 2008). All the prepared derivatives **72** were investigated for anti-inflammatory affinity (Figure 7). The detected increase in anti-inflammatory affinity was owing to the presence of 4-Cl, 4-OH and 4-NO2 in phenyl ring at five-position of pyrazoline ring of prepared derivatives.

Mohammed *et al*. evaluated the anti-inflammatory activity of hybrid sulfonamide-pyrazoles. Many compounds were less ulcerogenic than the reference drug indometacine (Figure 7) (Mohammed *et al*., 2014). Derivative **73** showed 81% inhibition of edema, which is better than that of diclofenac, and a selectivity index (SI) of 11.1, which was the best among all compounds synthesized. The ulcer selectivity index of derivative **73** was 2.79, while the value found for indomethacin was 12.82.

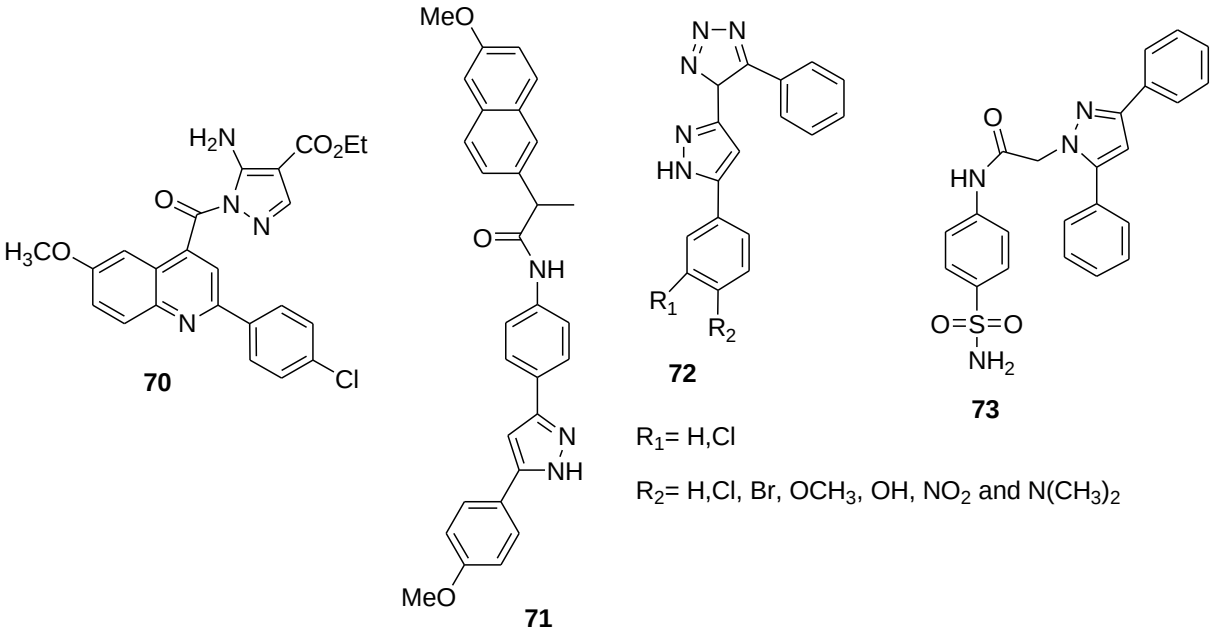

Figure 7: Chemical structure of pyrazoles with anti-inflammatory activity.

2.2.5. Anticancer Activity of Pyrazole Derivatives

Cancer is a diverse group of diseases characterized by abnormal cell growth with the potential to invade or spread to other parts of the body. Cancer is a worldwide health problem and the most frightening disease in humans. The great majority of cancers are caused by environmental

factors and carcinogens. Due to increasing pollution and the use of carcinogens, this fatal disease is increasing in prevalence. The majority of cancers are either resistant to chemotherapy or acquire resistance during treatment. Pyrazoles constitute an important heterocyclic family exhibiting anticancer activity, and many studies have been done to design new and potent anticancer drugs (Anam *et al*., 2017).

A series of functionally substituted pyrazole compounds have been synthesized (**74–75**) and evaluated *in vitro* for their antiproliferative effects on a panel of 60 cell lines by Nitulescu and colleagues (Mihai *et al.,* 2010). Promising results were obtained with *N*-benzoyl-*N′*-(3-(4-bromophenyl)-1*H*-pyrazol-5-yl)-thiourea (**75a**). SAR studies revealed that substituted pyrazolyl thiourea derivatives are more active than the related *N*-[(1-methyl-1*H*-pyrazole-4-yl)]-thiourea derivatives (Figure 8).

Prasad *et al*., reported novel 4,5-dihydropyrazole derivatives (**76–78**) exhibiting excellent anticancer activity compared to the reference drug cisplatin (Prasad *et al.,* 2013). Compound **77** having 4-chloro substitution showed excellent anticancer activity (IC_{50} = 4.94 μM) against HeLa (human cervix carcinoma cell lines), which implied that lipophilic and electron-withdrawing halobenzyl groups are beneficial for cytotoxic activity against HeLa cell lines (Figure 8).

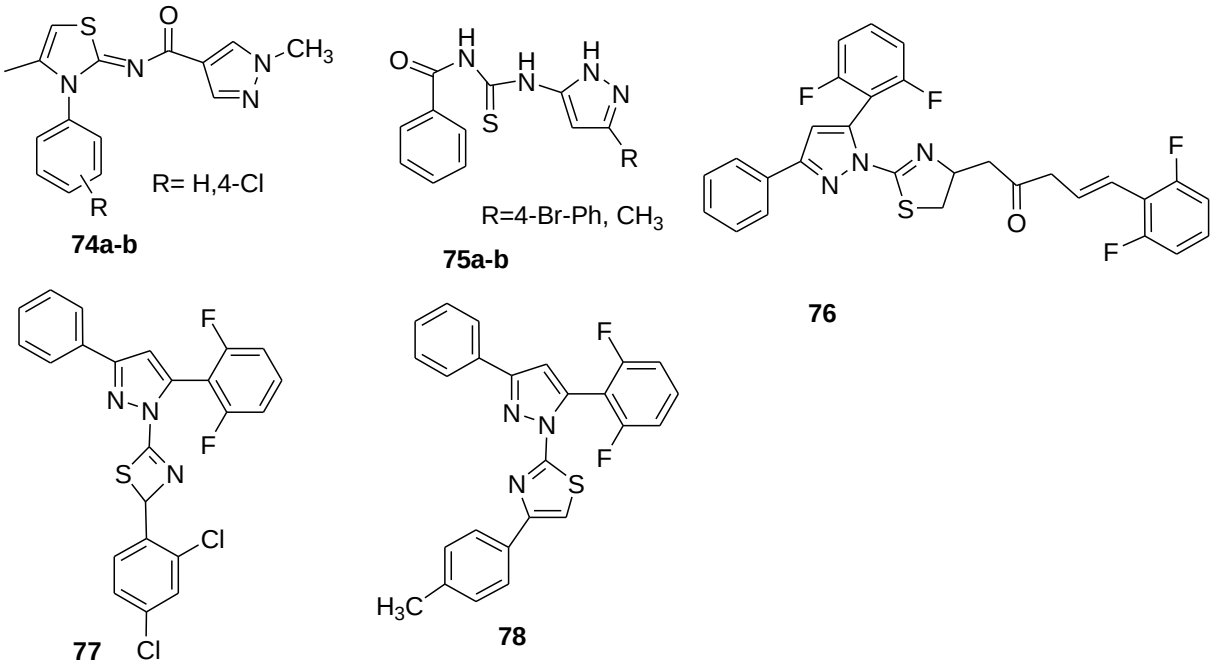

Figure 8: Chemical structure of pyrazoles with anticancer activity.

3. MATERIALS AND METHODS

3.1. Reagents and Chemicals

All solvents and chemicals were obtained commercially from Micro lab store and Fine chemicals PLC (Addis Ababa) and were used without further purification. Phenyl hydrazine (98 %), *p*-nitro acetophenone (98 %), *o*-hydroxy acetophenone (99 %), dimethylformamide (99.9 %), phosphorus oxy chloride (98 %), dichloromethane (99.5 %), distilled water, n-hexane (99.9 %), ethyl acetate (99.5 %), ethanol (98 %), methanol (99.8 %), diethyl ether (99 %), hydrochloric acid (37 %) and sodium hydroxide (99 %) were chemicals used during this work.

3.2. Apparatus and Instruments

Melting points were determined in open capillaries tubes using digital melting point apparatus, expressed in ^{o}C. Reaction progress was checked on pre-coated TLC plates and spots were visualized using UV lamp at 254 nm. The ^{1}H and ^{13}C NMR spectra of the compounds were recorded on Bruker avance 400 MHz NMR spectrophotometer using DMSO-d_6 as the solvent and the values are expressed in δ ppm. Rota-vapor, Funnels, round bottom flasks, vials, refrigerator, hot plate with magnetic stirrer, condenser, thermometer, electronic digital balance, filter papers, aluminum foil, oven, measuring cylinders, beakers, TLC chamber and capillary tubes were apparatus and instruments used during this work.

3.3. Experimental Procedures

3.3.1. General Procedure for Synthesis of *p*-Amino Acetophenone

p-Nitro acetophenone **79** (4.95 g, 0.03 mol) was added into three necked round bottom flask and ethyl alcohol (30 mL) was added. To this suspension iron powder (6.7 g, 0.12 mol), and HCl (1mL) were added and the reaction mixture was refluxed at 60 ^{o}C on oil bath. The progress of the reaction was monitored using TLC in *n*-hexane/ethyl acetate (3:2) solvent system. After completion of the reaction, the reaction mixture was filtered to remove the iron residues, which were washed with ethyl acetate (3 × 40 mL). The organic extracts were washed with H_2O (3 × 30 mL), brine (2 × 30 mL), dried over anhydrous Na_2SO_4, filtered and concentrated under reduced pressure using rotary evaporator (Orlandi *et al.*, 2018).

3.3.2. General Procedure for the Synthesis of Phenyl Hydrazones Intermediate (Derivatives)

To a solution of the appropriate acetophenone derivatives **79** (3.3 g, 20 mmol), **86** (2.7 g, 20 mmol) and **87** (2.72 g, 20 mmol) in methanol (40 ml), phenyl hydrazine **88** (2.16 g, 20 mmol) was added and refluxed for 3 hrs. After cooling the reaction mixture the phenyl hydrazone **91a-c** derivatives was crystallized from methanol and filtered, the higher yield intermediate was obtained. (Jadhav *et al*., 2020).

3.3.3. General Procedure for the Synthesis of Compound 2-(1-phenyl-1H-pyrazol-3-yl) Phenol (97)

The derivative of acetophenone phenyl hydrazone **91c** (3.6 g, 0.016 mol) was dissolved in DMF (15 ml) and then $POCl_3$ (1.5 ml, 0.016 mol) was added drop wise at 0 ^oC. After a complete addition of $POCl_3$, the reaction mixture warmed at room temperature and heated at 60-70 ^oC for 3 hrs. The reaction was poured on to crushed ice and then neutralized with 10 % aqueous NaOH solution. The precipitate was filtered and washed with water and recrystallize from ethanol, this process give a high yield compound **97** (Jadhav *et al*., 2020).

3.3.4. General Procedure for the Synthesis of Compounds 3-aryl-1-phenyl-1H-pyrazole-4-carbaldehyde Derivatives (102a-b)

The derivatives of acetophenone phenylhydrazone **91a** (1.78 g, 0.007 mol), **91b** (1.57 g, 0.007 mol) was dissolved in DMF (15 ml) and then $POCl_3$ (1.96 ml, 0.021 mol) was added drop wise at 0 ^oC. After a complete addition of $POCl_3$, the reaction mixture warmed at room temperature and heated at 60-70 ^oC for 3 hrs. The reaction was poured on to crushed ice and then neutralized with 10 % aqueous NaOH solution. The precipitate was filtered and washed with water and recrystallize from ethanol, this process give a high yield compounds **102a-b** (Jadhav *et al*., 2020).

3.3.5. Determination of Antibacterial Activity

3.3.5.1. Preparation of Inoculums/Cell Culture

The test bacterial species were transferred from the stock cultures and streaked on Mueller Hinton plates and incubated for 24 h at 37 °C. Well-separated bacterial colonies were then used as inoculums. Bacteria was transferred using bacterio- logical loop to autoclaved Mueller Hinton agar that was cooled to about 45 °C in a water bath and mixed by gently swirling the flasks. The medium was then poured to sterile Petri dishes, allowed to solidify and used for the biotest (Obinna *et al.*, 2009).

The antibacterial activities of synthesized compounds were done in collaboration with the Oromia Public Health Research and Referral Laboratory Center. *In vitro* antibacterial activities of synthesized compounds were done against Gram-negative bacterial species (*E. coli and P. aeruginosa*) and Gram-positive bacteria (*S. pyogenes* and *S. aureus*) by disk diffusion assay. The bacterial cultures were inoculated into the nutrient broth (inoculation medium) and incubated overnight at 37 ^{o}C. Inoculated medium were added aseptically to the nutrient medium and mixed thoroughly to get a uniform distribution. The solution was poured approximately 20 mL of sterile MHA in sterile culture plates and allowed to attain room temperature. Sterile agar-disc diffusion previously soaked in a known concentration (100, 50 and 25 mg/mL) synthesized compounds and standard drug Ceftazidime were prepared in DMSO using nutrient agar tubes and carefully placed at the center of the labeled seeded plate. The zones of growth inhibition around the disks were measured after 24 hrs of incubation at 37 °C. The inhibition zones were measured with a ruler and compared with the positive control disk (disk containing Ceftazidime) and expressed in mm (Shakhatreh *et al.,* 2016).

3.3.6. Evaluation of Antioxidant Activity by DPPH

The free radical scavenging activities of the synthesized compound were measured by 1,1-diphenyl-2-picryl-hydrazyl (DPPH) based on the method reported by Bhaskara *et al*. (Bhaskara *et al.,* 2015). With this method, it is possible to determine the radical scavenging power of an antioxidant by measuring the decrease in the absorbance of DPPH at 517 nm. As a result of the color changing from purple to yellow, the absorbance was decreased when the DPPH radical is

scavenged by an antioxidant through donation of hydrogen to form a stable DPPH molecule. Lower absorbance of the reaction mixture indicated higher free radical scavenging activity.

All synthesized compounds and Ascorbic acid were dissolved in DMSO to give 1 mg/mL; the solution were serially diluted to give concentration of 12.5, 25, 50 and 100 μg/mL. To 1 mL of each concentration, 1 mL DPPH (0.04 mg DPPH in 1mL of methanol) was added. Then all the prepared samples and standard were incubated in an oven at 37°C for 30 min and then absorbance was recorded at 517 nm using double beam UV-Vis spectrophotometer. Ascorbic acid was used as standard. The percentage inhibition was calculated using the following formula:-

$$\% \text{ of radical scavenging activity} = \frac{A_o - A_1}{A_o} \times 100, \qquad (\mathbf{1})$$

Where, *Ao* is the absorbance of control reaction and *A*1 is the absorbance of analyte.

IC_{50} was determined from excel curve after plotting % radical scavenging activities and concentration (µg/ml) respectively in excel. The % radical scavenging activity of synthesized compounds data were entered into excel sheet in adjacent columns and then the graph was plotted with a scatter diagram. From the plotted curve, IC_{50} was determined by using the equation below;

$$Y = mx, \qquad (\mathbf{2})$$

Where, Y is % of inhibition, x is Concentration of compound and m is slope of line

3.3.7. *In silico* Molecular Docking Study of Synthesized Compounds

Molecular docking is a method which predicts the preferred orientation of one molecule to a second when bound to each other to form a stable complex (Mishra *et al.,* 2019). The 2D structures of all synthesized compounds **97, 102a** and **102b** were drawn and each individual structure was analyzed by using Chem Draw 16.0. The selected molecules were treated quantum mechanically by applying DFT method using the Gaussian 09 program suite at the Becke-3-Lee-YangPar (B3LYP) level combined with the standard 6-31G (d,p) basis set. During the optimization procedure all the parameters were set in order to obtain a stable structure with

minimum energy. The global minimum energy of the title compound was determined from the structure optimization procedure. The 3D coordinates (PDB) of each molecule were obtained through optimized structure.

The crystal structure of receptor molecule *S. aureus tyrosyl-tRNA synthetase* (PDB ID: 1JIJ) and Human *myeloperoxidase* (PDB ID 1DNU) were downloaded from protein data bank. The protein preparation was done using the reported standard protocol by removing the co-crystallized ligand, selected water molecules and cofactors, the target protein file was prepared by leaving the associated residue with protein by using Auto Preparation of target protein file Auto Dock 4.2.6 (MGL tools 1.5.6). The graphical user interface program Auto Dock 4.2.6 was used to set the grid box for docking simulations. The grid was set so that it surrounds the region of interest in the macromolecule. The docking algorithm provided with Auto Dock Vina was used to search for the best docked conformation between ligand and protein. During the docking process, a maximum of nine conformers were considered for each ligand. The conformations with the most favorable (least) free binding energy were selected for analyzing the interactions between the target receptor and ligands by Discovery studio visualizer.

Auto Dock Vina with standard protocol was used to dock the protein *S. aureus tyrosyl-tRNA synthetase* (PDB ID: 1JIJ) and Human *myeloperoxidase* (PDB ID 1DNU) synthesized new ligands **97, 102a,** and **102b** into the active site of proteins. The molecular docking studies were carried out using Auto Dock Tools (ADT), which is a free graphic user interface (GUI) for the Auto Dock Vina program. The grid box was constructed using 20x20x20, pointing in x, y, and z directions, respectively, with a grid point spacing of 0.375 Å. The center grid box is of 62x30x62 Å for 1JIJ. Nine different conformations were generated for each ligand scored using Auto Dock Vina functions and were ranked according to their binding energies. The ligands are represented in different color, H-bonds and the interacting residues are represented in stick model representation.

3.3.8. *In silico* Pharmacokinetics (Drug-likeness), ADME, and Toxicity Analysis

Drug-likeness is a prediction that determines whether a particular pharmacological agent has properties consistent with being an orally active drug. The chemical structure of the compounds **97, 102a** and **102b** was converted to their canonical simplified molecular input line entry system (SMILE) and submitted to SwissADME tool to estimate *in silico* pharmacokinetic parameters. SwissADME predictor provides information on the number of hydrogen donors, hydrogen acceptors and rotatable bonds, and total polar surface area of a compound. The ligands were also subjected to Lipinski, screened using SwissADME and PreADMET predictors. The organ toxicities and toxicological endpoints of the ligands and their LD_{50} were predicted using Pro Tox II and OSIRIS Property Explorer. The analyses of the compounds were compared with that of a standard drug.

3.3.9. DFT Study

The selected molecules were treated quantum mechanically by applying DFT method using the Gaussian 09 program suite at the Becke-3-Lee-YangPar (B3LYP) level combined with the standard 6-31G (d,p) basis set. During the optimization procedure all the parameters were set in order to obtain a stable structure with minimum energy. The global minimum energy of the title compound was determined from the structure optimization procedure.

4. RESULTS AND DISCUSSION

4.1. The Synthesis of the Compounds

Compound **86** was synthesized according to the procedure developed by Orlandi *et al*. (Orlandi *et al.,* 2018). Starting material *p*-nitro acetophenone **79** was reduced by Fe powder/ HCl in ethanol solvent under reflux for 6 hrs to furnish *p*-amino acetophenone **86** with 73% yield (Scheme 13).

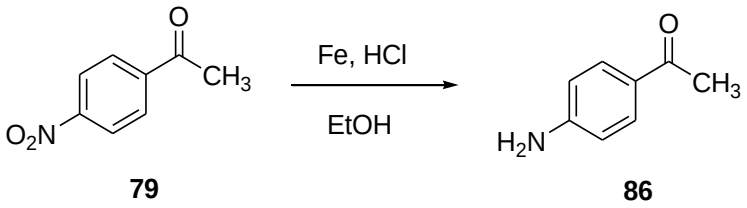

Scheme 13: Reduction of *p*-nitro acetophenone

The plausible mechanism of the reduction of *p*-nitro acetophenone by iron was depicted in the scheme 14.

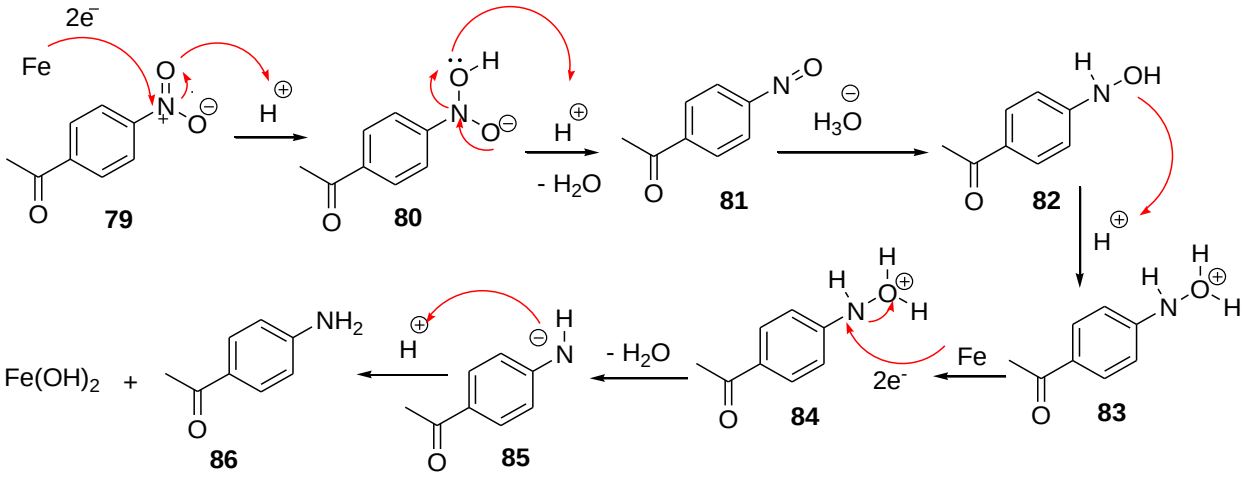

Scheme 14: The proposed mechanism of *p*-nitro acetophenone

Phenyl hydrazone derivatives **91a-c** were generated by reacting compounds of acetophenone derivatives *p*-nitroacetophenone **79** or *p*-aminoacetophenone **86** or *o*-hydroxyacetophenone **87** with phenyl hydrazine **88** in methanol under reflux for three hours with 79%, 89% and 94% (Scheme 15).

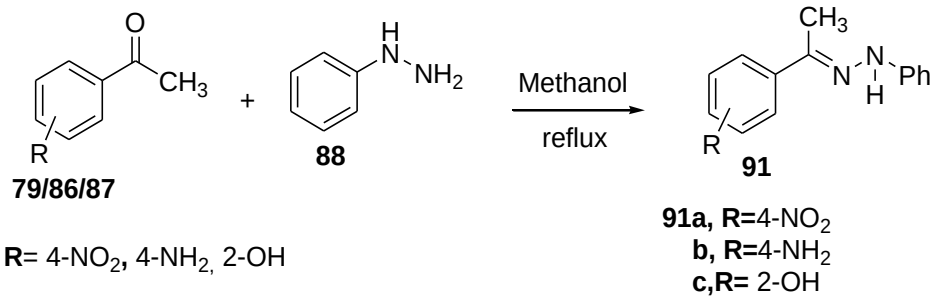

Scheme 15: Synthesis of phenyl hydrazone intermediate **91(a-c)**

The reasonable mechanism of the synthesis of phenyl hydrazone intermediate 91(a-c) was shown in the scheme 16.

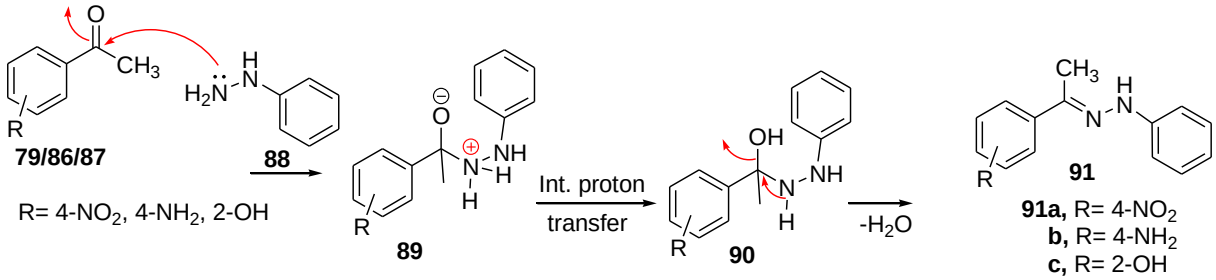

Scheme 16: The proposed mechanisms of phenyl hydrazone intermediate **91(a-c)**

Target compound 2-(1-phenyl-1H-pyrazol-3-yl) phenol **97** were synthesized according to the protocol developed by Archanad *et al.* (Jadhav *et al.*, 2020). The derivatives of acetophenone phenyl hydrazone **91c** were reacted Vilsmeier-Haack reagents which was produced by reacting DMF with $POCl_3$ 1:1 ratio. The reaction was neutralized with 10 % aqueous NaOH solution and the precipitate was filtered, this process to afford compound **97** with yield 75 % yields (Scheme 17).

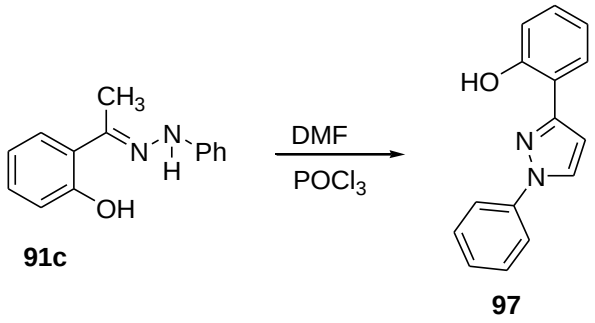

91c **97**

Scheme 17: Synthesis of compound 2-(1-phenyl-*1H*-pyrazol-3-yl) phenol **97**

The plausible mechanism of the reaction starts with tautomerization and Vilsmeier-Haack reagents were cyclized and activate the reaction as depicted in the following mechanism (Scheme 18).

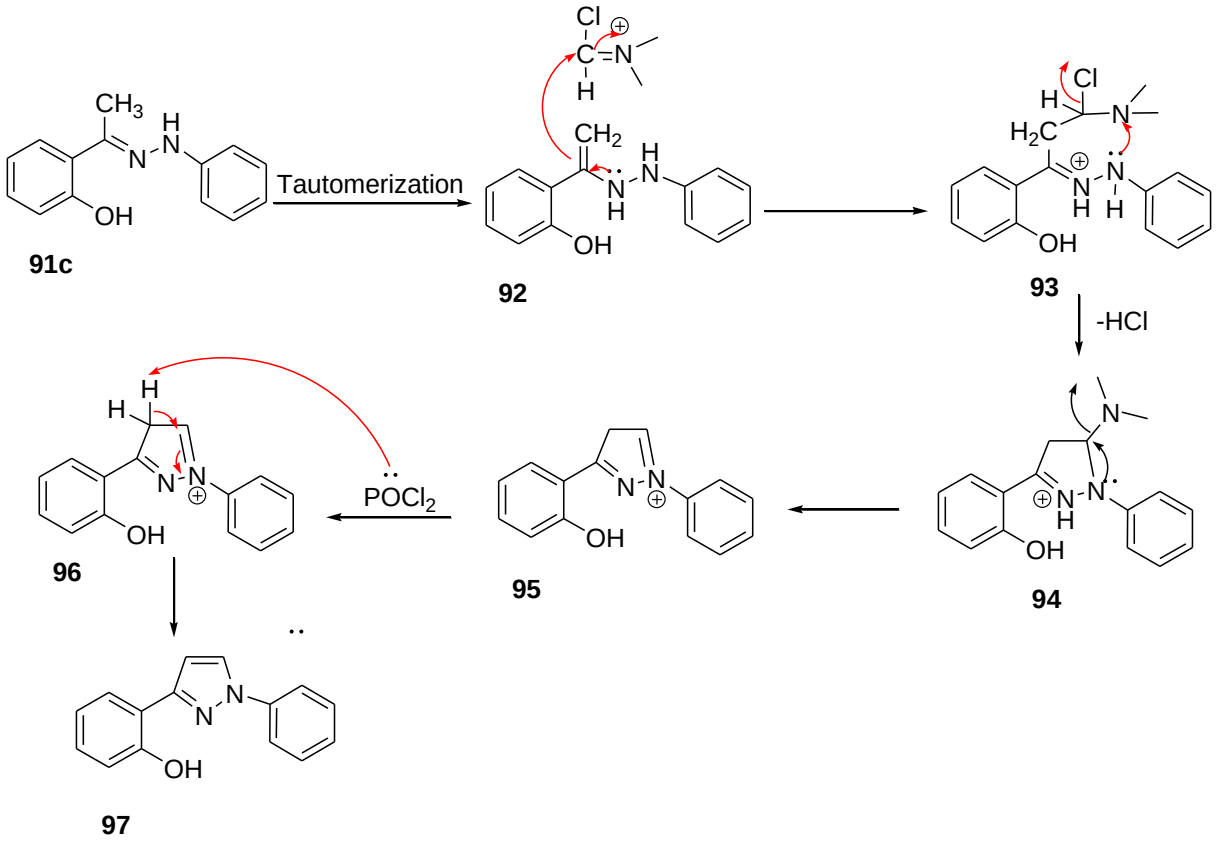

91c **92** **93** **94** **95** **96** **97**

Scheme 18: The proposed mechanism for synthesis of compound **97**

Target compound 3-aryl-1-phenyl-1H-pyrazole-4-carbaldehyde derivatives (**102a, b)** were synthesized according to the protocol developed by Archanad *et al.* (Jadhav *et al.*, 2020).

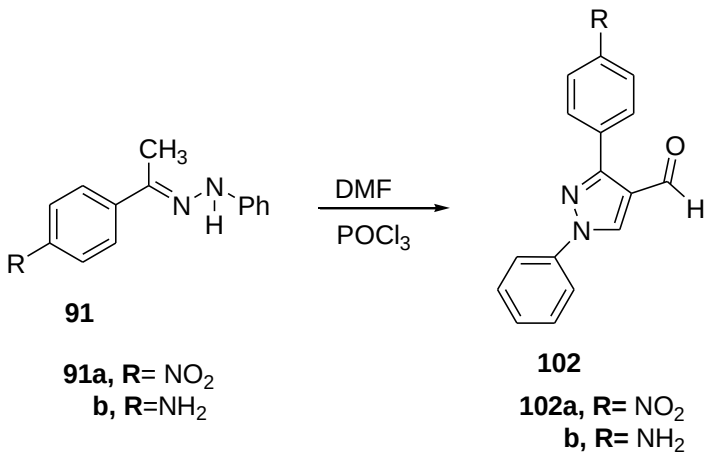

91

91a, R= NO_2
b, R=NH_2

102

102a, R= NO_2
b, R= NH_2

Scheme 19: Synthesis of 3-aryl-1-phenyl-*1H*-pyrazole-4-carbaldehyde derivatives **102a, b**

The derivatives of acetophenone phenyl hydrazone **91a, b** were reacted with Vilsmeier-Haack reagents which was produced by reacting DMF with $POCl_3$ in case of excess ratio. The reaction was refluxed for 4 hrs and neutralized with 10 % aqueous NaOH solution and the precipitate was filtered, and afforded compounds **102a** and **102b** with the high yield 84% and 86% respectively (Scheme 20**)**.

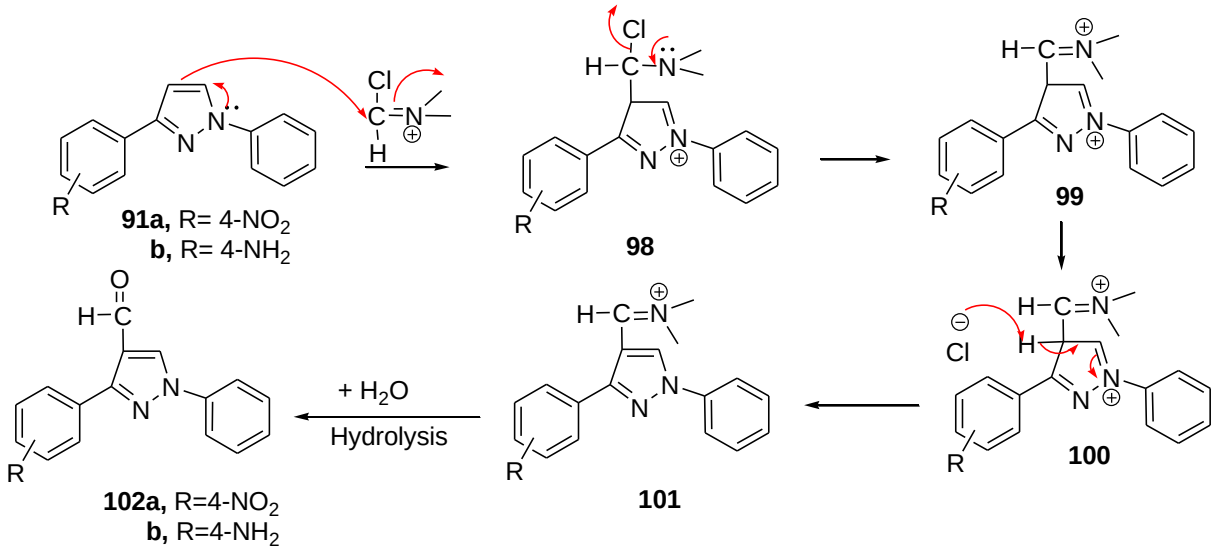

91a, R= 4-NO_2
b, R= 4-NH_2

102a, R=4-NO_2
b, R=4-NH_2

..

Scheme 20: The proposed mechanism for synthesis of compound **102a, b**

Physical constants and percentage yields of the synthesized compounds are presented in Table **1**. Progress of the reactions were monitored using TLC. The Rf values for each of the synthesized compounds were calculated (Table 1). The spots on the TLC plate were visualized using UV lamp at 254 nm.

Table 1: Physical characterization, percentage yield and Rf values of the synthesized compounds.

Compound	**Molecular formula**	**Color**	**M.p (°C)**	**Yield (%)**	**Rf** **n-hexane/ ethyl acetate (**3:2**)**
97	$C_{15}H_{12}N_2O$	Pink powder	115-120 °C	75	0.69
102a	$C_{16}H_{11}N_3O_3$	Red powder	129-132 °C	84	0.75
102b	$C_{16}H_{13}N_3O$	Old rose powder	170-175 °C	86	0.30 Ethyl acetate/n-hexane (9:1)

Target compounds **97, 102a** and **102b** were synthesized in high percentage of yield 75 %, 84 % and 86 % respectively. The synthesized compounds were readily soluble in dimethyl sulfoxide (DMSO), and partially soluble in methanol. Chemical structures of the synthesized compounds were fully characterized using ^{1}H and ^{13}C-NMR spectral data.

4. 2. Characterization of Synthesized Compounds

One-dimensional NMR experiments are fundamental in determining the resonance frequency of each ^{1}H or ^{13}C nucleus in the molecule, thus, both ^{1}H and ^{13}C NMR experiments were employed the most in elucidating the structures of the synthesized compounds in the current study. Moreover, the chemical shifts obtained gave important information about the nature and number of protons and carbons in the compounds of interest.

2-(1-phenyl-1H-pyrazol-3-yl) phenol (97)

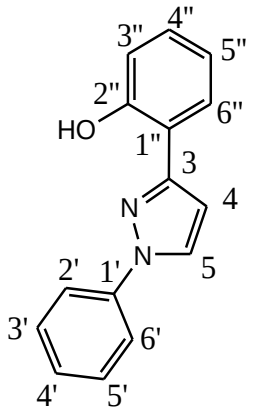

Compound **97** was obtained as Pink powder (75 %, yield) MP= 115-120 ^{o}C. R_f = 0.69 (*n*-hexane/ethyl acetate, (3:2) as eluent). ^{1}H NMR (400 MHz, DMSO) suggest aromatic proton at 7.89 (d, *J* = 7.9 Hz, 1H, H-6**''**), 7.54 (t, *J* = 7.7 Hz, 2H, H-3**'**, H-5**'**), 7.35 (d, *J* = 8 Hz, 2H, H-2**'**, H-6**'**), 7.24 (t, *J* = 7.7 Hz, 1H, H-4**'**), 7.18 (dd, *J* = 7.2 Hz, 1H, H-4**''**), 7.00 (t, *J* = 8.2 Hz, 1H, H-5**''**), 6.95 (d, *J* = 7.5 Hz, 1H, H-3**''**), 6.70 (d, *J* = 7.3 Hz, 1H, H-4) and peak at δ 8.63 (d, *J* = 7 Hz, 1H, H-5) shown pyrazole proton (Appendix 1**)**. The ^{13}C NMR (100 MHz, DMSO) along with DEPT-135 spectra of compound **97** possessed 13 carbons signals, including four quaternary and nine methines. Peak at δ 155.6 (phenol, C-2**''**), 151.6 (pyrazole,C-3), 139.5 (C-1**'**) and118.6 (C-1**''**) shown quaternary carbons and peak at δ 130.1 (C-4**''**), 129.8 (C-3**'**, C-5**'**), 129.4 (C-6**''**), 127.8 (C-5), 126.9 (C-4**'**), 119.8 (C-5**''**), 117.6 (C-2**'**, 6**'**), 117.0 (C-3**''**) and 107 (C-4) are shown methine carbons (Appendix 2). DEPT-135 (101 MHz, DMSO) spectrum of **97** showed 9 carbon signals (Appendix 3).

3-(-4-nitrophenyl)-1-phenyl-1H-pyrazole-4-carbaldehyde (102a)

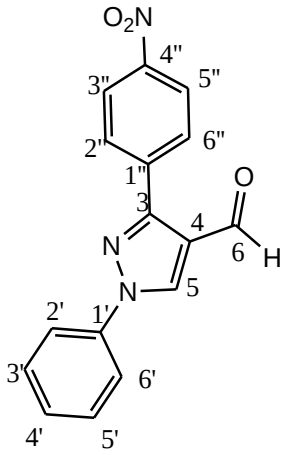

Compound **102a** was obtained as red powder (84 %, yield) MP= 129-132 ^{o}C. R_f = 0.75 (*n*-hexane/ethyl acetate, (3:2) as eluent). ^{1}H NMR (400 MHz, DMSO) suggest aromatic proton at δ 8.33 (d, *J* = 7.5 Hz, 2H, H-3’’, H-5’’), 8.17 (d, *J* = 7.4 Hz, 2H, H-2’’, H-6’’), 8.02 (d, *J* = 7.7, Hz, 2H, H-2’, H-6’), 7.52 – 7.02 (m, *J*= 8.1 Hz, 2H, H-3’, H-5’), 6.83 (t, *J* = 7.5 Hz, 1H, H-4’), A signal at δ 9.71 (s, 1H, H-6) shown aldehyde proton and peak at δ 8.22 (s, 1H, H-5) shown pyrazole proton (Appendix 4). The ^{13}C NMR (100 MHz, DMSO) spectrum of compound **102a** possessed 11 carbons signals, including one aldehyde, four quaternary and six methines. (Appendix **2**). A signal at δ 197.6 (C-6) shown aldehyde carbon, 150.3 (pyrazole,C-3), 148.4 (C-4’’), 141.7 (C-1’, C-1’’) and 113.7 (C-4) are quaternary carbons and signals at δ 130.0 (C-5), 129.4 (C-3’, C-5’), 126.1 (C-2’’, C-6’’), 124.2 (C-4’), 124.0 (C-3’’, C-5’’), and 120.3 (C-2’, C-6’) are methine carbons. **(**Appendix 5**)**.

3-(4-aminophenyl)-1-phenyl-1H-pyrazole-4-carbalddehyde (102b)

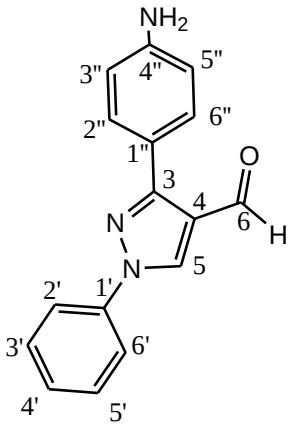

Compound **102b** was obtained as old rose powder with 86 % yield and MP= 170-175 ^{o}C. R_f = 0.3 (ethyl acetate/*n*-hexane, (9:1) as eluent). ^{1}H NMR (400 MHz, DMSO) suggest aromatic proton at 7.73 (t, *J*= 8 Hz, 2H, H-3', H-5'), 7.59 (d, *J* = 7.6 Hz, 2H, H-2', H-6'), 7.48 (t, *J*= 8.2 Hz, 1H, H-4'), 7.43 (d, *J* = 8.6 Hz, 2H, H-2'', H-6''), 7.30 (d, *J* = 7.4 Hz, 2H, H-3'', H-5''), 3.94 (s, 1H, NH), peak at δ 9.99 (s, 1H, H-6) shown aldehyde proton and peak at 8.00 (s, 1H, H-5) shown pyrazole proton (Appendix-7). The ^{13}C NMR (100 MHz, DMSO) spectrum of compound **102b** possessed 12 carbons signals, including one aldehyde carbon, five quaternary and six methines. A signal at δ 185.02 (C-6) shown aldehyde carbon, 153.9 (pyrazole,C-3), 151.9 (C-4''), 138.9 (C-1'), 122.6 (C-1'') and 118.5 (C-4) are quaternary carbons and signal at δ 130.1 (C-5), 129.9 (C-3', C-5'), 129.4 (C-2'', C-6''), 128.2 (C-4'), 119.69 (C-2', C-6') and 119.4 (C-3'', C-5'') are methine carbons. **(**Appendix 8**)**. DEPT-135 (101 MHz, DMSO) spectrum of **102b** showed 7 carbon signals (Appendix 9).

4.3. Antibacterial Activity of Synthesized Compounds

All synthesized compounds were tested for their *in-vitro* antibacterial activity against Gram-negative bacterial species (*E. coli and P. aeruginosa*) and Gram-positive bacteria (*S. pyogenes* and *S. aureus*) by disk diffusion assay at different concentration (100, 50 and 25 mg/mL). Ceftazidime was used as positive control. The zone of inhibition values indicated that all the synthesized compounds at three different concentration exhibited a varied range of 7.5-25 mm of antibacterial activities against all the tested bacterial strains (Table 2). Among synthesized compounds, compound **102a** showed modern inhibitory activity against Gram-negative, *E. coli* with 18.75±1.06 mm zone of inhibition at 100 mg/mL, *S. pyogenes* with 25±0.707 mm zone of inhibition at 100 mg/mL and *S. aureus* with 12.5±0.707 mm zone of inhibition at 100 mg/mL. Compound **102b** showed high inhibitory activity against *S. aureus* with 15.5±0.707 mm zone of inhibition at 100 mg/mL. Compound **97** showed less antibacterial activity against four tested bacterial strains. All the synthesized compounds showed high inhibitory activity against Gram-positive, *S. aurues* at 100 mg/mL with 15.5±0.707 – 7.5±0.707 mm zone of inhibition against tested bacterial strains.

Table 2: Zone of bacterial growth inhibition diameter (mm)

Compounds	**Conc.**	**Inhibition diameter (mm)**±SD			
		Gram negative		**Gram positive**	
		E. coli	***P*. aeruginosa**	***S. pyogenes***	***S. aureus***
97	100mg/mL	6.20±0.282	6.15±0.212	6.00±0.707	9.50±1.414
	50mg/mL	6.10±0.141	6.10±0.141	6.00±0.707	8.50±0.707
	25mg/mL	6.00±0.011	6.00±0.707	6.00±0.707	7.50±0.040
102a	100mg/mL	18.75±1.06	12.5±0.707	25.0±0.707	12.5±0.707
	50mg/mL	14.5±0.707	9.5±0.707	22.0±1.41	11.0±1.41
	25mg/mL	6.65±0.212	8.75±0.353	18.5±0.707	10.25±1.06
102b	100mg/mL	6.45±0.495	6.00±0.707	6.15±0.070	15.5±0.707
	50mg/mL	6.15±0.212	6.00±0.707	6.05±0.070	15.0±0.707
	25mg/mL	6.00±0.707	6.00±0.707	6.00±0.040	14±0.495
Ceftazidime	30µg/mL	26.0±1.414	23.5±2.12	15.5±2.121	13.5±0.707

SD= standard Deviation

4.4 Antioxidant Activity of Synthesized Compounds

DPPH is a simple method and used to determine the radical scavenging power of an antioxidant by measuring the decrease in the absorbance of DPPH at 517 nm. In the DPPH scavenging assay, of synthesized compounds were investigated for their free radical scavenging activity via their reaction with the stable DPPH radicals. The reduction of the DPPH was followed *via* the decrease in absorbance at 517 nm. Synthesized compounds significantly reduced the DPPH. The DPPH radical scavenging activities (%) of all synthesized compounds **97**, **102a** and **102b** were found to be 81 %, 72.2 % and 85.1 % respectively at 100 µg/ml (Table 3) and ascorbic

acid was found to be 92.2 %. It was observed that the DPPH scavenging activity increased with increasing concentration of the samples in the assay. For the various concentrations, compound **102b** exhibited slightly highest percent inhibition of the DPPH with IC_{50} of **1.805** as compared to the other synthesized compounds. The positive control, ascorbic acid showed maximum scavenging effect at very high concentration with IC_{50} of **1.636** (Figure 9).

Table 3: % radical scavenging activity of synthesized compounds and positive reference

Conc. (µg/ml)	Compound code							
	97		**102a**		**102b**		**Ascorbic acid**	
	A	% S.A	A	% S.A	A	% S.A	A	% S.A
12.5	0.145	73.1	0.21	61.1	0.12	77.7	0.049	90.9
25	0.122	77.4	0.18	66.6	0.10	81.4	0.048	91.1
50	0.112	79.2	0.16	70.4	0.09	83.3	0.045	91.6
100	0.101	81	0.15	72.2	0.08	85.1	0.042	92.2
IC_{50}		1.90		2.16		1.805		1.636

Conc.-Concentration, A- Absorbance, % S.A- Percentage scavenging activity

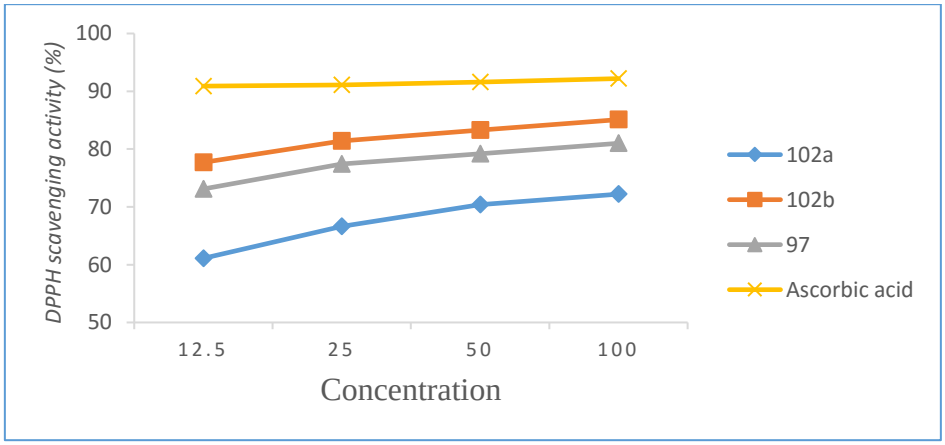

Figure 9: DPPH scavenging activity (%) of synthesized compounds and ascorbic acid

4.5. *In silico* Molecular Docking Study

Molecular docking studies are generally employed to investigate the binding energy and to further validate the molecular mechanisms for ligands at the active site of a protein. To understand the binding mode of the ligands, all the synthesized compounds were subjected to molecular docking studied against selected proteins viz. *S. aureus tyrosyl-tRNA synthetase* (PDB ID 1JIJ) using Auto-dock Version 4.2.6

In this study, the molecular docking analysis of the synthesized compounds **97, 102a-b** was carried out to investigate their binding interaction within the binding sites of *S. aureus tyrosyl-tRNA synthetase* and the results were compared with standard anti-bacterial agent in class Ceftazidime. The synthesized compounds **97, 102a-b** were found to have minimum binding energy ranging from – 8.0 to – 8.4 kcal/mol (Table 4). Comparing with Ceftazidime (– **8.8** kcal/mol), the synthesized compounds **97, 102a-b** have shown comparable binding affinity and similar residual interaction profile with many amino acid residues. The compounds **97** (– 8.3 kcal/mol), **102a** (– 8.4 kcal/mol), and **102b** (– 8.0 kcal/mol), have shown comparable binding affinity and similar residual amino acid binding within the binding pockets of 1JIJ as compared to Ceftazidime (Figure 11-14). The *in silico* interaction results have shown that the synthesized compounds, **97, 102a-b** have comparable binding affinity, among them **102a** has shown the best binding score (– 8.4 kcal/mol). Based on the molecular docking analysis results, all the synthesized compounds have shown comparable residual interactions, as well as all the docking results are in good agreement with *in-vitro* analysis. Hence, these compounds might prove to be comparable anti-bacterial agents with Ceftazidime. The binding affinity, H-bond and residual interaction of all the synthesized compounds are summarized in Table 4.

Table 4: Molecular docking results of novel synthesized compounds against *S. aureus tyrosyl-tRNA synthetase* (PDB ID 1JIJ)

S. No	Ligands	Binding Affinity (kcal/mol)	H-bond	Residual interactions	
				Hydrophobic, Electrostatic and Others	Van der Waals
102a	$C_{16}H_{11}N_3O_3$	**– 8.4**	ASP-40:HN, TYR-170:HH, ASP-195:OD1, GLY-49:O	Electrostatic-Pi-anion-ASP-195:OD1 Electrostatic-Pi-anion-ASP-195:OD2 Hydrophobic-Pi-Alkyl-ALA-39	LEU-223, ASP-80, GLY-193, GLN-174, GLY-49, HIS-50, GLY-38, PHE-54, GLN-196, PRO-53
97	$C_{15}H_{12}N_2O$	**– 8.3**	GLY-38:HN, ALA-39:CA, ASP-80:OD2, ASP-40:HN	Electrostatic-Pi-anion-ASP-40:OD1 Hydrophobic-Pi-Alkyl-LEU-70 Hydrophobic-Pi-Alkyl-ALA-39	ASP-80, TYR-170, GLN-174, THR-75, ASN-124, ASP-177, TYR-36, HIS-50, THR-42, ALA-39, GLN-196, ILE-200, CYS-37, GLN-190
102b	$C_{16}H_{13}N_3O$	**– 8.0**	GLY-193:HN, TYR-36:OH, ASP-177:OD1, GLY-192:CA	Electrostatic-Pi-cation-LYS-84:NZ	THR-42, ARG-88, ASP-80, TYR-170, GLN-190, ASP-40, ALA-39, LEU-70, GLY-192, GLN-196, GLY-38, CYS-37, GLN-174

	Ceftazidime ($C_{22}H_{22}N_6O_7S_2$)	**– 8.8**	ASP-40:HN, ARG-88:HH11, ARG-88:HH12(DHA = 107.246), ARG-88:HH12(DHA = 114.197), GLY-193:HN, GLN-196:HE21, ALA-39:CA, LYS-84:CE, HIS-47:NE2	Electrostatic-Attractive Charge-LYS-84:NZ Electrostatic-Attractive Charge-ARG-88:NH1 Pi-Sulfur-HIS-47 Pi-Sulfur-HIS-50 Hydrophobic-Alkyl-ALA-43 Hydrophobic-Pi-Alkyl-HIS-47 Hydrophobic-Pi-Alkyl-TRP-241	ALA-39, ASP-80, ASN-124, LEU-70, TYR-170, THR-75, GLY-72, GLN-174, GLY-38, THR-42, ASP-195, HIS-47, PRO-53, CYS-37, GLY-192, VAL-191

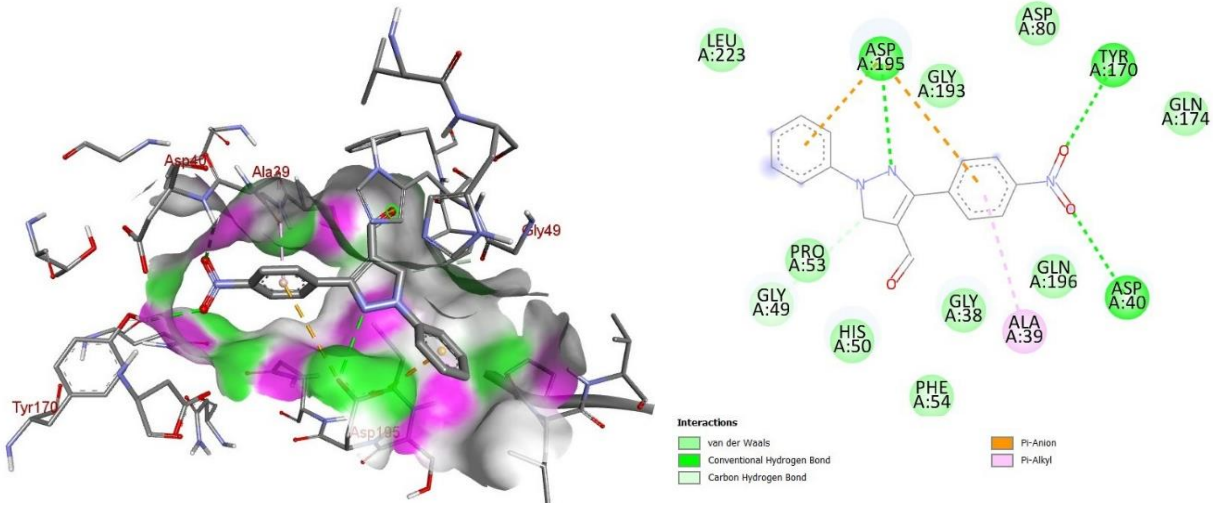

Figure 10: The 2D and 3D binding interactions of compound **102a** against *S. aureus tyrosyl-tRNA synthetase* (PDB ID: 1JIJ). Hydrogen bond between compounds and amino acids are shown as green dash lines, π-anion interactions are shown as orange lines. Hydrophobic interactions are shown as pink lines.

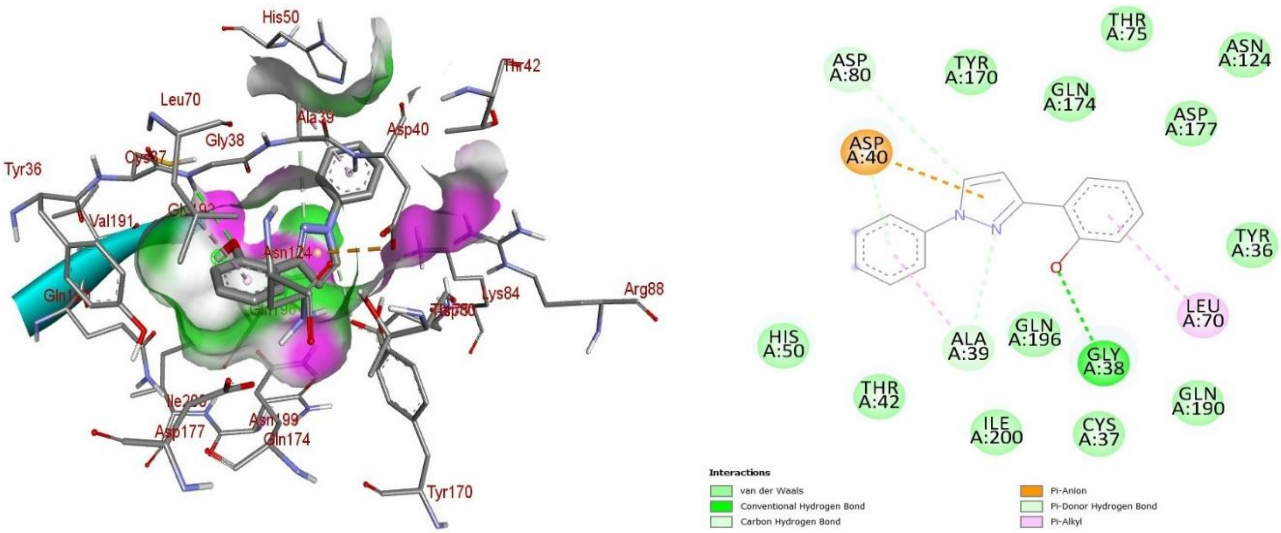

Figure 11: The 2D and 3D binding interactions of compound **97** against *S. aureus tyrosyl-tRNA synthetase* (PDB ID: 1JIJ). Hydrogen bond between compounds and amino acids are shown as green dash lines, π-anion interactions are shown as orange lines. Hydrophobic interactions are shown as pink lines.

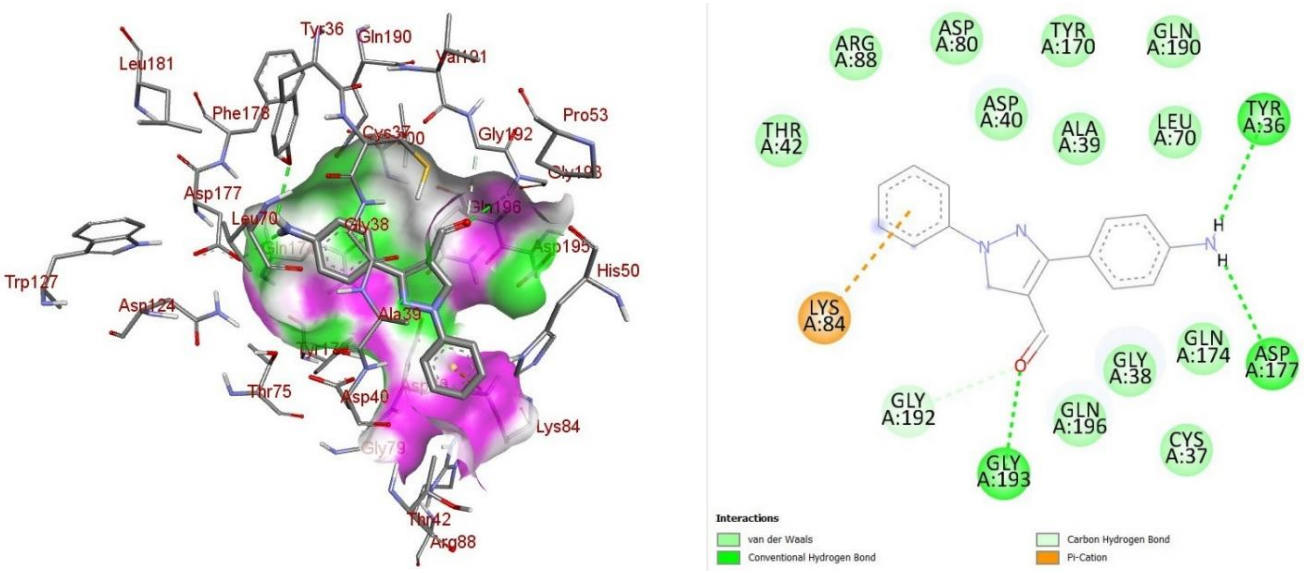

Figure 12: The 2D and 3D binding interactions of compound **102b** against *S. aureus tyrosyl-tRNA synthetase* (PDB ID: 1JIJ). Hydrogen bond between compounds and amino acids are shown as green dash lines, π-cation interactions are shown as orange lines.

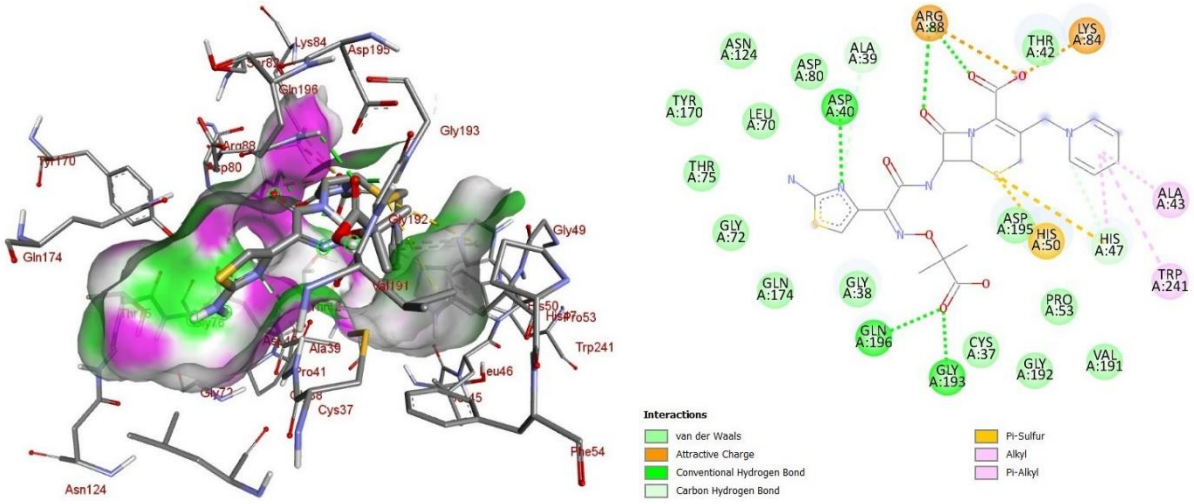

Figure 13: The 2D and 3D binding interactions of standard drug **Ceftazidime** against *S. aureus tyrosyl-tRNA synthetase* (PDB ID: 1JIJ). Hydrogen bond between compounds and amino acids are shown as green dash lines, Electrostatic interactions are shown as orange lines. Hydrophobic interactions are shown as pink lines.

To understand the binding mode of the ligands, all the synthesized compounds were subjected to molecular docking studied against selected proteins viz. Human myeloperoxidase (PDB ID 1DNU) using Auto-dock Version 4.2.6.

In this study, the molecular docking analysis of the synthesized compounds **97, 102a-b** was carried out to investigate their binding interaction within the binding sites of Human *myeloperoxidase* and the results were compared with standard anti-bacterial agent in class Ceftazidime and antioxidant ascorbic acid. The synthesized compounds **97, 102a-b** were found to have minimum binding energy ranging from – 8.5 to – 9.3 kcal/mol (Table 5). Comparing with Ceftazidime (– 9.4 kcal/mol) and ascorbic acid (– 8.1 Kcal/mol) the synthesized compounds **97, 102a-b** have shown comparable binding affinity and similar residual interaction profile with many amino acid residues. The compounds **97** (– 8..5 kcal/mol), **102a** (– 9.3 kcal/mol), and **102b** (– 8.8 kcal/mol), have shown comparable binding affinity and similar residual amino acid binding within the binding pockets of 1DNU as compared to Ceftazidime and ascorbic acid (Figure 15-19). The *in silico* interaction results have shown that the synthesized compounds, **97, 102a-b** have comparable binding affinity, among them **102a** has shown the best binding score (– 9.3 kcal/mol). Based on the molecular docking analysis results, all the synthesized compounds have shown comparable residual interactions, as well as all the docking results are in good agreement with *in-vitro* analysis. Hence, these compounds might prove to be comparable antioxidant agents with Ceftazidime. The binding affinity, H-bond and residual interaction of all the synthesized compounds are summarized in Table 5.

Table 5: Molecular docking results of novel synthesized compounds against Human *myeloperoxidase* (PDB ID 1DNU)

S. No	Ligands	Binding Affinity (kcal/mol)	H-bond	Residual interactions	
				Hydrophobic, Electrostatic and Others	**Van der Waals**
102a	$C_{16}H_{11}N_3O_3$	**-9.3**	Gln-91, Thr-100, Arg-333	Electrostatic-Pi-cation-Arg-239:NH2 Electrostatic-Pi-cation-ARG-333:NH1 Pi-Sulfur-MET-87 Hydrophobic-Amide-Pi Stacked-GLY-90:C,O; GLN-91:N	PHE-332, GLY-335, ASP-94, ASP-98, ILE-339, HIS-336, HIS-95, GLU-242, THR-329, PHE-99
97	$C_{15}H_{12}N_2O$	**-8.5**	PHE-332:O	Electrostatic-Pi-cation-ARG-239:NH2 Electrostatic-Pi-anion-ASP-94:OD2 Hydrophobic-Pi-Sigma-GLN-91 Pi-Sulfur-MET-87 Hydrophobic-Pi-Pi T-Shaped-HIS-95 Hydrophobic-Pi-Pi T-Shaped-HIS-336 Hydrophobic-Amide-Pi Stacked-GLY-90:C,O; GLN-91:N Hydrophobic-Pi-Alkyl-ARG-333	LEU-338, GLY-335, THR-329

102b	$C_{16}H_{13}N_3O$	**-8.8**	ARG-333:HH12, ARG-424:HE, ASP-98:OD2, ASP-94:OD1	Electrostatic-Pi-cation-ARG-239:NH2 Electrostatic-Pi-cation-ARG-333:NH1 Electrostatic-Pi-anion-ASP-94:OD2 Hydrophobic-Pi-Alkyl-ARG-239	PHE-366, PHE-99, GLU-242, PHE-407, GLU-102, THR-100, PHE-332, THR-329
	Ceftazidime ($C_{22}H_{22}N_6O_7S_2$)	**-9.4**	ASN-162:HD21, ARG-31:HN, ARG-323:HH12 (DHA = 145.523), ARG-323:HH12 (DHA = 104.57), ARG-323:HH22, ASP-321:OD1, VAL-30:CA, ILE-160:O	Hydrophobic-Alkyl-ALA-28 Hydrophobic-Alkyl-ALA-152 Hydrophobic-Alkyl-CYS-153 Hydrophobic-Pi-Alkyl-VAL-30 Hyd. Bond; Electrostatic-Salt Bridge-Attractive Charge-ARG-323:HH22	LEU-33, ASN-162, ILE-160, PRO-34, ALA-35, VAL-30, ARG-31, PHE-29, THR-159, ILE-160, CYS-153
	Ascorbic Acid ($C_6H_8O_6$)	**-8.1**	GLN-91:HE21, THR-100:HN, ARG-239:HH21, ARG-333:HE, ARG-333:HH11, ARG-239:CD, ARG-333:CA	Electrostatic-Pi-anion-ASP-94:OD2 Hydrophobic-Pi-Alkyl-ARG-333	HIS-336, PHE-332, PHE-99, THR-329, HIS-95, ASP-98

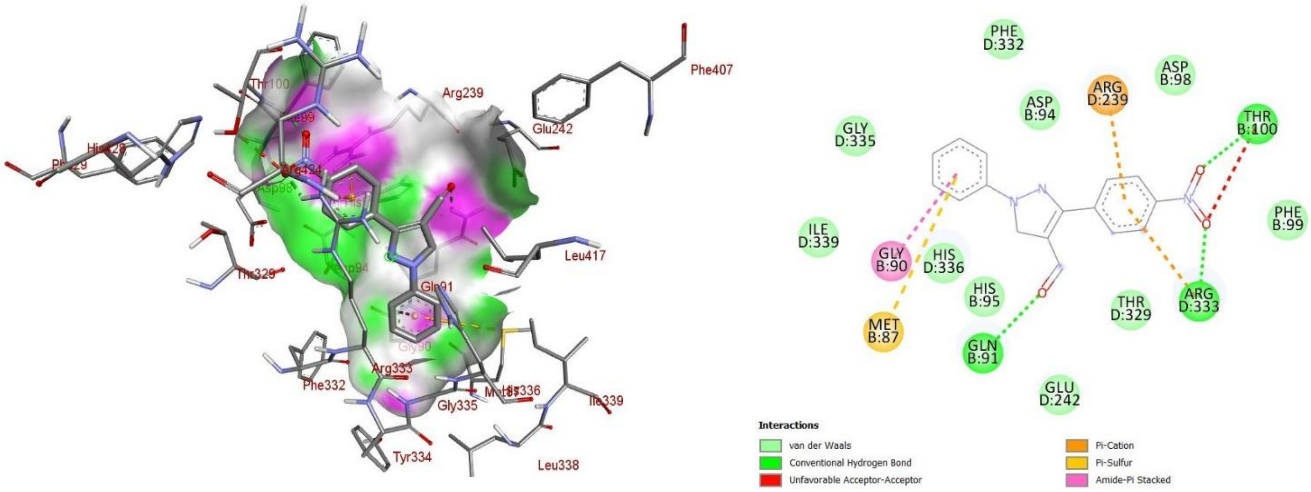

Figure 14: The 2D and 3D binding interactions of compound **102a** against Human *myeloperoxidase* (PDB ID: 1DNU). Hydrogen bond between compounds and amino acids are shown as green dash lines, π-cation/ π-sulfur interactions are shown as orange lines. Hydrophobic interactions are shown as pink lines.

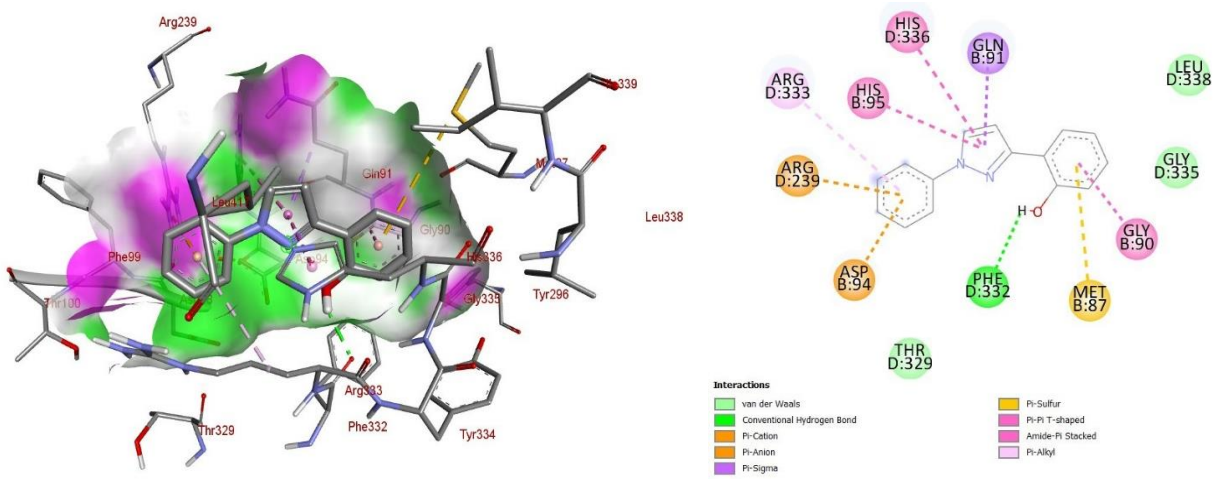

Figure 15: The 2D and 3D binding interactions of compound **97** against Human *myeloperoxidase* (PDB ID: 1DNU). Hydrogen bond between compounds and amino acids are shown as green dash lines, π-anion/ π-cation/ π-sulfur interactions are shown as orange lines. Hydrophobic interactions are shown as pink lines.

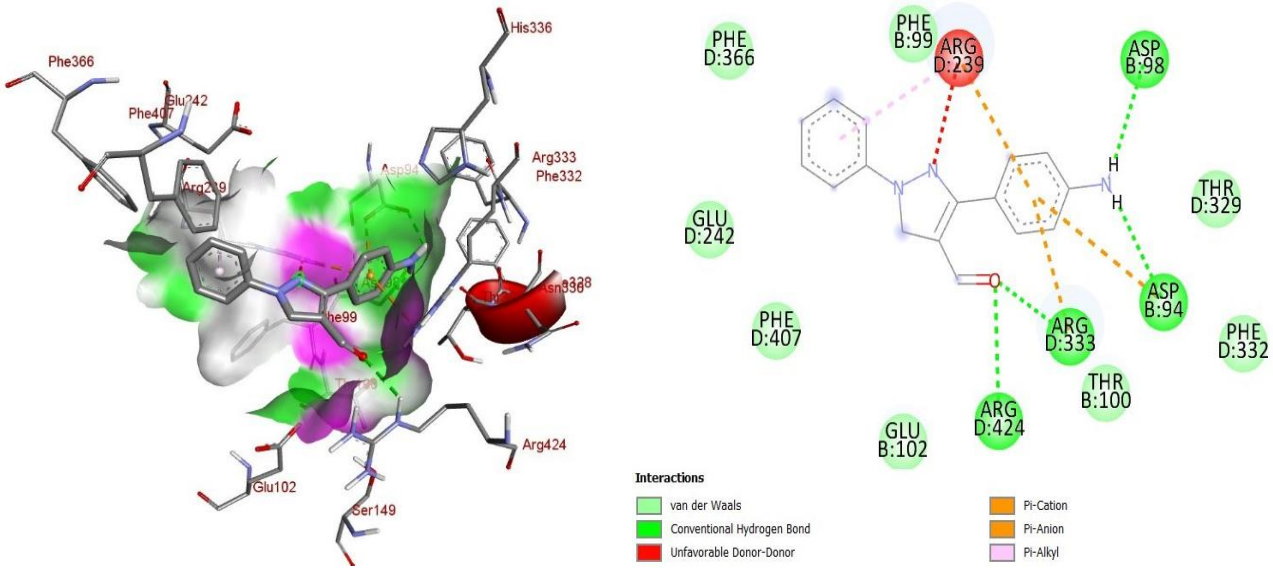

Figure 16: The 2D and 3D binding interactions of compound **102b** against Human *myeloperoxidase* (PDB ID: 1DNU). Hydrogen bond between compounds and amino acids are shown as green dash lines, π-anion/ π-cation interactions are shown as orange lines. Hydrophobic interactions are shown as pink lines

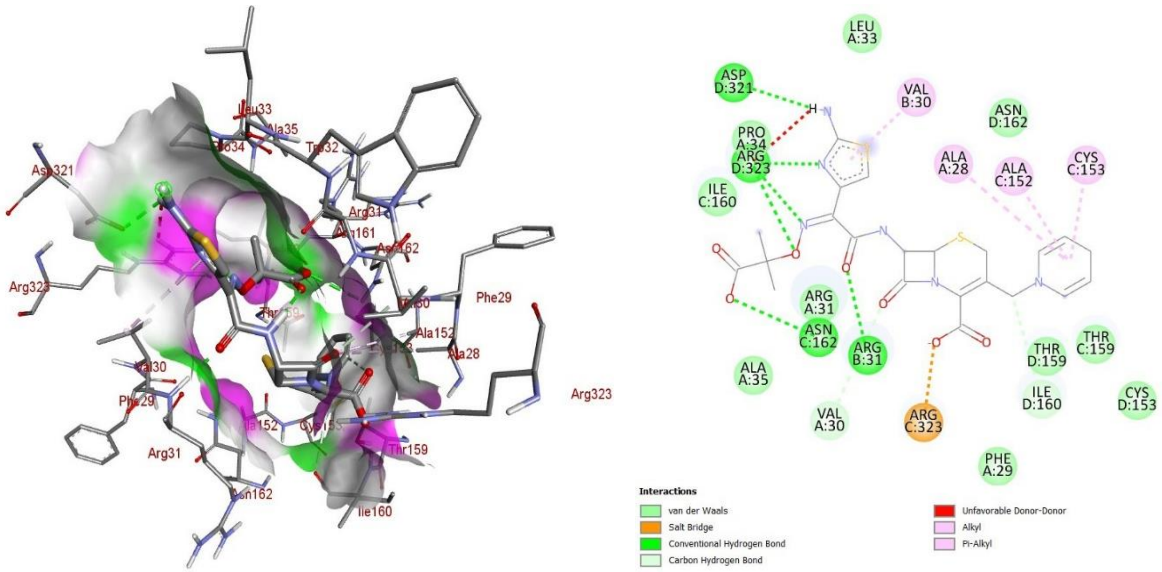

Figure 17: The 2D and 3D binding interactions of standard drug **Ceftazidime** against Human *myeloperoxidase* (PDB ID: 1DNU). Hydrogen bond between compounds and amino acids are shown as green dash lines, Electrostatic interactions are shown as orange lines. Hydrophobic interactions are shown as pink lines.

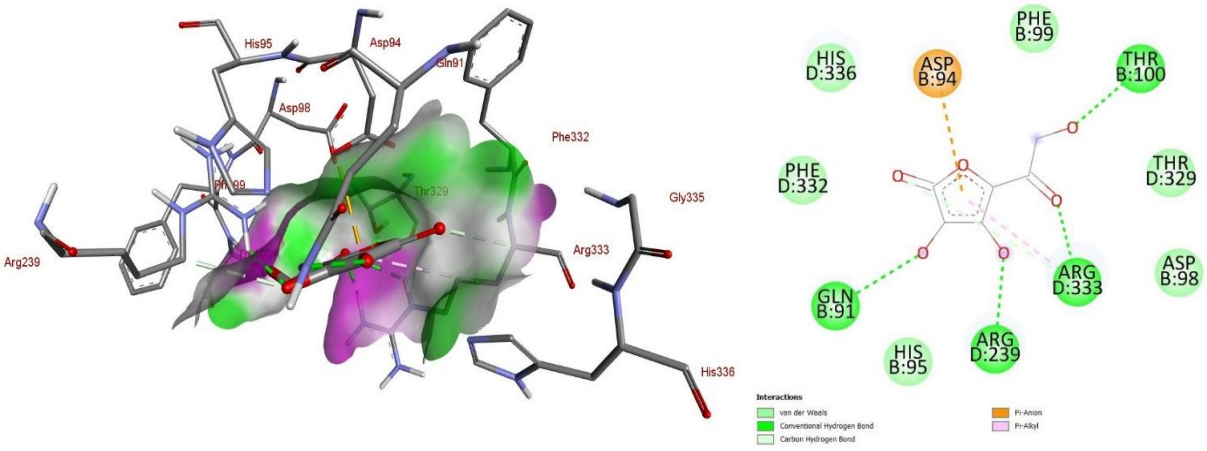

Figure 18: The 2D and 3D binding interactions of standard drug ascorbic acid against Human *myeloperoxidase* (PDB ID: 1DNU). Hydrogen bond between compounds and amino acids are shown as green dash lines, π-anion interactions are shown as orange lines. Hydrophobic interactions are shown as pink lines.

4.6. *In Silico* Pharmacokinetics (Drug-likeness), ADME and Toxicity Analysis

The drug likeness of the synthesized compounds were characterized according to 'Lipinski's rule of five'. As per the Lipinski's rule, the potential molecules should have the physicochemical properties like, (i) less than 5 hydrogen-bond donors (HBDs), (ii) less than 10 hydrogen-bond acceptors (HBAs), (iii) a molecular mass less than 500 Da and (iv) log P not greater than 5 and (v) total polar surface area (TPSA) should not be > 140 Å. The SwissADME computed results showed that all the synthesized compounds **97, 102a-b** in the present study are satisfying the Lipinski's rule of five with zero violations (Table 6). Hence, all the synthesized compounds might be candidates for further *in-vivo* antibacterial studies.

Table 6: Drug-likeness predictions of compounds, computed by SwissADME

S. No.	Ligands	M.W (g/mol)	NHD	NHA	NRB	TPSA ($A^{\circ 2}$)	Log *P* (iLOGP) Lipophilicity	Log *S* (ESOL) Water Solubility	Synthetic Accessibility	Lipinski's rule of five with zero violations
102a	$C_{16}H_{11}N_3O_3$	293.28	0	4	4	80.71	2.10	-3.76	2.46	0
97	$C_{15}H_{12}N_2O$	236.27	1	2	2	38.05	2.74	-3.89	2.10	0
102b	$C_{16}H_{13}N_3O$	263.29	1	2	3	60.91	2.13	-3.37	2.34	0
	Ceftazidime ($C_{22}H_{22}N_6O_7S_2$)	546.58	3	9	10	244.76	-2.68	-1.37	5.25	2
	Ascorbic Acid ($C_6H_8O_6$)	176.12	4	6	2	107.22	-0.31	0.23	3.47	0

NHD = number of hydrogen donors, NHA = number of hydrogen acceptors, NRB = number of rotatable bonds, and TPSA = total polar surface area.

Evaluation of ADMET properties of newly synthesized compounds is pivotal in drug discovery. The skin absorption of molecules is indicated by skin permeability value (Kp) in cm/s. The more negative the value of logKp the less the skin absorption. The skin permeability, Kp, values of all molecules (-5.47 to -6.25 cm/s) comparable to ascorbic acid (- 8.54 cm/s) and Ceftazidime (-11.23 cm/s) inferring low skin permeability. In addition to that, Absorption and distribution of drug molecules are measured by gastrointestinal (GI) and Blood brain barrier (BBB) permeation. The Swiss ADME prediction parameters have shown that none of the compounds has Blood brain barrier (BBB) permeation. Drug metabolism has been mainly governed by a range of cytochromes (CYP's). Among them CYP1A2, CYP2C19, CYP2C9, CYP2D6 and CYP3A4 are paramount for biotransformation of drug molecules. The *in silico* computed results of Absorption, Distribution, Metabolism, and Excretion (ADME) for synthesized compounds **97, 102a-b,** Ceftazidime and ascorbic acid are given in Table 7.

Table 7: ADME predictions of compounds, computed by SwissADME and PreADMET

S. No.	Ligands	Skin Permeation Value (Log *Kp*) cm/s	GI Absorption	BBB Permeability	Inhibitor Interaction					
					Pgp substrate	CYP1A2 inhibitor	CYP2C19 inhibitor	CYP2C9 inhibitor	CYP 2D6 inhibitor	CYP 3A4 inhibitor
102a	$C_{16}H_{11}N_3O_3$	-6.07	High	No	No	Yes	Yes	Yes	No	No
97	$C_{15}H_{12}N_2O$	-5.47	High	Yes	No	Yes	Yes	No	Yes	No
102b	$C_{16}H_{13}N_3O$	-6.25	High	Yes	No	Yes	Yes	No	Yes	No
	Ceftazidime ($C_{22}H_{22}N_6O_7S_2$)	-11.23	Low	No	No	No	No	No	No	No
	Ascorbic Acid ($C_6H_8O_6$)	-8.54	High	No	No	No	No	No	No	No

GI = gastrointestinal, BBB = blood brain barrier, P-gp = P-glycoprotein, and CYP = cytochrome-P

Acute toxicity predictions result such as LD_{50} values and toxicity class classification [1 (toxic) to 6 (non-toxic)] reveals that none of the ligands has shown acute toxicity and were found better than Ceftazidime. All synthesized compounds **97, 102a and 102b** have shown toxicity class classification **4** (harmful if swallowed). The toxicological prediction gives results of endpoints such as Hepatotoxicity, Carcinogenicity, mutagenicity, immunogenicity, and cytotoxicity. Pro-Tox II and OSIRIS property explorer prediction analysis have shown in Table 8. Hence, based on ADMET prediction analysis, compounds **97, 102a-b** have shown good toxicity predictions.

Table 8: Toxicity prediction of compounds, computed by ProTox-II and OSIRIS property explorer

S. No.	Ligands	LD_{50} (mg/Kg)	Toxicity Class	Organ Toxicity					
				Hepatotoxicity	Carcinogenicity	Immunotoxicity	Mutagenicity	Cytotoxicity	Irritant
102a	$C_{16}H_{11}N_3O_3$	670	4	Active	Active	Inactive	Active	Inactive	No
97	$C_{15}H_{12}N_2O$	1400	4	Active	Active	Inactive	Active	Inactive	No
102b	$C_{16}H_{13}N_3O$	670	4	Active	Active	Inactive	Active	Inactive	No
	Ceftazidime ($C_{22}H_{22}N_6O_7S_2$)	10000	6	Inactive	Inactive	Inactive	Inactive	Inactive	No
	Ascorbic Acid ($C_6H_8O_6$)	3367	5	Inactive	Inactive	Inactive	Inactive	Inactive	No

4.7. DFT Study

4.7.1. Molecular Geometry

The optimized structures of the title compounds **97, 102a, b** along with force on nucleus i.e. 0.000 are shown in Figure 19. The global minimum energy obtained by the DFT structure optimization procedure for the investigated compounds is summarized in Table 9. The bond lengths, Mulliken Charges, Electrostatic Potential Surface, 2D Contour and HOMO-LUMO Structures are shown in Figure 20-25.

4.7.2. Frontier Molecular Orbital Analysis

The excitation energy of a molecule can be calculated by finding the energy difference between the Highest Occupied Molecular Orbital (HOMO) and the Lowest Unoccupied Molecular Orbital (LUMO), and it is an excellent indicator of electronic transition absorption in the molecular systems. These molecular orbitals provide insight into the reactivity nature and the physical and structural properties of molecules. The positive and negative phase was represented

in red and green color in the figures. The HOMO, LUMO energies and the energy gap for the investigated compounds were calculated using B3LYP/6-31G (d,p) method. Owing to the HOMO–LUMO orbital interaction, LP-LP, and LP-bond pair type interactions were observed to be predominant in the investigated compounds according to the molecular orbital theory. The calculated HOMO, LUMO energies, the energy gap and dipole moment are shown in Table 9. The molecular orbital analysis for the investigated compounds based on their optimized geometry indicates that the frontier molecular orbitals are mainly composed of π type-atomic orbitals. An electronic system with larger HOMO-LUMO gap should be less reactive than one with a smaller gap. Moreover, the HOMO–LUMO energy gap clearly explains the eventual charge transfer taking place within the molecule. The power of an electronegative atom in a compound to attract an electron towards it was introduced by Pauling. The parameters such as hardness (η), ionization potential (I), electronegativity (χ), chemical potential (μ), electron affinity (A), global softness (σ) and global electrophilicity (ω) are calculated.

The ionization energy (IE) can be expressed through HOMO orbital energies, and electron affinity (EA) can be expressed through LUMO orbital energies. The hardness (η) corresponds to the gap between HOMO and LUMO orbital energies. The hardness has been associated with the stability of the chemical system. All the calculated values of quantum chemical parameters of the investigated molecules using the B3LYP method with 6-31G (d,p) basis set are summarized in Table 9

From the results in Table 9 it is clear that for the molecules investigated **102b** has the minimum energy gap of 3.6742 eV and **97** has the maximum energy gap of 4.7059 eV. These facts further indicate that **102b** would be highly reactive among all the synthesized compounds.

Table 9: The various Quantum chemical parameters of synthesized compounds **97, 102a-b**

S. No.	Compounds	Optimized energy (Hartree)	E_{HOMO} (eV)	E_{LUMO} (eV)	Energy Gap ΔE (eV)	Electro negativity χ (eV)	Pauling Hardness η (eV)	Global Softness σ (eV^{-1})	Global Electrophilicity ω (eV	Dipole Moment (Debye)
97	$C_{15}H_{12}N_2O$	-763.55437	-5.6863	-0.9804	4.7059	3.33335	2.35295	0.42499	2.36112	3.1852982
102a	$C_{16}H_{11}N_3O_3$	-1006.1577	-6.5605	-2.4572	4.1032	4.50885	2.05165	0.48741	4.95448	9.8504022
102b	$C_{16}H_{13}N_3O$	-857.01605	-4.9969	-1.3227	3.6742	3.1598	1.8371	0.54434	2.71742	2.6480827

4.7.3. Mulliken Population Analysis

The Mulliken population analysis of the title compounds was performed at DFT-B3LYP/6-31G (d,p) level to obtain the values of the atomic charges and the results are shown in Figure 21. All calculated values indicate the extensive charge delocalization in the investigated molecules. The positive charges are localized over the hydrogen atoms.

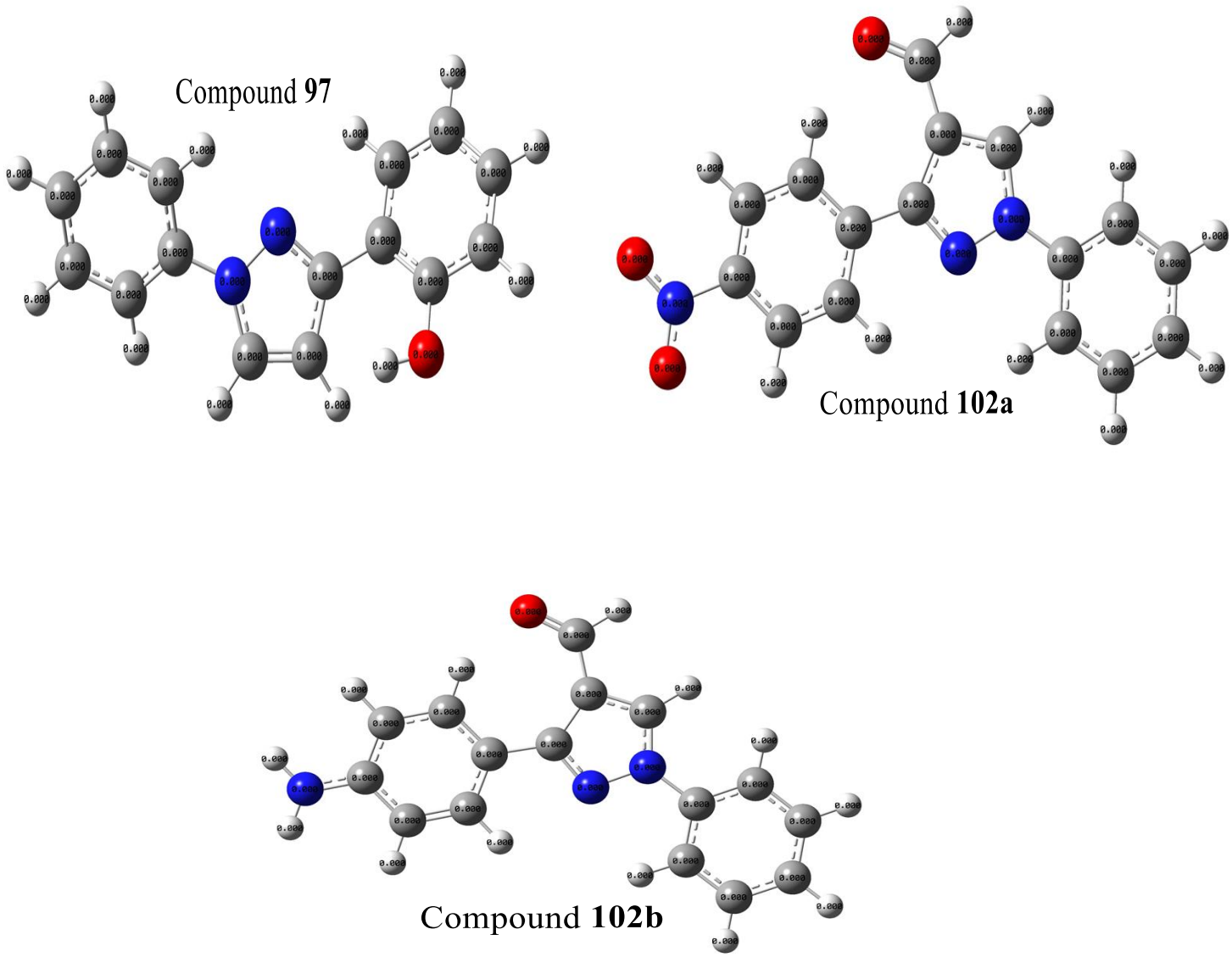

Figure 19: Optimized Structures of Compounds **97, 102a-b** depicting force on nucleus.

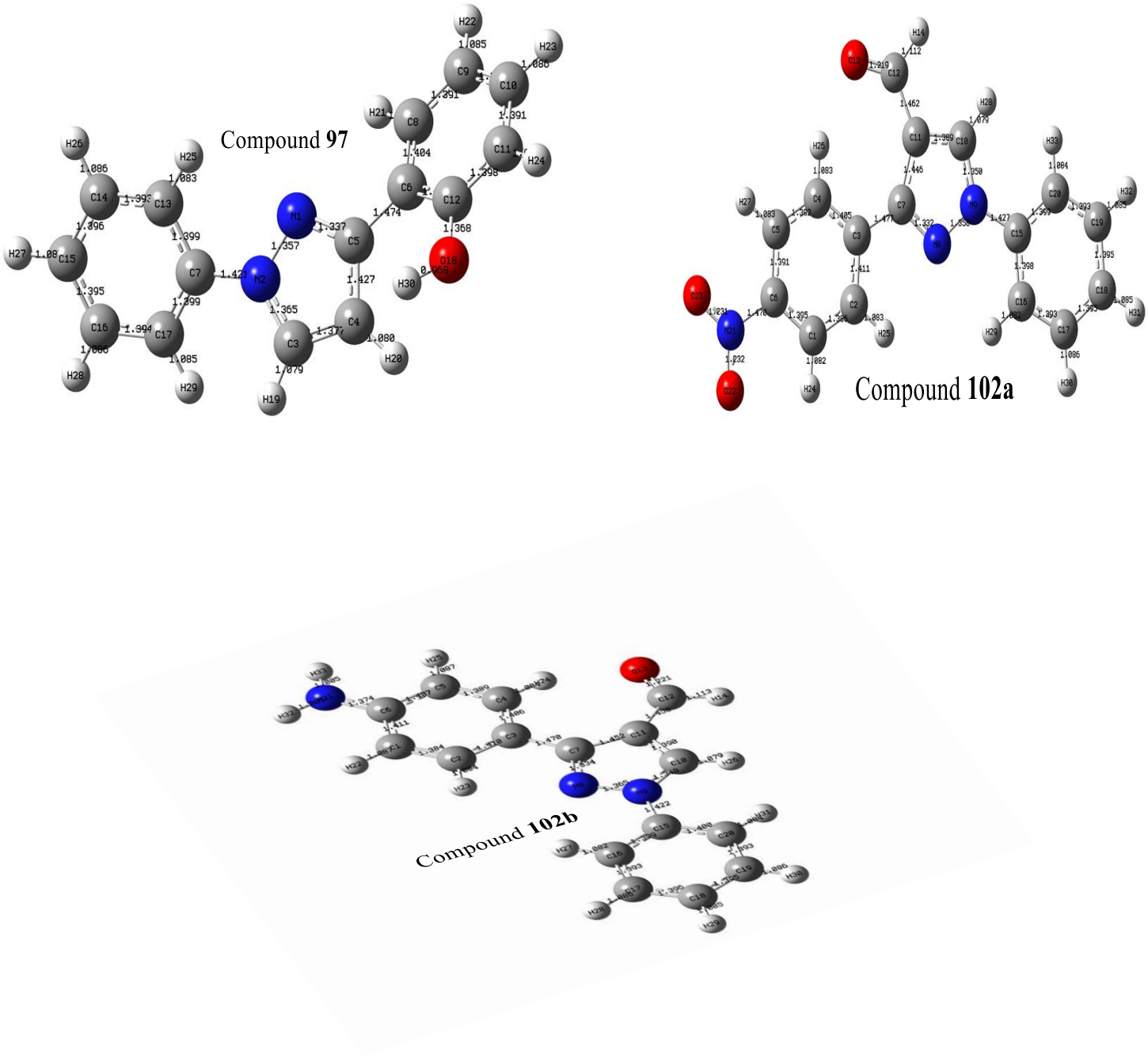

Figure 20: Optimized Structures of Compounds **97, 102a-b** depicting Bond Length.

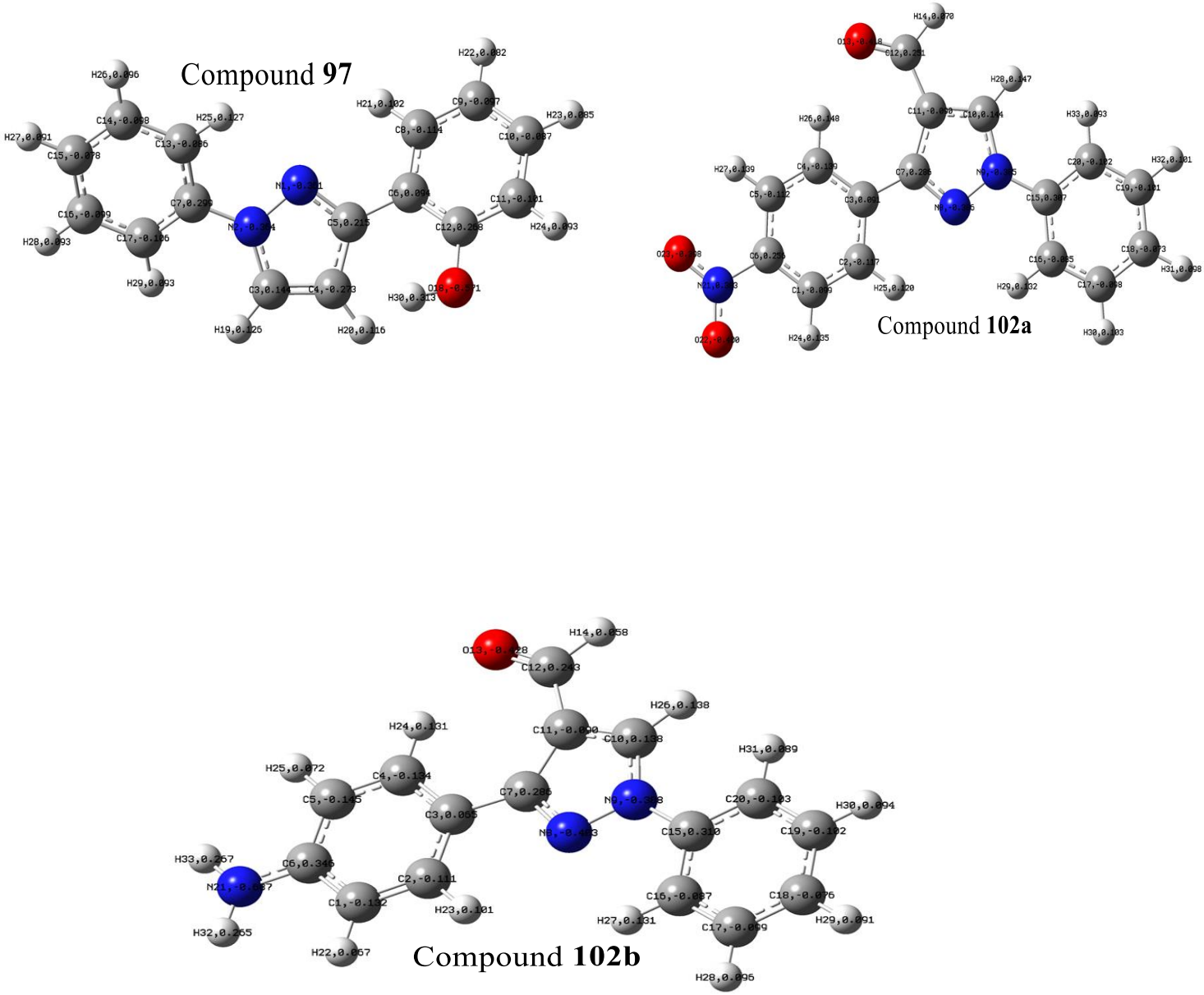

Figure 21: Optimized Structures of Compounds **97, 102a-b** depicting Mulliken Charges.

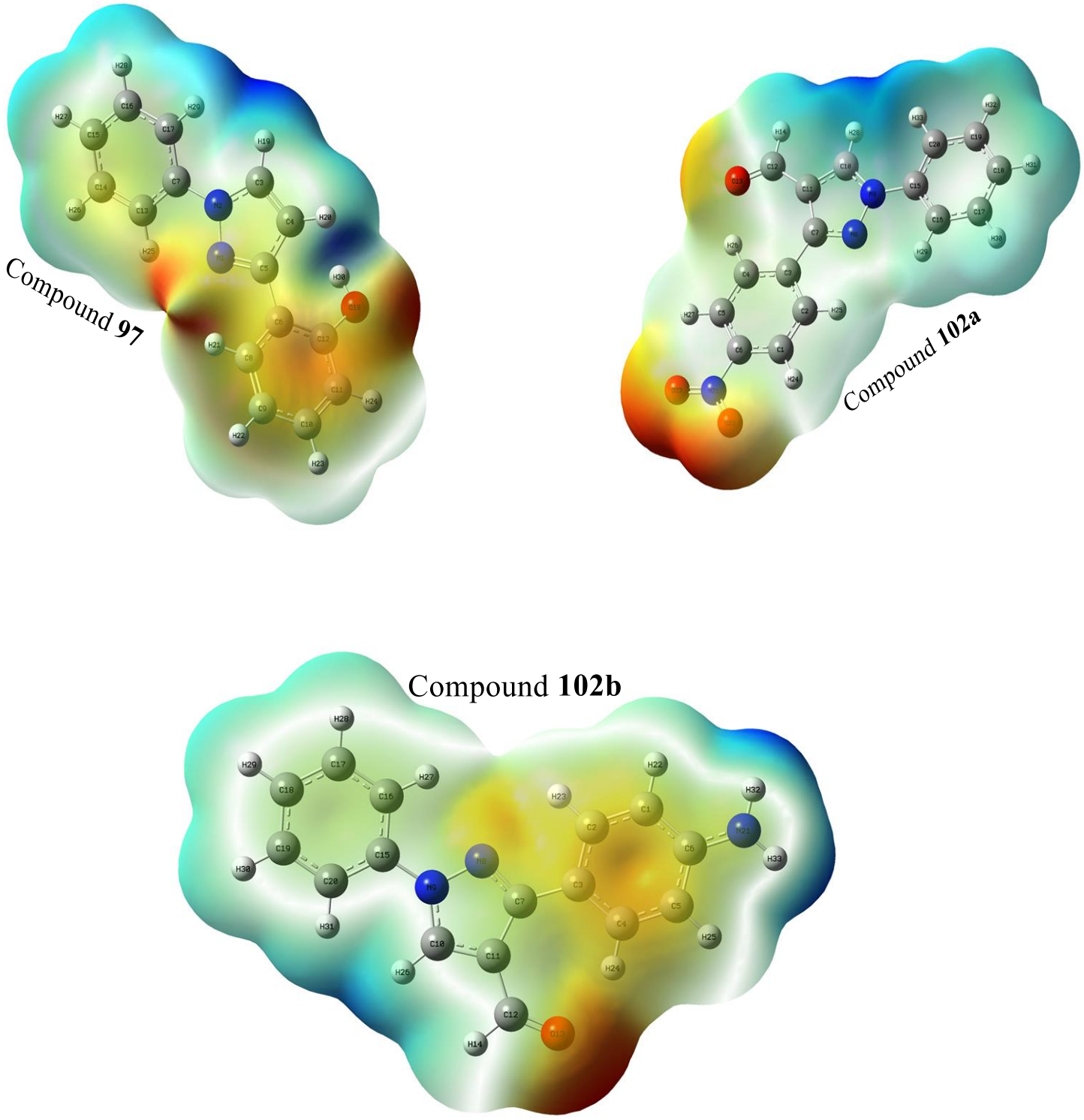

Figure 22: Optimized Structures of Compounds **97, 102a-b** depicting Molecular Electrostatic Potential Surface.

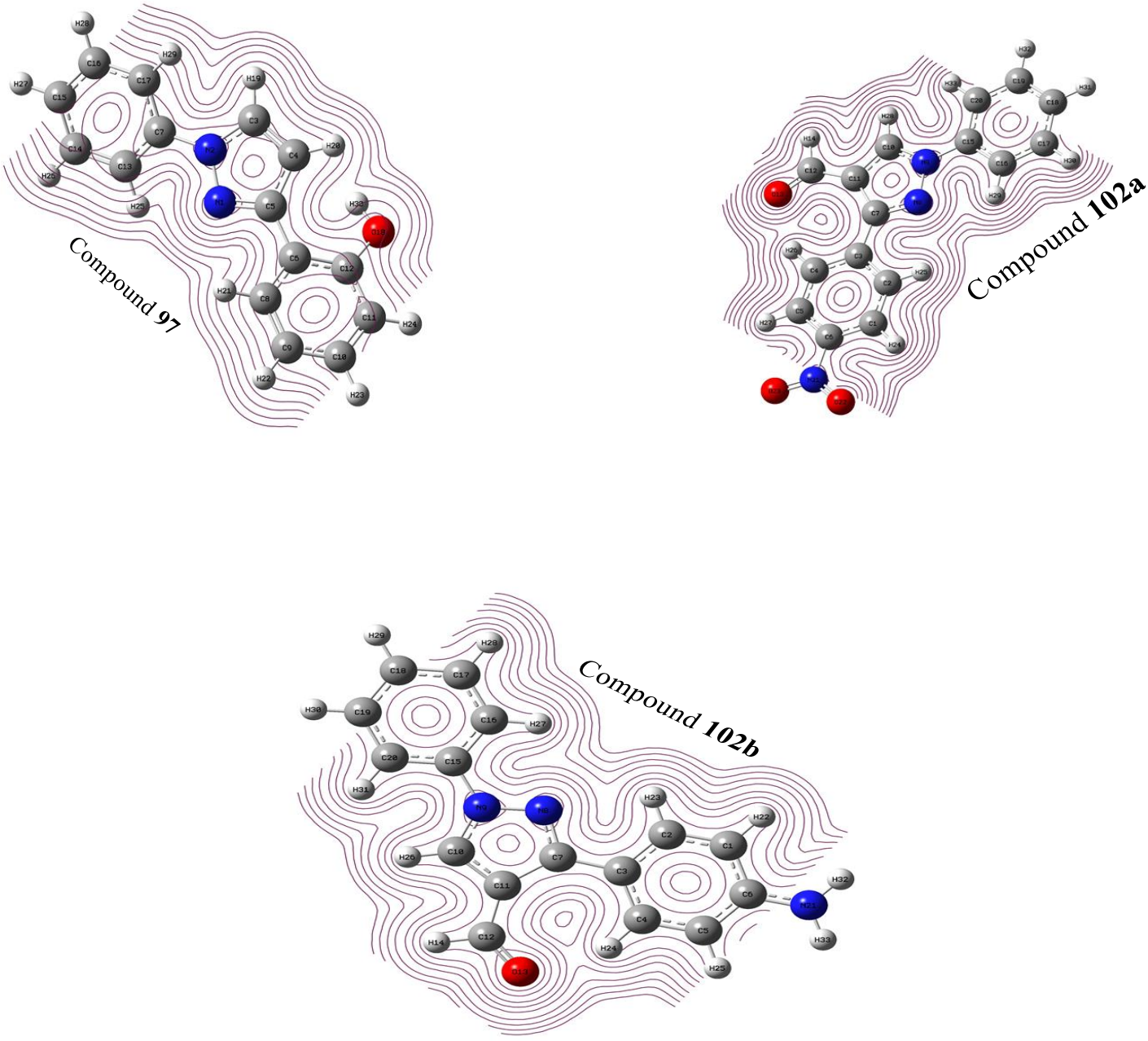

Figure 23: Optimized Structures of Compounds **97, 102a-b** depicting 2D Contour.

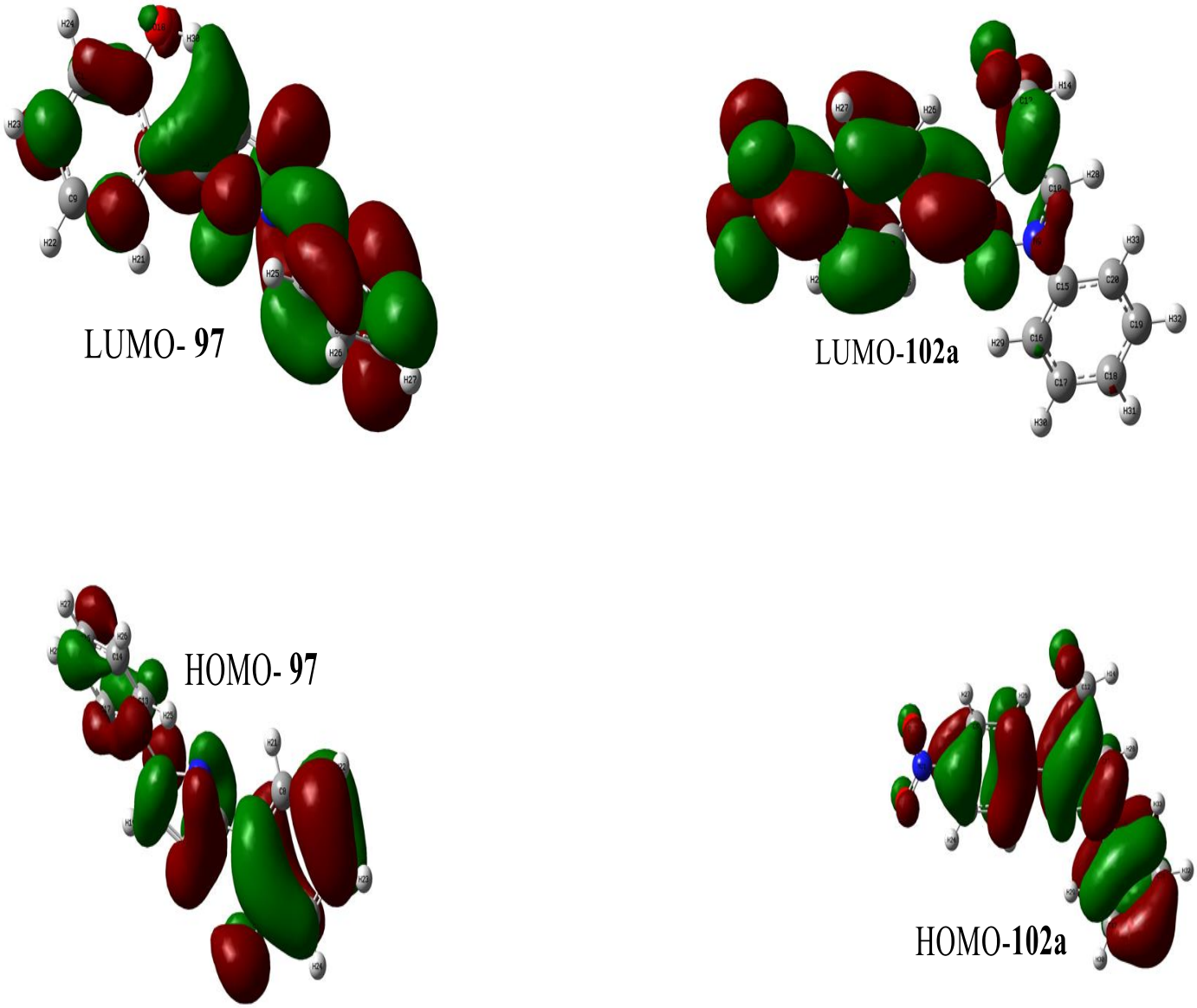

Figure 24: HOMO-LUMO Structures of Compounds **97, 102a**

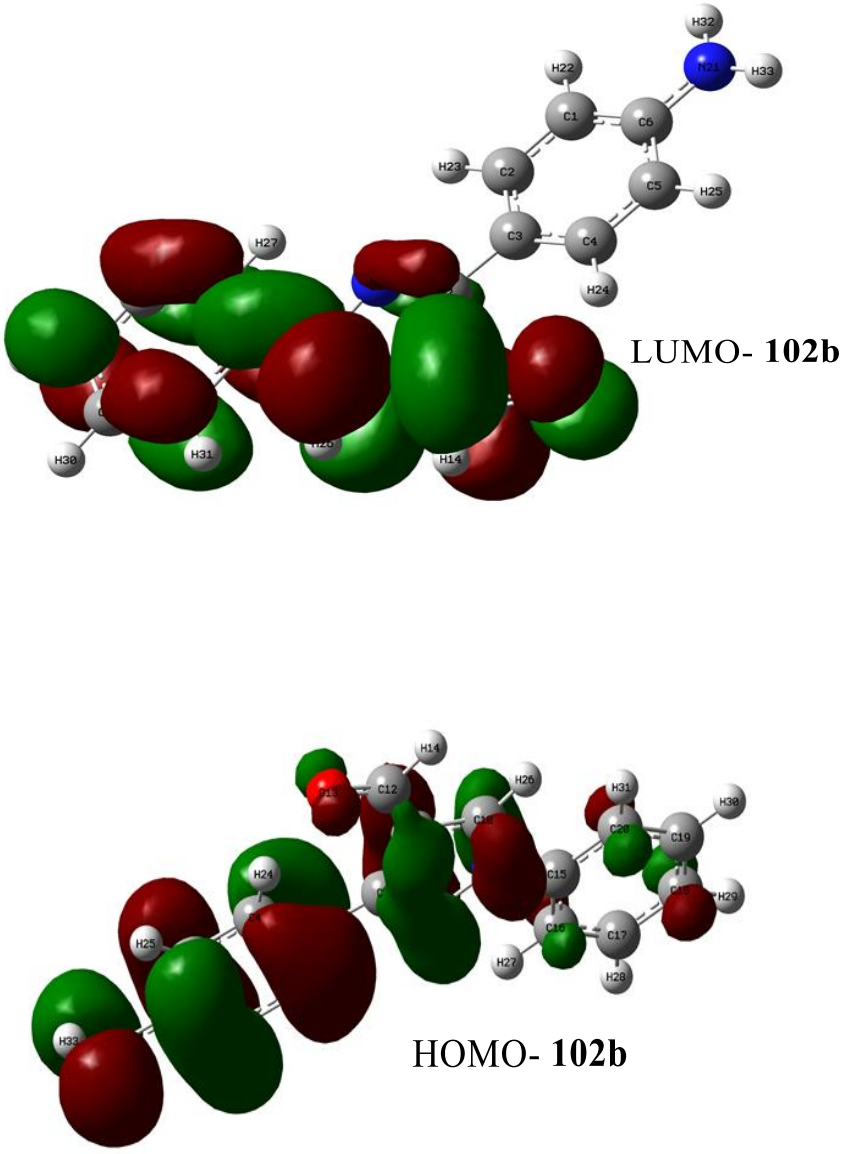

Figure 25: HOMO-LUMO Structures of Compound **102b**

5. CONCLUSIONS AND RECOMMENDATION

5.1. Conclusions

Pyrazoles represent a major pharmacophore with various biological properties, and some pyrazole containing derivatives have already been used for therapeutic purposes. Our literature review shows that pyrazole derivatives are pharmacologically very potent and, therefore, their design and synthesis is the potential area of research. Previous reports also show that the structural modifications of the basic structure of pyrazole, have allowed the preparation of new derivatives with a broad spectrum of biological activity, with the most important structural variations concerning the substituents at the 1-position, the carbon at the 3-position and the substituent at the 5-position. Previous studies have shown that the structural modification on the different positions of the basic molecule allows for improving its pharmacological profile, giving it antimicrobial, anticonvulsant, analgesic, anti-inflammatory, anti-viral, anti-malarial and anti-cancer properties. Therefore, researchers all over the world have been drawn their attention to the design and synthesize more potent pyrazole derivatives having great diversity of biological activity. The research work described in this thesis demonstrates the synthesis and chracterization of novel chemical entities of pyrazole derivatives such as pyrazole derivatives **97**, **102a** and **102b** through Vilsmeier-Haack reaction and condensation reaction. All the synthesized compounds show significant to moderate antimicrobial activities against four bacterial strains. Additionally, all the synthesized compounds showed high antioxidant activity. Antioxidants play important roles in the maintenance of cellular integrity and thus are critical in maintaining the homeostasis of the host immune system. Several cancer chemopreventive compounds having antioxidant properties have been documented to potentiate radiation therapy–induced cytotoxic effects on cancer cells while reducing its toxicity on normal surrounding tissues. The results of *in silico* molecular docking of the synthetized compounds are in good agreement with *in-vitro* analysis. The drug likeness of the synthesized compound satisfies the Lipinski's rule of five with zero violations. Hence, all the synthesized compounds might be candidates for further *in-vivo* antibacterial studies and thus have a potential as a lead molecule in the research of antimicrobial drug discovery programs.

5.2. Recommendation

Based on the present study the following further works were recommended:

- Synthesis of more derivatives of pyrazoles should be carried out.
- Determining Minimum inhibitory concentration (MIC) of the synthesized compounds should be conducted in addition to antibacterial results.
- The antibacterial activity was carried out on four strain (*E. coli*, *P. aeruginosa*, *S. pyogenes and S. aureus*), therefore the synthesized compounds should be investigated on other strains.
- It is necessary to evaluate anticancer, antifungal and anti-inflammatory activities of these synthesized compounds.

6. REFERENCES

Abdel-wahab, B. F., Khidre, R. E., & Farahat, A. A. (2011). Pyrazole-3 (4) -carbaldehyde : synthesis , reactions and biological activity. *Arkivoc*, *2011*, 196–245.

Abunada, N. M., Hassaneen, H. M., Kandile, N. G., & Miqdad, O. A. (2008). Synthesis and Biological Activity of Some New Pyrazoline and Pyrrolo[3,4-c]pyrazole-4,6-dione Derivatives: Reaction of Nitrilimines with Some Dipolarophiles. *Molecules*, *13*, 1011–1024.

Altun, A., Ok, S., & Mert, S. (2014). Synthesis , structure e activity relationships , and in vitro antibacterial and antifungal activity evaluations of novel pyrazole carboxylic and dicarboxylic acid derivatives. *Eur. J. Med. Chem*, *78*, 86–96. https://doi.org/10.1016/j.ejmech.2014.03.033

Anam Ansari , Abad Ali, M. A. and S. (2017). Review_ biologically active pyrazole derivatives. *New J. Chem*, *41*, 16–41. https://doi.org/10.1039/C6NJ03181A

Assali, M., Abualhasan, M., Sawaftah, H., Hawash, M., & Mousa, A. (2020). Synthesis , Biological Activity , and Molecular Modeling Studies of Pyrazole and Triazole Derivatives as Selective COX-2 Inhibitors. *Hind J Chem*, *1*, 1–14. https://doi.org/doi.org/10.1155/2020/6393428

Balbi, A., Anzaldi, M., Macciò, C., Aiello, C., Mazzei, M., & Gangemi. (2011). Synthesis and biological evaluation of novel pyrazole derivatives with anticancer activity. *Euro. J. Med. Chem.*, *46*(11), 5293–5309. https://doi.org/10.1016/j.ejmech.2011.08.014

Bhaskara Reddy, M. V., Srinivasulu, D., Peddanna, K., Apparao, C., & Ramesh, P. (2015). Synthesis and Antioxidant Activity of New Thiazole Analogues Possessing Urea, Thiourea, and Selenourea Functionality. *Synth Commun*, *45*(22), 2592–2600. https://doi.org/10.1080/00397911.2015.1095929

Chawla, R., Sahoo, U., & Arora, A. (2010). Microwave assisted synthesis of some novel 2-pyrazoline derivatives as possible antimicrobial agents. *Act. Polon. Pharm.*, *67*(1), 55–61.

De, A., Sarkar, S., & Majee, A. (2021). Recent advances on heterocyclic compounds with antiviral properties. *Chemistry of Heterocyclic Compounds*, *12*, 410–416. https://doi.org/10.1007/s10593-021-02917-3

El-Feky, S. A. H., Abd El-Samii, Z. K., Osman, N. A., Lashine, J., Kamel, M. A., & Thabet.

(2015). Synthesis, molecular docking and anti-inflammatory screening of novel quinoline incorporated pyrazole derivatives using the Pfitzinger reaction II. *Bioorg. Chem.*, *58*, 104–116. https://doi.org/10.1016/j.bioorg.2014.12.003

El-sehemi, A. G., Bondock, S., & Ammar, Y. A. (2013). Transformations of naproxen into pyrazolecarboxamides : search for potent anti-inflammatory , analgesic and ulcerogenic agents. *Med Chem Res*, *23*, 827–838. https://doi.org/10.1007/s00044-013-0650-0

Faisal, M., Saeed, A., Hussain, S., & Dar, P. (2019). Recent developments in synthetic chemistry and biological activities of pyrazole derivatives. *J. Chem. Sci*, *131*(70), 1–30. https://doi.org/10.1007/s12039-019-1646-1

Holst, J. (2020). Global Health - Emergence, hegemonic trends and biomedical reductionism. *Globalization and Health*, *16*(1), 1–11. https://doi.org/10.1186/s12992-020-00573-4

Hu, H., Ge, C., Ding, L., & Zhang, A. (2010). Synthesis of Novel 1-[(2,6-Dichloro-4-trifluoromethyl)phenyl]-3- aryl-1H-pyrazole-4-carbaldehydes. *Molecules*, *15*, 7472–7481. https://doi.org/10.3390/molecules15107472

Jadhav, A. D., & Barhate, P. (2020). Synthesis and spectral studies of pyrazole derivatives proven effective as antibacterial & antifungal activity. *Hetero Letters Org*, *10*, 439–445. https://doi.org/10.13140/RG.2.2.28244.01924

Karrouchi, K., Radi, S., Ramli, Y., Taoufik, J., Mabkhot, Y. N., & Al-Aizari, F. A. (2018). Synthesis and pharmacological activities of Pyrazole derivatives: A review. *Molecules*, *23*(1), 1–85. https://doi.org/10.3390/molecules23010134

Kaur, H., Kumar, S., Singh, I., & Kumar, A. (2010). Synthesis , characterization and antibacterial activity of various substituted oxadiazolylpyrazolinyl / isoxazolinylcoumarin. *IJPSR*, *1*(1), 58–65.

Kendre, B. V, Landge, M. G., & Bhusare, S. R. (2015). Synthesis and biological evaluation of some novel pyrazole , isoxazole , benzoxazepine , benzothiazepine and benzodiazepine derivatives bearing an aryl sulfonate moiety as antimicrobial and anti-inflammatory agents. *Arab. J. Chem*, 1–7. https://doi.org/10.1016/j.arabjc.2015.01.007

Kohli, P., Steg, G., Cannon, C. P., Jr, C. S., & Eagle, K. A. (2014). NSAID Use and Association with Cardiovascular Outcomes in Outpatients with Stable Atherothrombotic Disease. *Am J Med*, *127*(1), 53–60. https://doi.org/10.1016/j.amjmed.2013.08.017

Kumar, P., Kaushik, P., Sharma, C., & Kaushik, D. (2012). Synthesis and biological evaluation

of some pyrazole derivatives as anti- inflammatory-Antibacterial agents. *Med Chem Res*, 1–11. https://doi.org/10.1007/s00044-011-9853-4

Mantzanidou, M., Pontiki, E., & Hadjipavlou-litina, D. (2021). Pyrazoles and Pyrazolines as Anti-Inflammatory Agents. *Molecules*, *26*, 3439. https://doi.org/doi.org/10.3390/molecules26113439

Mihai, G., Draghici, C., & Vasile, A. (2010). Synthesis of new pyrazole derivatives and their anticancer evaluation. *Eur. J. Med. Chem*, *45*(11), 4914–4919. https://doi.org/10.1016/j.ejmech.2010.07.064

Mishra, R., Mazumder, A., Mazumder, R., Mishra, P., & Chaudhary, P. (2019). Docking study and result conclusion of heterocyclic derivatives having urea and acyl moiety. *Asian J. Biomed. Pharm. Sci.*, *9*(67), 13–17. https://doi.org/10.35841/2249-622x.67.19-082

Mohammed, K. O., & Nissan, Y. M. (2014). Synthesis, Molecular Docking and Biological Evaluation of Some Novel Hydrazones and Pyrazole Derivatives as Anti-inflammatory Agents. *Chem Biol Drug Des*, *84*, 473–488. https://doi.org/10.1111/cbdd.12336

Mohareb, A. A. and M. (2016). New approaches for the synthesis of pyrazole, thiophene, thieno[2,3- b]pyridine, and thiazole derivatives together with their anti-tumor evaluations. *Med Chem Res*, *23*, 564–579. https://doi.org/10.1007/s00044-013-0664-7

Nagamallu, R., Srinivasan, B., Ningappa, M. B., & Kariyappa, A. K. (2015). Synthesis of novel coumarin appended bis(formylpyrazole) derivatives: Studies on their antimicrobial and antioxidant activities. *Bioorg. and Med. Chem. Lett.*, *26*, 690–694. https://doi.org/10.1016/j.bmcl.2015.11.038

Nagy Khalifa, Hoda Fahmy and Eman Nossier. (2019). Novel synthesis of pyrazole-containing thiophene, 2-alkyloxy- pyridine and thieno[2,3-. *Bull. Chem. Soc*, *33*(3), 505–515. https://doi.org/doi.org/10.4314/bcse.v33i3.11

Nakao, S., Mabuchi, M., & Shimizu. (2014). Design and synthesis of prostate cancer antigen-1 (PCA-1 / ALKBH3) inhibitors as anti-prostate cancer drugs. *Bioorg Med Chem Lett*, *24*, 1071–1074.

Obinna, C., Nwodo, S., Olayinka, O., & O, I. C. (2009). Antibacterial effects of extracts of Ocimum gratissimum and piper guineense on Escherichia coli and. *Afr. J. Food Sci*, *3*, 077–081.

Orlandi, M., Brenna, D., Harms, R., Jost, S., & Benaglia, M. (2018). Recent Developments in

the Reduction of Aromatic and Aliphatic Nitro Compounds to Amines. *Org. Process Res. Dev*, *22*, 430−445. https://doi.org/10.1021/acs.oprd.6b00205

Prasad, Y. R., Kumar, G. V. S., & Chandrashekar, S. M. (2013). Synthesis and biological evaluation of novel 4 , 5-dihydropyrazole derivatives as potent anticancer and antimicrobial agents. *Med Chem Res*, *22*, 2061–2078. https://doi.org/10.1007/s00044-012-0191-y

Rodionov, A. N., Simenel, A. A., Korlyukov, A. A., Kachala, V. V, Peregudova, S. M., & Yu, E. (2011). Synthesis and properties of 5-ferrocenyl-1 H -pyrazole-3-carbaldehydes. *J. Organomet. Chem*, *696*(10), 2108–2115. https://doi.org/10.1016/j.jorganchem.2010.11.018

S. B. JADHAV, R. A. SHASTRI, K. V. G. and S. V. G. (2009). Synthesis and Antimicrobial Studies of Some Novel Pyrazoline and Isoxazoline Derivatives. *Euro.J.Chem*, *6*, 183–188. https://doi.org/10.1155/2009/361564

Sahu, S. K., Banerjee, M., Samantray, A., & Behera, C. (2008). Synthesis , Analgesic , Anti-inflammatory and Antimicrobial Activities of Some Novel Pyrazoline Derivatives. *Trop J Pharm Res*, *7*(2), 961–968.

Sankappa Rai, A. Isloor, P. S. (2014). Synthesis and in vitro biological evaluation of new pyrazole chalcones and heterocyclic diamides as potential anticancer agents. *Arab. J. CHEM.*, 1–5. https://doi.org/10.1016/j.arabjc.2014.01.018

Selvam, T., Kumar, P., Saravanan, G., & Prakash, C. (2012). Microwave-assisted synthesis , characterization and biological activity of novel pyrazole derivatives. *J Saudi Chem Soc*. https://doi.org/10.1016/j.jscs.2011.12.006

Shakhatreh, M. A. K., Al-Smadi, M. L., Khabour, O. F., Shuaibu, F. A., Hussein, E. I., & Alzoubi, K. H. (2016). Study of the antibacterial and antifungal activities of synthetic benzyl bromides, ketones, and corresponding chalcone derivatives. *Drug Design, Development and Therapy*, *10*, 3653–3660. https://doi.org/10.2147/DDDT.S116312

Thuy Hang Nguyen Thi, Yen Tran Thi, Le Anh Nguyen, Ngoc Binh Vo, Q. A. N. (2019). Design, Synthesis and Biological Activities of New Pyrazole Derivatives Possessing Both Coxib and Combretastatins Pharmacophores. *Chem and Biod.*, 1–11. https://doi.org/10.1002/cbdv.201900108

Venância, J., Fazolin, P., Gabriella, A., & Miguita. (2017). Bioorganic & Medicinal Chemistry

Recently reported biological activities of pyrazole compounds. *Bio. Org & Med Chem*, *25*, 5891–5903. https://doi.org/10.1016/j.bmc.2017.09.035

Xing, M., Ren, T. Z. Y., & Yang, N. P. X. (2014). Synthesis , biological evaluation , and molecular docking studies of pyrazolyl-acylhydrazone derivatives as novel anticancer agents. *Med Chem Res*, *23*, 3274–3286. https://doi.org/10.1007/s00044-014-0909-0

7. APPENDICES

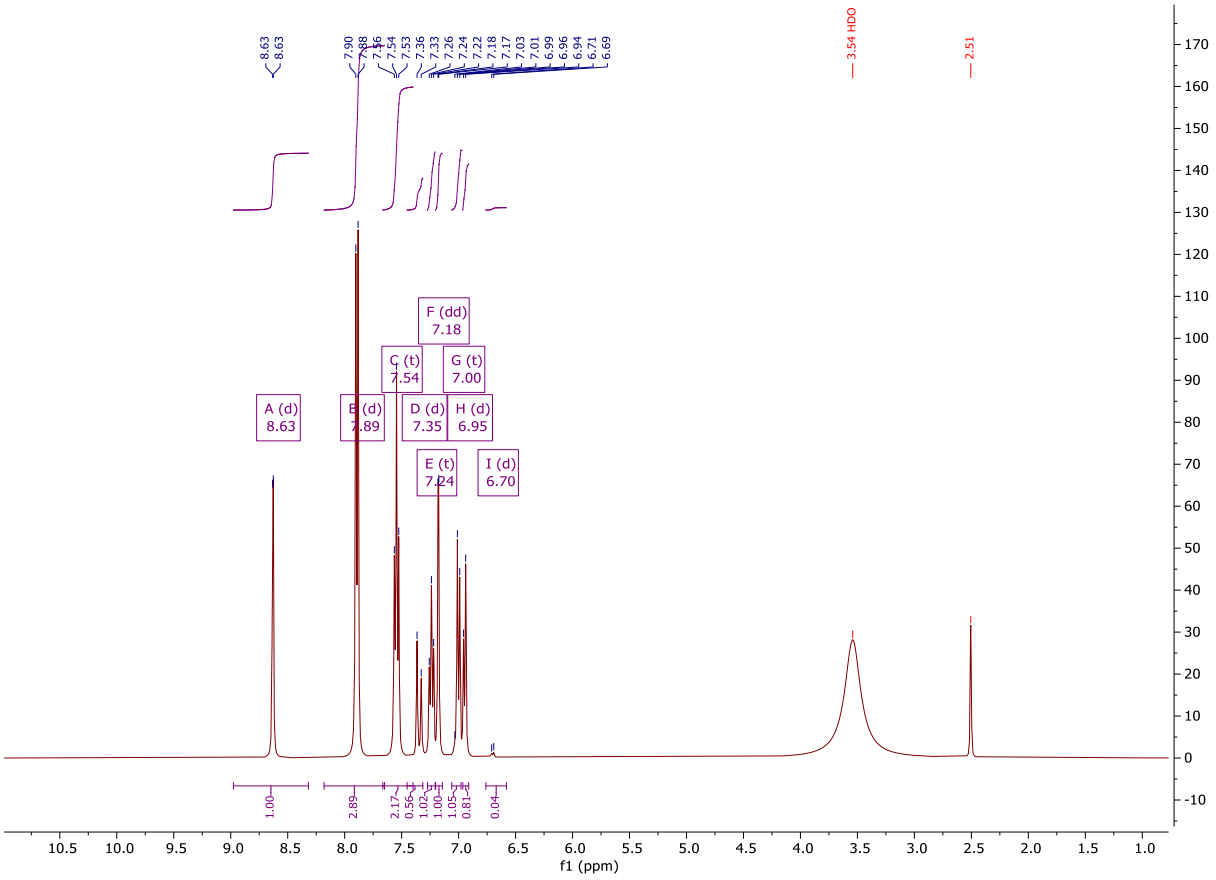

Appendix 1: ^{1}H-NMR (400 MHz, DMSO) spectrum of compound **97**

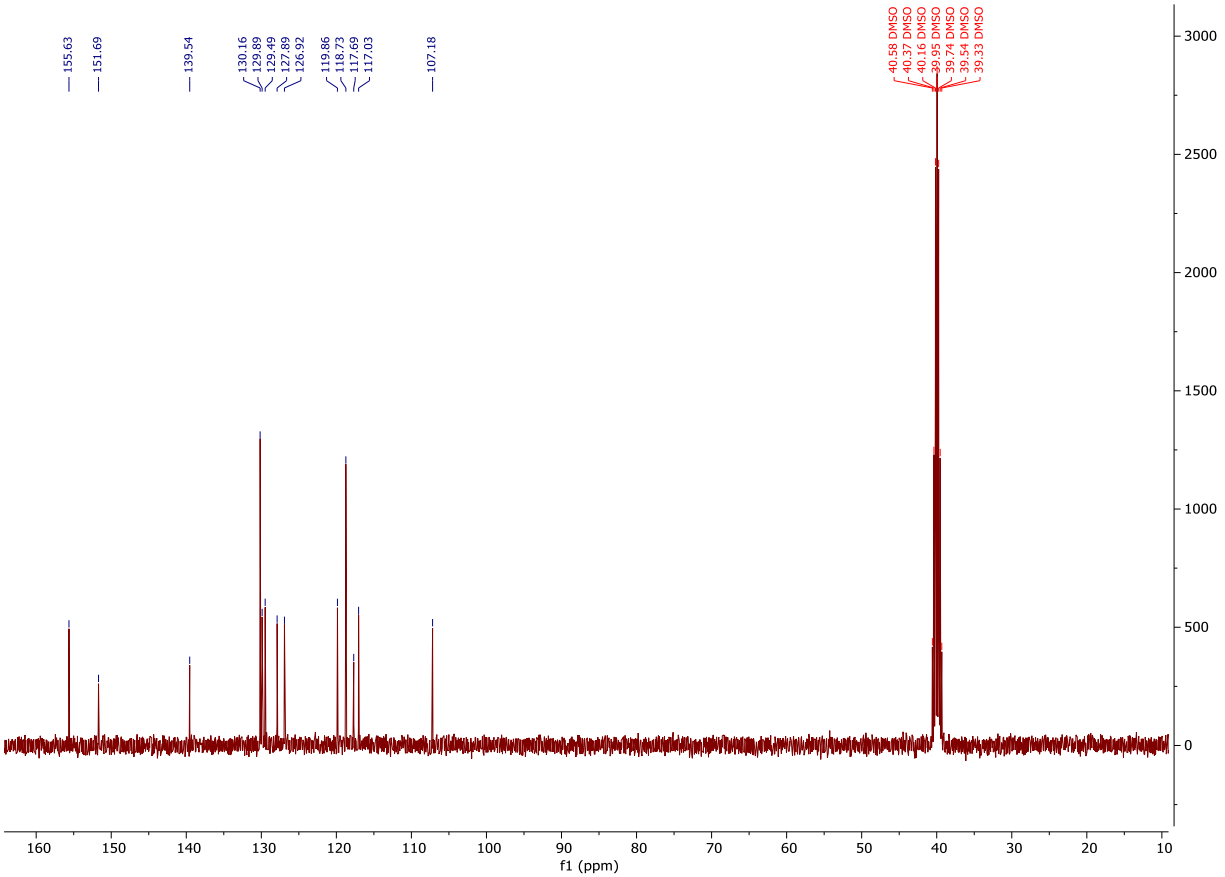

Appendix 2: ^{13}C-NMR (101 MHz, DMSO) spectrum of compound **97**

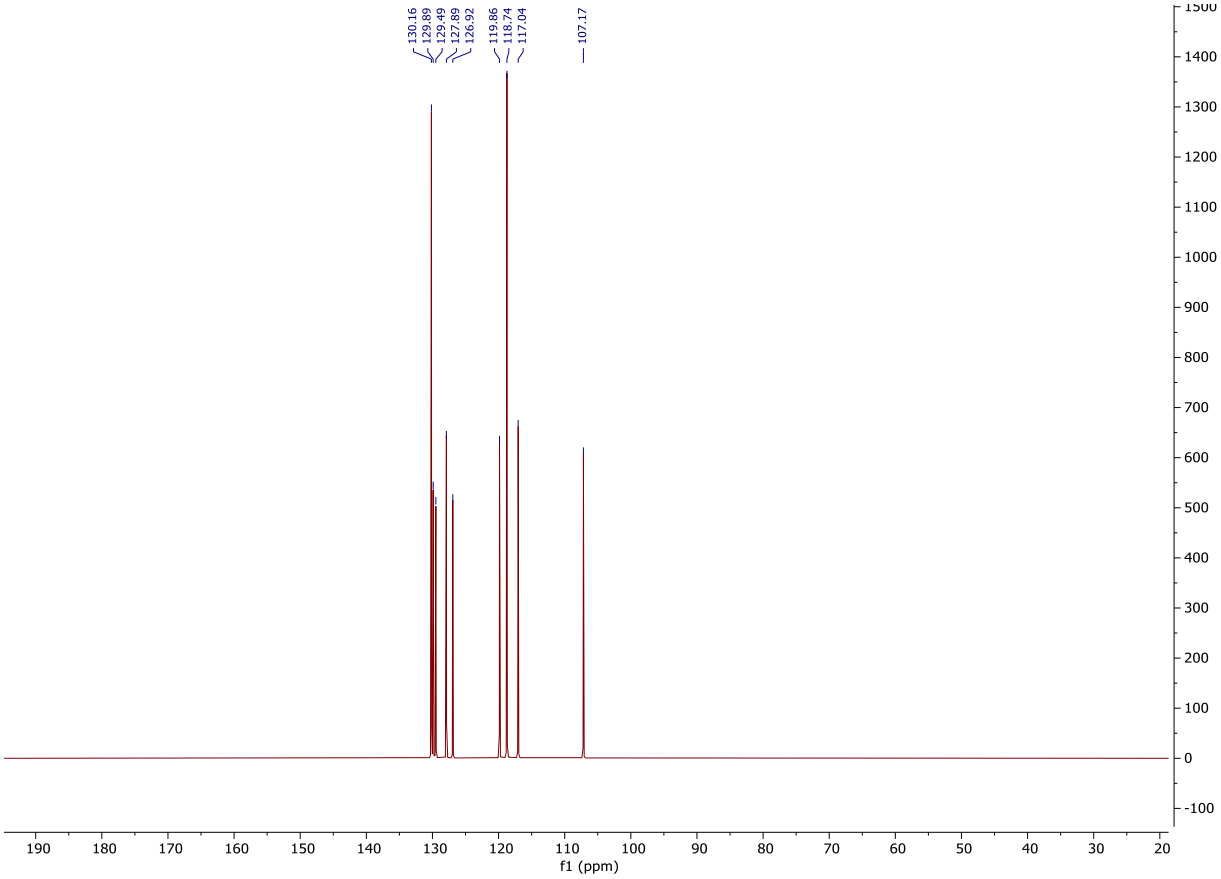

Appendix 3: DEPT-135 (101 MHz, DMSO) spectrum of compound **97**

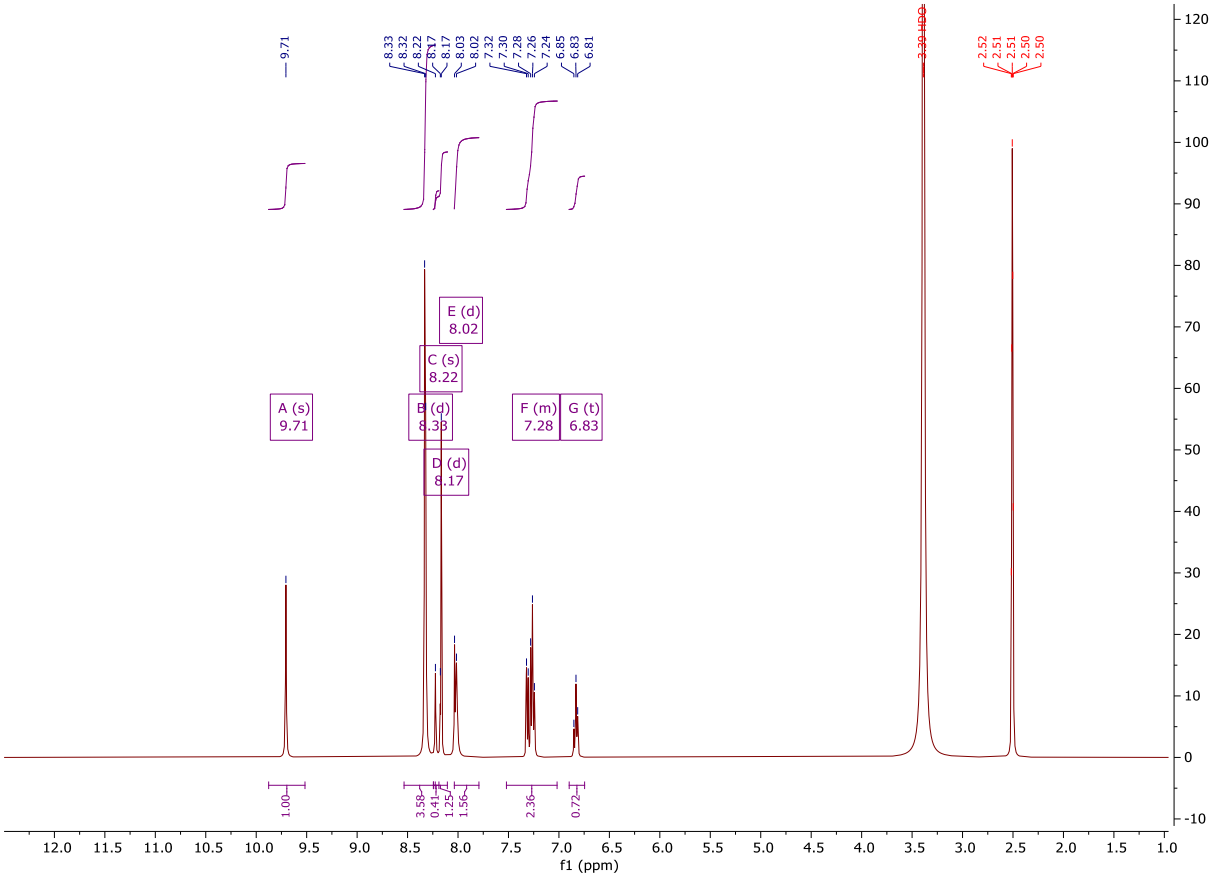

Appendix 4: ^{1}H-NMR (400 MHz, DMSO) spectrum of Compound **102a**

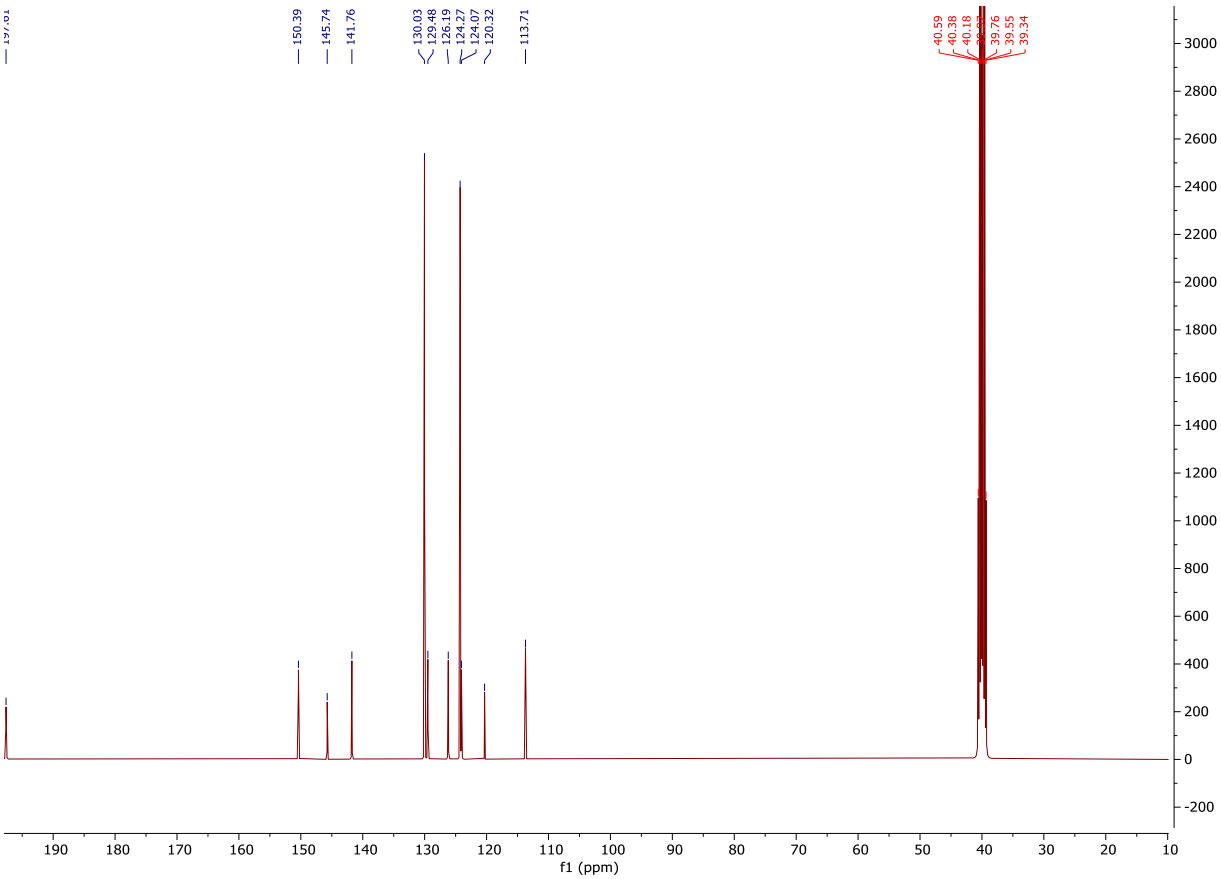

Appendix 5: ^{13}C-NMR (101 MHz, DMSO) spectrum of compound **102a**

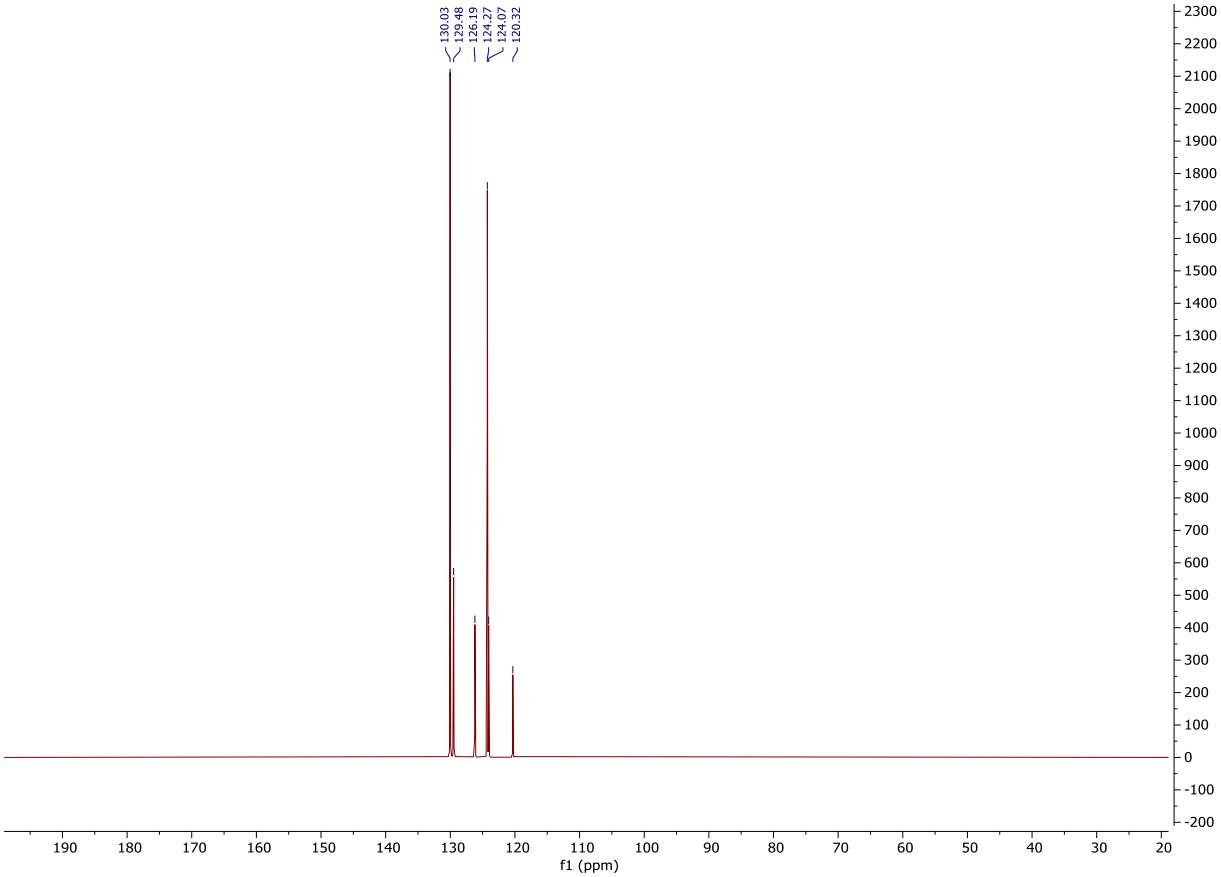

Appendix 6: DEPT-135 (101 MHz, DMSO) spectrum of compound **102a**

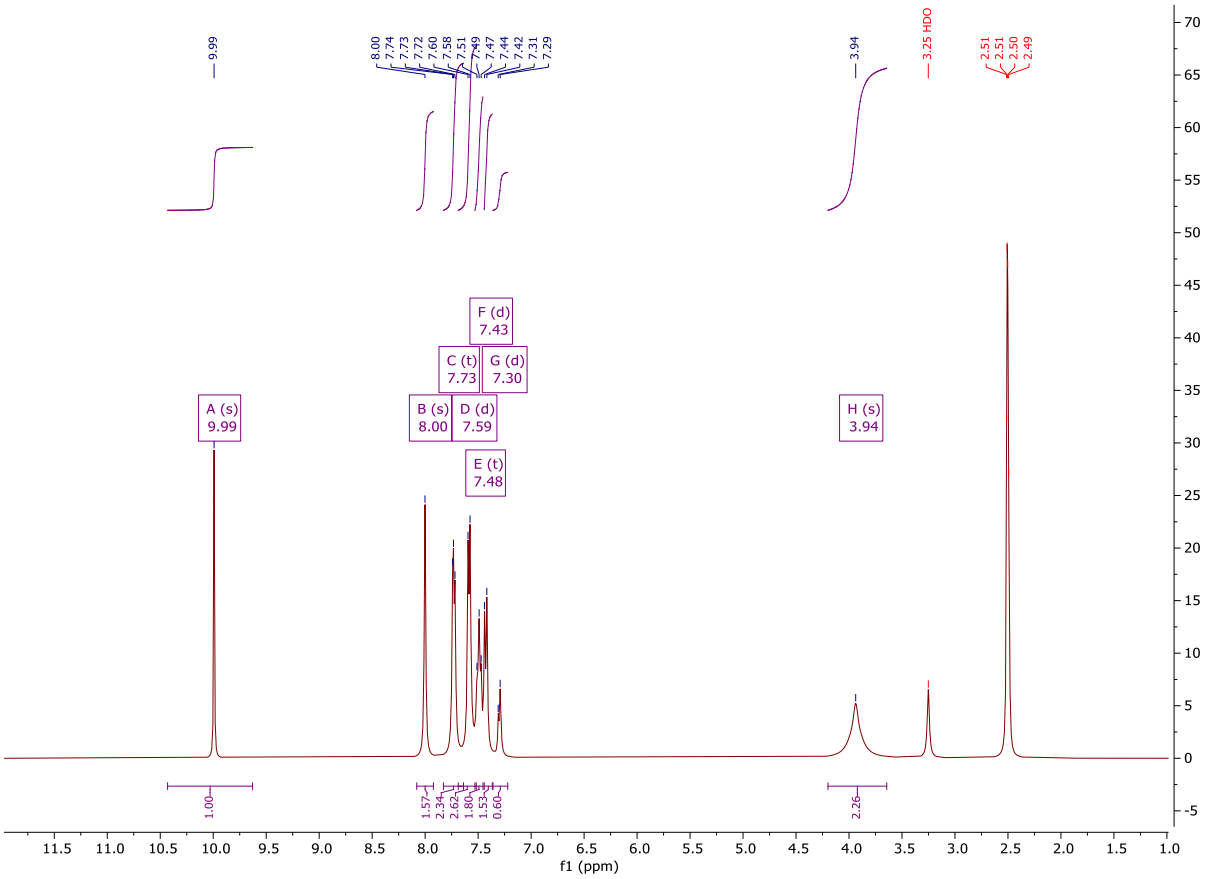

Appendix 7: ^{1}H-NMR (400 MHz, DMSO) spectrum of compound **102b**

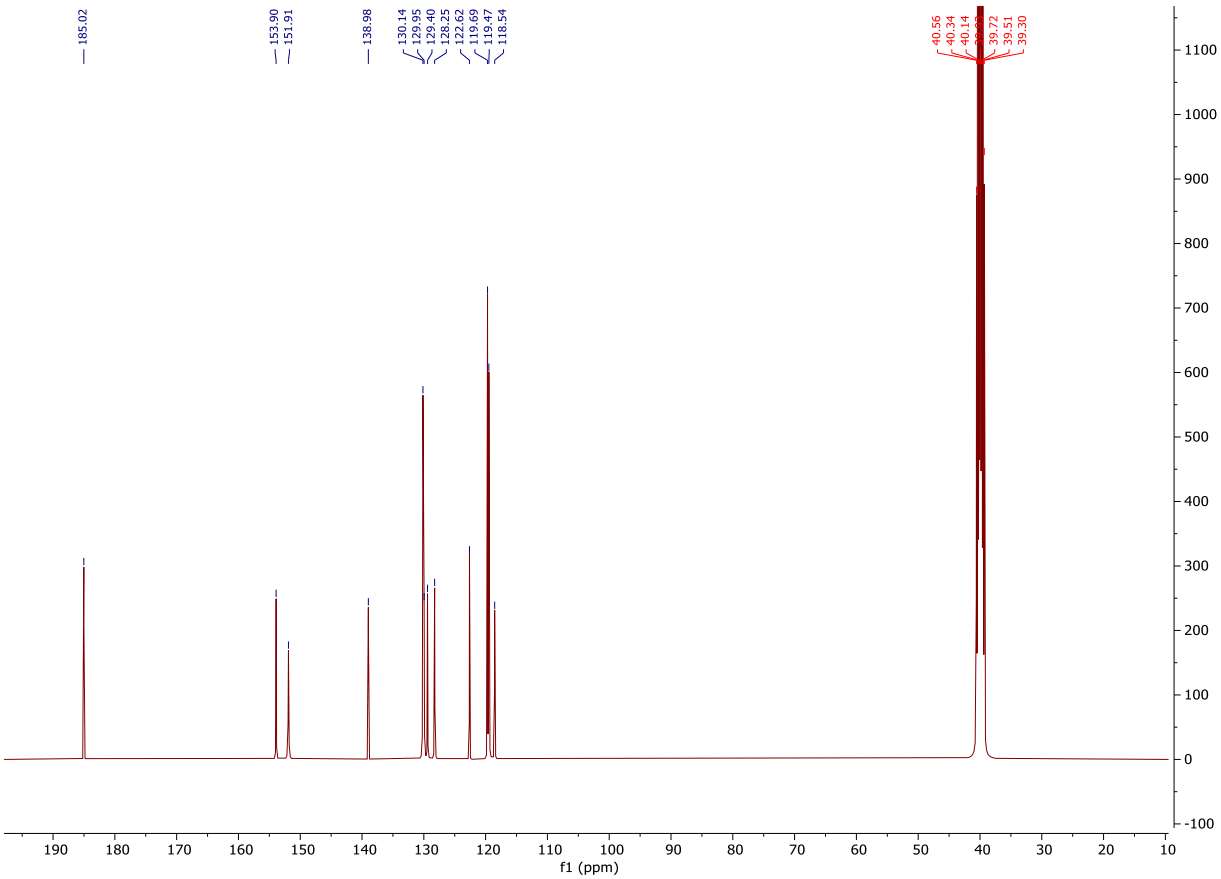

Appendix 8: ^{13}C-NMR (101 MHz, DMSO) spectrum of compound **102b**

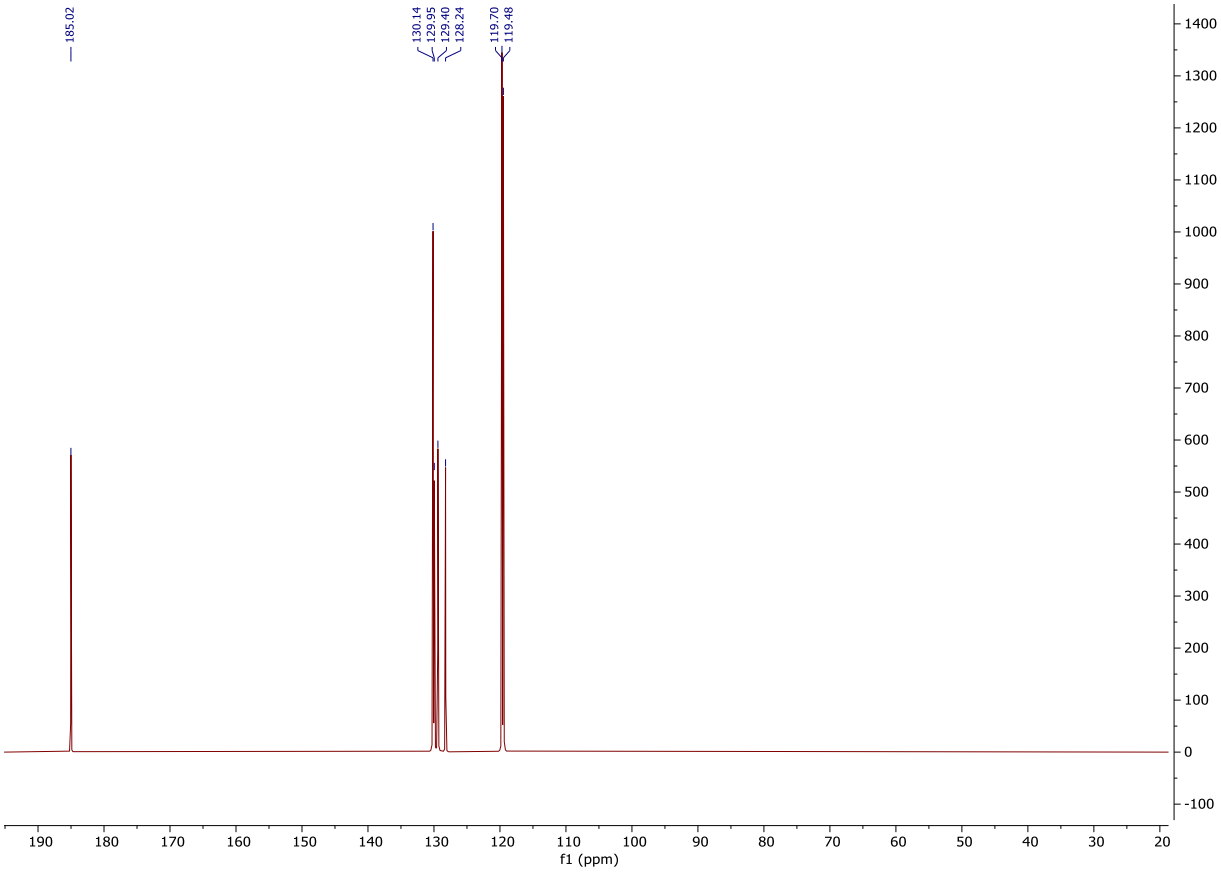

Appendix 9: DEPT-135 (101 MHz, DMSO) spectrum of compound **102b**

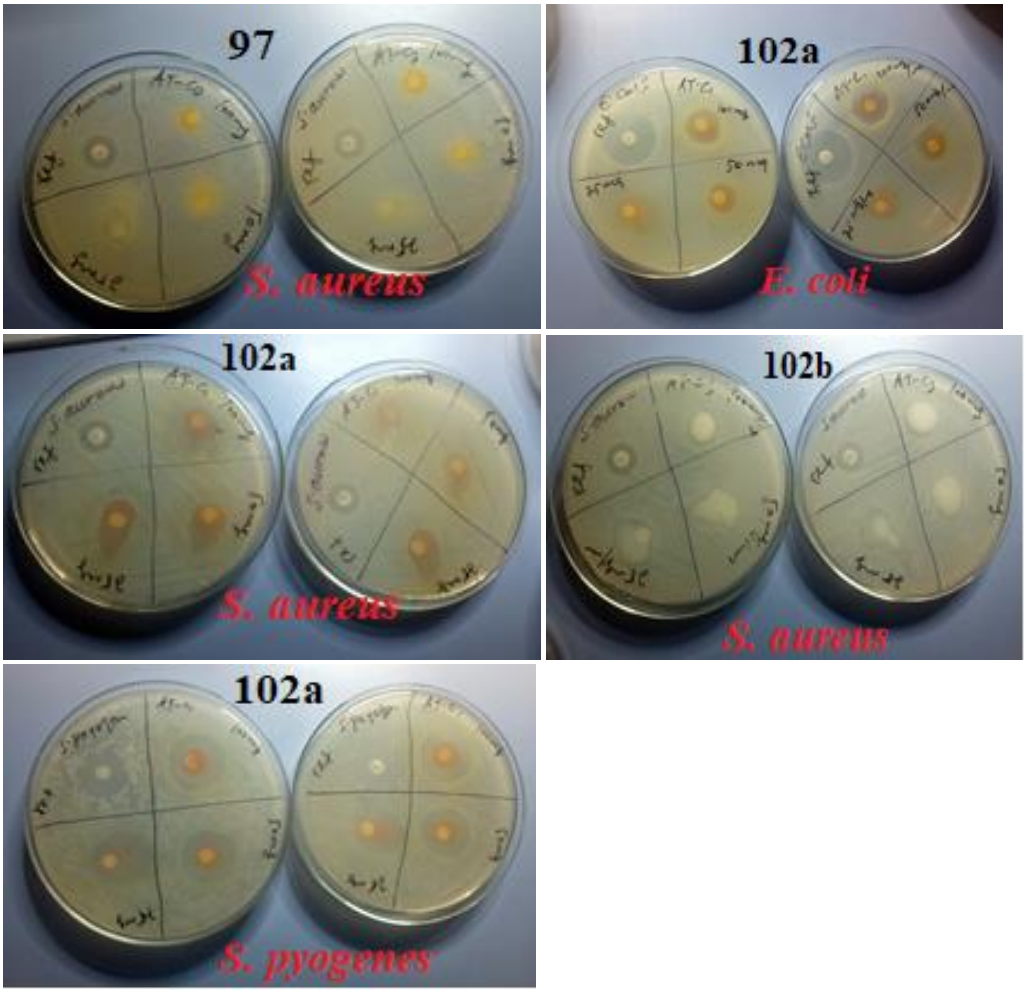

Appendix 10: Mean inhibition zone of bacterial growth (mm)